

# Optimized Energy Hub Scheduling Using Evolutionary Algorithms

Zur Erlangung des akademischen Grades eines

**DOKTORS DER INGENIEURWISSENSCHAFTEN (Dr.-Ing.)**

von der KIT-Fakultät für  
Maschinenbau  
des Karlsruher Instituts für Technologie (KIT)

angenommene

**DISSERTATION**

von

**M.Sc. Rafael Poppenborg**  
geb. in Ahlen

Tag der mündlichen Prüfung:

Hauptreferent:

Korreferent:

10.12.2024

Prof. Dr.-Ing. Veit Hagenmeyer

Prof. Dr.-Ing. Thomas Kolb



This document is licensed under a Creative Commons Attribution-ShareAlike 4.0 International License (CC BY-SA 4.0): <https://creativecommons.org/licenses/by-sa/4.0/deed.en>

# Abstract

The ambitious targets for reducing Greenhouse Gas (GHG) emissions necessitate the increased utilization of Renewable Energy Sources (RESs) and their integration into the existing grid infrastructure. Additionally, the growing dependence of various sectors on electrical energy poses significant challenges for the power grid as demand fluctuates greatly. An Energy Hub Gas (EHG) represents a promising approach to support the operation of energy grids formed by these developments. The EHG concept combines various technical components into a sector-coupling system to support the power grid with ancillary and balancing services, helping to cope with fluctuating generation from renewable energies and varying demand. Additionally, the EHG facilitates the provision of (renewable) energy sources, such as green hydrogen, for industrial processes that are difficult to electrify.

In this thesis, a co-simulation approach is used to integrate several separate models from different technical areas into an EHG system model. This approach offers flexibility in modeling aspects and modularity needed for easy adaptability for other use cases. The concept is evaluated using two different test cases. The two configured EHG demonstrate their ability to provide flexibility by reducing the difference between maximum and minimum load flow from and into the higher level grid infrastructure by up to 30%. Additionally, the average energy exchange is reduced by 8%. By relieving the load on the surrounding grid infrastructure, additional renewable energy potential is unlocked, and the curtailment of existing energy is reduced.

Optimized planning of Distributed Energy Resources (DERs) is crucial for the Energy Hub (EH) concept. However, this planning represents an NP-hard optimization problem and requires the use of powerful heuristic algorithms. One such heuristic approach is an Evolutionary Algorithm (EA). However, like all heuristics, they can produce inferior quality solutions and may need a lot of computation time if the search space is complex. Therefore, in this thesis, the applied EAs are adapted and improved by considering the predicted objective values of the optimization. Specifically, Machine Learning (ML) methods trained on previous solutions are used to predict the objective values of the optimization. Based on these predictions, the computational effort of the EA is directed to particularly difficult areas of the search space. This adjustment is achieved through a dynamic interval length assignment during the translation from genotype to phenotype. The approach is evaluated based on the optimization results using several ML prediction algorithms on two different EAs. The results show a significant increase in the Degree of Fulfillment (DOF) by up to 8.6%. Hereby, this thesis demonstrates that the EHG can make an important contribution to the operation of future power grids.



# Kurzfassung

Die ambitionierten Ziele zur Verringerung der Treibhausgasemissionen erfordern die verstärkte Nutzung erneuerbarer Energiequellen und ihre Integration in die bestehende Netzinfrastruktur. Außerdem stellt die Elektrifizierung verschiedener Sektoren das Stromnetz vor erhebliche Herausforderungen. Der Energy Hub Gas (EHG) ist ein vielversprechender Lösungsansatz zur Unterstützung des Energienetzbetriebs. Das EHG-Konzept kombiniert verschiedene technische Komponenten zu einem sektorgekoppelten Systemverbund, der das Stromnetz unterstützt fluktuierende Erzeugung und Nachfrage zu bewältigen. Zusätzlich ermöglicht der EHG die Bereitstellung von (erneuerbaren) Energieträgern, wie z.B. grünem Wasserstoff, für industrielle Prozesse, die schwer zu elektrifizieren sind.

In dieser Arbeit wird ein Co-Simulationsansatz verwendet, um mehrere separate Modelle aus verschiedenen technischen Bereichen in ein EHG-Systemmodell zu integrieren. Dieser Ansatz bietet die notwendige Flexibilität für eine einfache Anpassung des Systemmodells an unterschiedliche Anwendungsfälle. Anhand von zwei Testfällen wird die Flexibilitätsbereitstellung des EHG demonstriert, indem die Differenz zwischen maximalem und minimalem Lastfluss von und in die übergeordnete Netzinfrastruktur um bis zu 30% verringert wird. Zusätzlich wird der durchschnittliche Energieaustausch um 8% reduziert. Durch die Entlastung der umgebenden Netzinfrastruktur werden zusätzliche Potenziale zur erneuerbaren Energieerzeugung erschlossen und die Abregelung vorhandener Erzeugungsanlagen reduziert.

Die Optimierung der Betriebsführung stellt jedoch ein NP-schweres Problem dar und erfordert leistungsfähige heuristische Algorithmen, wie z.B. Evolutionäre Algorithmen (EA). Heuristiken können jedoch Lösungen minderer Qualität erzeugen und benötigen u.U. viel Rechenzeit bei komplexen Suchräumen. Daher werden die angewandten EA-Optimierungen angepasst und erweitert auf Basis des vorhergesagten besten Zielfunktionswertes. Methoden des maschinellen Lernens (ML), die auf früheren Lösungen trainiert wurden, werden verwendet, um den erreichten Zielfunktionswert der Optimierung vorherzusagen. Basierend auf diesen Vorhersagen wird der Rechenaufwand des EA auf besonders schwer zu optimierende Bereiche des Suchraums fokussiert. Diese Anpassung wird durch eine dynamische Intervalllängenbestimmung im Zuge der Übersetzung vom Genotyp zum Phänotyp realisiert. Unterschiedliche ML-Vorhersagealgorithmen werden auf zwei verschiedene EAs angewandt und anhand der erzielten Optimierungsergebnisse evaluiert. Die Ergebnisse zeigen eine signifikante Verbesserung um bis zu 8,6%. Damit wird in dieser Arbeit gezeigt, dass ein EHG durch seine Flexibilitätsbereitstellung einen wichtigen Beitrag zum Betrieb zukünftiger Stromnetze leisten kann.



# Contents

<b>Abstract</b> . . . . .	<b>i</b>
<b>Kurzfassung</b> . . . . .	<b>iii</b>
<b>Abbreviations and Symbols</b> . . . . .	<b>vii</b>
<b>1 Introduction</b> . . . . .	<b>1</b>
<b>2 Fundamentals</b> . . . . .	<b>5</b>
2.1 Energy Hub . . . . .	5
2.2 Co-Simulation . . . . .	8
2.2.1 Mosaik . . . . .	9
2.2.2 Process Operation Framework . . . . .	10
2.3 Energy Management System . . . . .	10
2.4 Multi Objective Optimization . . . . .	13
2.5 Evolutionary Optimization . . . . .	16
2.5.1 Creating a Start Population . . . . .	16
2.5.2 Encoding and Decoding . . . . .	17
2.5.3 Evaluation and Fitness Functions . . . . .	19
2.5.4 Creating Next Generation and Termination . . . . .	20
2.6 Mixed Integer Linear and Quadratic Programming . . . . .	21
2.7 No Free Lunch Theorem . . . . .	22
<b>3 Schedule Optimization</b> . . . . .	<b>23</b>
3.1 Scheduling . . . . .	23
3.2 Methods for Optimized Scheduling of DERs . . . . .	24
3.2.1 Comparison of MILP and EA . . . . .	25
3.3 The Energy Hub Gas . . . . .	26
3.3.1 Related Work . . . . .	27
3.3.2 Simulation Setup . . . . .	29
3.3.3 Component Models . . . . .	31
3.3.4 Test Case Description . . . . .	33
3.3.5 Industrial Area in Karlsruhe (Germany) . . . . .	34
3.3.6 Industrial Area in Northern Germany . . . . .	36
3.3.7 Specification of the Optimization Problem . . . . .	38
3.3.8 Comparison of GLEAM and DEAP . . . . .	39

3.3.9 Evaluation of the Energy Hub Gas . . . . .	43
3.4 Dynamic Fitness Mapping for EA-based Optimization . . . . .	50
3.4.1 Related Work . . . . .	51
3.4.2 Concept of Dynamic Mapping . . . . .	53
3.4.3 Evaluation of the Dynamic Objective Mapping Function . . . . .	57
<b>4 Adaptive Schedule Optimization . . . . .</b>	<b>61</b>
4.1 Problem Statement . . . . .	61
4.2 Basic Approach . . . . .	62
4.2.1 Related Work . . . . .	64
4.2.2 Concept . . . . .	66
4.2.3 Evaluation of the Basic Approach . . . . .	70
4.2.4 Results . . . . .	71
4.3 Hybrid Evolutionary Algorithm for Scheduling Energy Hubs . . . . .	72
4.3.1 Related Work . . . . .	73
4.3.2 Concept . . . . .	74
4.3.3 Population Generation and Coding . . . . .	75
4.3.4 Chromosome Interpretation . . . . .	75
4.3.5 Interval Length Assignment . . . . .	77
4.3.6 Boundary Condition Enforcement and Evaluation . . . . .	78
4.3.7 Forecast Methods . . . . .	79
4.3.8 Evaluation Criteria . . . . .	81
4.3.9 Evaluation of the Hybrid Optimization . . . . .	81
4.3.10 Results with GLEAM . . . . .	84
4.3.11 Results with DEAP . . . . .	87
<b>5 Discussion . . . . .</b>	<b>91</b>
5.1 Energy Hub Gas . . . . .	91
5.2 Hybrid Optimization . . . . .	92
5.2.1 Insights from Results . . . . .	93
5.2.2 Forecast of Optimization Quality . . . . .	94
5.2.3 Limitations and Benefits . . . . .	95
<b>6 Conclusion . . . . .</b>	<b>97</b>
<b>List of Figures . . . . .</b>	<b>101</b>
<b>List of Tables . . . . .</b>	<b>103</b>
<b>Previous Publications . . . . .</b>	<b>105</b>
Journal Article . . . . .	105
Conference Proceedings . . . . .	105
<b>References . . . . .</b>	<b>107</b>



# Abbreviations

## Abbreviations

<b>3PM</b>	Three-phase Methanation
<b>API</b>	Application Programming Interface
<b>BB</b>	Branch-and-Bound
<b>BGP</b>	Bio Gas Plant
<b>CHP</b>	Combined Heat and Power Plant
<b>CPES</b>	Cyber Physical Energy System
<b>CWS</b>	Cascaded Weighted Sum
<b>DEAP</b>	Distributed Evolutionary Algorithms in Python
<b>DER</b>	Distributed Energy Resource
<b>DL</b>	Deferrable Load
<b>DOF</b>	Degree of Fulfillment
<b>DP</b>	Dynamic Programming
<b>DSO</b>	Distribution System Operator
<b>DWD</b>	Deutscher Wetterdienst
<b>ECP</b>	Electrical Connection Point
<b>EA</b>	Evolutionary Algorithm
<b>EH</b>	Energy Hub
<b>EHG</b>	Energy Hub Gas
<b>EMS</b>	Energy Management System
<b>FMI</b>	Functional Mock-up Interface
<b>FMU</b>	Functional Mock-up Unit
<b>GHG</b>	Greenhouse Gas
<b>GLEAM</b>	General Learning Evolutionary Algorithm and Method

<b>ICT</b>	Information and Communication Technology
<b>IEC</b>	International Electrotechnical Commission
<b>KIT</b>	Karlsruhe Institute of Technology
<b>KNN</b>	K-Nearest Neighbors
<b>LP</b>	Linear Programming
<b>LR</b>	Lagrangian Relaxation
<b>MAE</b>	Mean Absolute Error
<b>MDER</b>	Managed Distributed Energy Resource
<b>MILP</b>	Mixed Integer Linear Program
<b>MINLP</b>	Mixed Integer Non-Linear Program
<b>MIQP</b>	Mixed Integer Quadratic Program
<b>ML</b>	Machine Learning
<b>MOO</b>	Multi Objective Optimization
<b>N-HITS</b>	Neural Hierarchical Interpolation for Time Series Forecasting
<b>NLP</b>	Non-Linear Programming
<b>NN</b>	Feed Forward Neural Network
<b>NSGA2</b>	Non-dominated Sorting Genetic Algorithm
<b>PEM</b>	Polymer Electrolyte Membrane Electrolysis
<b>PF</b>	Pareto Front
<b>PL</b>	Priority List
<b>PO</b>	Pareto Optimization
<b>PoC</b>	Proof of Concept
<b>PROOF</b>	Process Operation Framework
<b>PSD</b>	Power Spectral Density
<b>PSO</b>	Particle Swarm Optimization
<b>PV</b>	Photovoltaic
<b>QP</b>	Quadratic Programming
<b>RE</b>	Renewable Energy
<b>RES</b>	Renewable Energy Source
<b>RF</b>	Random Forest

<b>RMSE</b>	Root Mean Squared Error
<b>RQ</b>	Research Question
<b>SCOOP</b>	Scalable Concurrent Operations in Python
<b>SLP</b>	Successive Linear Programming
<b>SOC</b>	State-Of-Charge
<b>SOO</b>	Single Objective Optimization
<b>TC1</b>	Test Case One
<b>TC2</b>	Test Case Two
<b>TFT</b>	Temporal Fusion Transformer
<b>TMY</b>	Typical Meteorological Year
<b>TSO</b>	Transmission System Operator
<b>UC</b>	Unit Commitment
<b>VAE</b>	Variational Autoencoder
<b>WPP</b>	Wind Power Plant
<b>WS</b>	Weighted Sum



# 1 Introduction

In the Paris Agreement<sup>1</sup>, 196 countries committed themselves to the goal of keeping the global warming well below 2 °C by reducing their Greenhouse Gas (GHG) emissions. Beyond that, the German target is to reach a net-zero energy system by the year 2045. To achieve this goal, it is necessary, on the one hand, to expand and accelerate the deployment of Renewable Energy Sources (RESs), and, on the other hand, to ensure the integration of these into the existing grid infrastructure. The share of RES generation in the gross electricity consumption for the year 2023 in Germany is 51.8%<sup>2</sup>, which illustrates the magnitude of the required changes in the coming years in order to achieve the set goals. If we look at the gross final energy demand, the situation is even more dramatic. Only 22.0% of this demand is currently sourced from renewable generation<sup>2</sup>.

The established grid infrastructure was developed for a traditional downstream energy flow, originating from large centralized energy plants. With a high penetration of RESs in the energy system, as demanded by the set goals, this strict downstream flow disappears, and instead, energy may flow in any direction, constituting a bi-directional grid. Consequently, new energy security challenges emerge, particularly around fair energy access and environmental sustainability [102]. In particular, feed-in fluctuation by RESs generation, but also peaks in demand due to the electrification of several sectors, cause challenges concerning grid stability. Hence, the ability to adjust both the generation and consumption of useful energy in terms of flexibility provision is paramount for future energy grids. A possible source for flexibility could be the use of Distributed Energy Resources (DERs), which often are controllable small-scale facilities that can be categorized as generation, conversion, and storage systems. DERs can provide the needed flexibility to the grid by deviating from their planned operation schedules [29, 55, 99]. Especially, the Energy Hub (EH) concept, introduced by [57, 58, 59, 60], offers a promising approach to address the upcoming challenges. This concept combines the mentioned DERs with a wide range of existing and market-ready technologies. The EH concept has already shown in several works that it is able to reduce volatility in the electrical grid and provide grid service [135, 103, 104]. However, the energy system needs to be considered in total, not only the

---

<sup>1</sup> [https://unfccc.int/sites/default/files/resource/parisagreement\\_publication.pdf](https://unfccc.int/sites/default/files/resource/parisagreement_publication.pdf)  
visited 22.08.2024

<sup>2</sup> [https://www.bmwk.de/Redaktion/DE/Downloads/Energie/zeitreihen-zur-entwicklung-der-erneuerbar-en-energien-in-deutschland-1990-2023.pdf?\\_\\_blob=publicationFile&v=6](https://www.bmwk.de/Redaktion/DE/Downloads/Energie/zeitreihen-zur-entwicklung-der-erneuerbar-en-energien-in-deutschland-1990-2023.pdf?__blob=publicationFile&v=6)  
visited 22.08.2024

electrical side. The EH concept allows a holistic control of the energy supply with its sector coupling ability. An effective and smart interconnection between energy generation and usage increases local flexibility for electricity grid operation while providing renewable energy carriers, such as green hydrogen, for hard-to-de-fossilize sectors. The decentralized approach may help accelerate the energy transition to a more sustainable energy system by possibly reducing the required electricity grid extension. This could be possible by lowering the interconnection power flow between different voltage levels due to the reduced fluctuation and the direct use of energy generated by surrounding RESs in a lower voltage level. This local balancing promises to act as a preventive congestion management measure. Moreover, interconnecting different (energy) sectors through conversion and storage units may address the different time constants between, e.g., electricity and gas supply infrastructures. Overall, the integration of gas infrastructure, storage units, and different energy carriers offers an opportunity to reduce the operation cost for congestion management and re-dispatch for the electrical grid while gradually de-fossilizing non-electricity demand sectors.

However, the optimized scheduling of such EHs, or more generally DERs, is still a challenge. The complexity of the optimization task can be attributed to the following three main reasons:

- Operation of weather-dependent RESs causes uncertainty, as consumer-driven load variations on various time scales do,
- non-linearities caused by multi-objectives and complex boundary conditions,
- various control variables span a huge search space.

This leads to an NP-hard optimization problem [30, 133] and calls for powerful heuristic algorithms to find high-quality solutions within a reasonable time. The complexity due to the high dimensionality as stated in [97] is hard to formulate in a simplified manner as Mixed Integer Linear Program (MILP) and difficult, that is, needing excessive time and computational effort, to solve as a Mixed Integer Non-Linear Program (MINLP). Furthermore, the large search space challenges naive search heuristics, such as Monte Carlo optimization. In [123], empirical comparisons show the advantage of Evolutionary Algorithms (EAs) over classical methods with multimodal functions. Moreover, as stated in [101], EAs can directly deal with arbitrary linear and nonlinear conditions. In summary, EA based optimization algorithms are a viable approach and are already applied to cope with these challenges [107, 83, 24, 86, 87]. With the goal of advancing EH scheduling and promoting the usefulness of EHs in practical use cases, this thesis proposes and evaluates novel EH scheduling approaches based on the following research questions:

RQ 1: To what extent can DERs be instrumented to provide flexibility and grid supporting services?

RQ 2: Which (dis-)advantage can a dynamization of EA-based optimized scheduling provide to enhance flexibility provision by DERs?

RQ 3: To what extent can a Machine Learning (ML) model improve the dynamization of EA-based scheduling?

For this purpose, a modular EH co-simulation model is set up to evaluate the flexibility provision of this concept and to answer Research Question (RQ) 1. When trying to fulfill an external control signal, further referred to as target schedule, an EH using an EA for the optimization of its operation schedule for each DER can suffer from difficulties when responding to those parts of the target schedule exhibiting high variability, as stated in [31]. In the present thesis, the target schedule for the total power output of the EH is provided by a Distribution System Operator (DSO) or Transmission System Operator (TSO) to enhance the grid operation and avoid congestion. With an employed generic EA, the solutions suggested by the algorithm are translated to schedules for the controlled DERs and evaluated by an Energy Management System (EMS). In the literature, this mapping from EA solutions to schedules is based chiefly on time intervals with a fixed length of 15 minutes. Increasing the time resolution to achieve a more accurate approximation would likely improve results, though it would also require additional computation effort without any guarantee for improvement. However, if increasing the temporal resolution of the entire schedule is too costly or not possible, one approach may be to modify the temporal resolution of individual schedule parts dynamically. The general concept to solve the mentioned challenges and answer RQ 2 is that the EA should focus its computational effort on specific time segments in the schedule. This allows the computational effort to concentrate on segments with higher frequency fluctuations instead of those with lower frequency fluctuations. In other words, the computational effort required to find a solution within a specific time frame is scaled according to the time resolution in the schedule. Therefore, finding time segments that are more difficult to optimize is crucial. Finally, ML-based forecasting models are investigated to gain knowledge about the optimization result in advance. Given this information, the dynamic time interval length adaption can control the allocation of the computational effort and provide an answer to RQ 3. The allocation can be achieved by a dynamic genotype-phenotype mapping within the EMS.

The thesis is structured as follows to address the previously stated RQs: First, in Chapter 2, the basic concepts used throughout the thesis are briefly introduced. Second, Chapter 3 presents an overview of the scheduling problem in general and specific methods to solve it in the context of DERs. Furthermore, an approach to deal with the challenges that come with the implementation of a generic EA for scheduling DERs is described. The mapping of objective functions calculated by an EMS into a fitness value within the EA and its evolutionary operators are adapted to a newly introduced Degree of Fulfillment (DOF). Additionally, the Energy Hub Gas (EHG) as an exemplary instance of the EH concept is introduced, and insights into the modeling and simulation environment are given. In Chapter 4, the general idea of dynamic interval length

adjustment is described. Based on the results from a first experiment, the use of ML-based forecasting to direct the computational effort on difficult search space areas is presented. In Chapter 5, the combined results of the proposed approaches are discussed in detail. Finally, Chapter 6 concludes the present work, followed by a brief outlook on possible future work.

Parts of the thesis are partially based on previous works listed under "Previous Publications". These parts have been significantly extended.



## 2 Fundamentals

In the following chapter, the basic concepts and fundamentals used over the course of this thesis are briefly described. Starting with the introduction of the EH concept, an overview of the co-simulation frameworks used for multi domain investigations is given. Following, a deeper insight into the concept of EAs as a heuristic optimization method for the previously described scheduling problem is presented. Finally, the equation-based optimization by MILP is described as a widely used alternative.

### 2.1 Energy Hub

The idea of an EH was first introduced by [57, 60] in 2007 and is defined as following: EHs consist of multiple [facilities], that can convert, condition and store multiple forms of energy. Formulated more [abstractly], they define a black box with energy inputs and outputs of different types, which [are internally transformed from one type to another and may be] stored for later use. [5]

Transformation, conversion, and storage of various forms of energy in decentralized plant networks as flexibility resources called EH is a promising approach for smoothing out and balancing local generation and demand as stated in [103], especially if RES are integrated. In [135] usage of the EH concept on an neighbourhood scale is proposed, which fits as one [application for the EH concept]. However, the EHG model described in [Section 3.3] is designed to serve not only for small neighbourhood use cases, but is also applicable to industrial areas as well as small cities and at interconnections to the transmission grid. [5]

In general the concept itself can be used to serve a wide range of applications.

“Mathematically, the transformation process can be interpreted as a coefficient matrix  $H_{ab}$  that connects multiple energy inputs  $I_\omega$  to a number of energy outputs  $O_\sigma$ .” [5]

“A generic conversion formulation with multiple in- and outputs for a single unit [, representing an EH instance,] can be described by three parts: power output vector  $L$ , the converter coupling matrix  $C$ , and the power input vector  $P$ .” [5] Both  $P$  and  $L$  are vectors comprising all considered energy carriers  $\varepsilon = [\alpha, \beta, \dots, \omega]$ , e.g., [hydrogen, natural gas, ..., heat] into one vector.

**Table 2.1:** Conversion types [57].

Type of Coupling	Coupling Factor	Energy Carriers
Lossless transmission	$c_{\alpha\beta} = 1$	$\alpha = \beta$
Lossy transmission	$0 < c_{\alpha\beta} < 1$	$\alpha = \beta$
Lossless conversion	$c_{\alpha\beta} = 1$	$\alpha \neq \beta$
Lossy conversion	$0 < c_{\alpha\beta} < 1$	$\alpha \neq \beta$
No coupling	$c_{\alpha\beta} = 0$	any $\alpha, \beta$

The coupling matrix  $C$  consists of all instrumented energy conversions  $[\alpha, \beta, \dots, \omega] \rightarrow [\alpha, \beta, \dots, \omega]$ , where the element  $c_{\alpha\beta}$  is the conversion factor for a transformation from  $\alpha$  to  $\beta$ , e.g., hydrogen to natural gas. Adopted from [57], these connections can generically be formulated as:

$$\underbrace{\begin{pmatrix} L_\alpha \\ L_\beta \\ \vdots \\ L_\omega \end{pmatrix}}_L = \underbrace{\begin{bmatrix} c_{\alpha\alpha} & c_{\beta\alpha} & \dots & c_{\omega\alpha} \\ c_{\alpha\beta} & c_{\beta\beta} & \dots & c_{\omega\beta} \\ \vdots & \vdots & \ddots & \vdots \\ c_{\alpha\omega} & c_{\beta\omega} & \dots & c_{\omega\omega} \end{bmatrix}}_C \cdot \underbrace{\begin{pmatrix} P_\alpha \\ P_\beta \\ \vdots \\ P_\omega \end{pmatrix}}_P \quad (2.1)$$

The components  $c_{\alpha\beta}$  of the coupling matrix  $C$  are called coupling coefficients and map in- to output power.  $c_{\alpha\beta}$  can either convert between different energy carriers in the case of  $\alpha \neq \beta$ , or transmit one energy carrier to itself  $\alpha = \beta$ . In both cases,  $c_{\alpha\beta}$  can be between 0 and 1, or equal to 1, making it a lossy or lossless conversion/transmission. The special case where  $c_{\alpha\beta}$  is equal to 0 represents no coupling between given carriers. [The different conversion characteristics are summarized in Table 2.1.] [5]

“ $C$  can be dependent on the power input or other factors, e.g., the control performed by an EMS on a conversion unit, therefore  $C = f(P, t, \dots)$ , which” [5], in general, makes the EH model non-linear. Another important property of Equation (2.1) is stated in [57]: From two energy carriers on upwards, it represents an under-determined system of equations, which results in  $C$  not being invertible. In other words, there are degrees of freedom for the solution of an optimization. Only in case Equation (2.1) is regular, it describes a one-to-one mapping with a single solution for  $P$  at given  $L$ .

In [57], two important characteristics of the converter coupling matrix are stated, that can be summarized as

$$0 \leq \sum_{\beta \in \zeta} c_{\alpha\beta} \leq 1 \forall \alpha, \beta \in \zeta \subseteq \varepsilon. \quad (2.2)$$

The sum over any subset  $\zeta$  from  $\varepsilon$  must be larger than 0 but less or equal to 1, meaning that no energy conversion can increase the overall amount of energy available from the inputs. [5]

Furthermore, for a converter with several in- and outputs or several converters with the same in- or output, it may be necessary to split the input of an energy carrier so as not to violate the energy conservation as stated in Equation (2.2). Therefore, dispatch factors are introduced that split inputs into multiple inputs for different facilities  $P_{\alpha N_{B_\alpha}}$ . With  $N_{B_\alpha}$  the number of converters that utilize the same input energy carrier  $\alpha$ . To quantify the flow going through each junction, the dispatch factors  $\nu_{\alpha k}$  are introduced as

$$K_{\alpha k} = \nu_{\alpha k} K_\alpha \quad (2.3)$$

where  $k \in B_\alpha = \{1, 2, \dots, N_{B_\alpha}\}$  is the  $k$ th dispatch and  $B_\alpha$  the set of all possible junctions one energy carrier  $\alpha$  has. The energy conservation is considered according to Equation (2.2) for the dispatch factor by

$$0 \leq \nu_{\alpha k} \leq 1 \quad \forall \alpha \in \varepsilon, \forall k \in B_\alpha, \text{ and} \quad (2.4)$$

$$\sum_{k \in B_\alpha} \nu_{\alpha k} = 1 \quad \forall \alpha \in \varepsilon. \quad (2.5)$$

“Beside conversion, the energy storage needs special consideration. The desired EH can not only convert but also store energy over a certain time. The storage of energy results in time dependencies of all modelling variables.” [5] In [57], any energy storage is interpreted in terms of an interface that exchanges power  $Q_\alpha$  with the surrounding system. The internal power flow  $\tilde{Q}_\alpha$  that includes charging and discharging efficiencies of the storages is introduced as

$$\tilde{Q}_\alpha = e_\alpha Q_\alpha, \quad \text{with} \quad (2.6)$$

$$e_\alpha = \begin{cases} e_\alpha^+ & \text{if } Q_\alpha \geq 0 \quad (\text{charging/standby}) \\ \frac{1}{e_\alpha^-} & \text{else} \quad (\text{discharging}). \end{cases} \quad (2.7)$$

$e_\alpha$  describes the combined charging ( $e_\alpha^+$ ) and discharging ( $e_\alpha^-$ ) efficiency that connects the internal power flow  $\tilde{Q}_\alpha$  with the power flow  $Q_\alpha$  that is observed from the outside. With the help of the internal power flow in combination with the stored energy  $E_\alpha(T)$  of a carrier  $\alpha$  the storage equation at a time  $T$  is formulated as

$$E_\alpha(T) = E_\alpha(0) + \int_0^T \tilde{Q}_\alpha(t) dt \approx E_\alpha(0) + \int_0^T \dot{E}_\alpha(t) dt, \quad (2.8)$$

with the internal power flow being approximately equal to the time derivative of the stored energy  $\frac{dE_\alpha}{dt} = \dot{E}_\alpha \approx \tilde{Q}_\alpha$ .

In [57], the storage influence on the total power output of an EH is summarized in the storage flow vector

$$M^{eq} = CQ + M. \quad (2.9)$$

In this representation  $Q$  is the storage power output before, and  $M$  the power output after an energy carrier is converted. Each component of  $M^{eq}$  can be restated as

$$M_{\beta}^{eq} = c_{\alpha\beta}Q_{\alpha} + M_{\beta} = \frac{c_{\alpha\beta}}{e_{\alpha}}\dot{E}_{\alpha} + \frac{1}{e_{\beta}}\dot{E}_{\beta}, \quad (2.10)$$

with  $e_{\alpha}$ ,  $e_{\beta}$  the charging or discharging efficiencies, according to Equation (2.4), for respective energy carrier, and  $\dot{E}$  the change in energy of an energy carriers storage. The relationship between the total storage influence of storage units with respect to its change in energy can be formulated in matrix notation to fit the concept of the coupling matrix  $C$  as follows:

$$\underbrace{\begin{pmatrix} M_{\alpha}^{eq} \\ M_{\beta}^{eq} \\ \vdots \\ M_{\omega}^{eq} \end{pmatrix}}_{M^{eq}} = \underbrace{\begin{bmatrix} s_{\alpha\alpha} & s_{\beta\alpha} & \dots & s_{\omega\alpha} \\ s_{\alpha\beta} & s_{\beta\beta} & \dots & s_{\omega\beta} \\ \vdots & \vdots & \ddots & \vdots \\ s_{\alpha\omega} & s_{\beta\omega} & \dots & s_{\omega\omega} \end{bmatrix}}_S \cdot \underbrace{\begin{pmatrix} \dot{E}_{\alpha} \\ \dot{E}_{\beta} \\ \vdots \\ \dot{E}_{\omega} \end{pmatrix}}_{\dot{E}} \quad (2.11)$$

thereby representing the complete EHs output power as

$$L = CP - S\dot{E} = [C \ -S] \begin{bmatrix} P \\ \dot{E} \end{bmatrix}. \quad (2.12)$$

[5]

## 2.2 Co-Simulation

A monolithic simulation model implemented in one simulation software system would be one option for implementing the plant network and the behavior of all IT components. But there are several disadvantages or trade-offs that come with this solution, as stated in [110]: First, there is a need to find a development environment that covers all used domains. Second, experts for each sub-system or domain need to work strongly together and have to use the same implementation environment to build the system simulation model. Third, models of the different storage and conversion technologies, or the implementations of the IT control logic cannot be easily reused

in other application settings. Finally, the performance of the whole model, and therefore the scalability of the system model is limited by the execution environment of this single simulator. [5]

As the EH modeling presented in the previous Section 2.1 shows, various domains need to be considered. Several technical domains are taken into account by the sector coupling character of the EH concept, such as electricity, natural gas, and heat. Furthermore, the EH concept calls for the ability of flexible adjustment of the considered components to investigate different EH instances. Thus, for simulating and evaluating EH use cases, the use of co-simulation frameworks is an eligible solution.

There is abundant and vast literature proposing various kinds of co-simulation approaches that can be used to model, simulate, and evaluate complex systems such as Smart Grids. Due to the interdisciplinarity needed for modelling each component of a complex sector-coupled energy system, various heterogeneous tools must be connected into a system simulation, e.g., by use of a co-simulation approach. However, many co-simulation approaches are limited to particular scenarios. Moreover, they do not allow to integrate many different kinds of simulators that could provide a more universal co-simulation framework for simulating real complex multi-domain energy system models, such as the EH use case consisting of multiple physical components and technical plants, energy carriers, IT communication, and control components.

Preliminary work [117] has shown the challenges of developing co-simulation frameworks that allow for the integration of (dynamic) plants, converters and also infrastructure models (electricity, gas, heat). Furthermore, there are also some co-simulation frameworks, e.g., Mosaik and the PROOF, that are more flexible and allow to combine, and reuse a bigger number of existing component models executed in different simulator tools to create complex system models and execute Smart Grid scenarios. [5]

### 2.2.1 Mosaik

As described in [122, 129], the Mosaik framework is designed as a flexible solution specifically for CPES/smart grids research with a focus on co-simulations across multiple domains. Its architecture consists of a simulator management module for configuring and integrating different component models. This is implemented for different simulators by, e.g., using FMUs and enabling data exchange between the simulators, and a scheduler acting as master for coordinating the execution steps and the exchange of data between simulations. For implementing system models, Mosaik offers two APIs to system modellers:

- the component API that has to be implemented by users for connecting simulators to Mosaik,
- the scenario API for setting up co-simulation scenarios by using the Mosaik scheduler as a master for controlling data flow and execution of simulator operations according to a test scenario.

Note, that with Mosaik, modelers will model their system by writing programming code in Python using the Mosaik APIs. [5]

## 2.2.2 Process Operation Framework

[As described in] [96, 95], the PROOF is a generic, modular, and highly scalable framework that automates the startup, synchronization, and management of scientific computational workflows. By using container-automation, distributed message oriented middleware and a microservice-based architecture it enables novel distributed process execution and coordination. It also supports trans-disciplinary, multi-domain co-simulations as part of larger workflows including different simulation tools [and programming languages] (e.g., Python, Matlab, FMU, Julia, Java, etc.). Moreover, an easy-to-use web user interface is provided to allow system modelers to easily set up, perform and control workflows or co-simulations, which can be executed remotely on a computing cluster without the need to think about the underlying computing infrastructure as an execution environment.

While the integration of different simulator types and tools within PROOF needs some programming effort for setting up the tools as reusable building blocks for creating workflows and system simulations, the setup of a system model itself is done using a graphical editor in a declarative way. PROOF is also part of a larger ecosystem where scenario data can directly be fetched from different data sources and injected into a simulation workflow. Output and intermediate results can be written to data storage on the cluster and, e.g., visualized in dashboards. [5]

## 2.3 Energy Management System

Energy management is defined by the Association of German Engineers as a “forward-looking, organized and systematic coordination of energy procurement, conversion, distribution and utilization in order to cover requirements whilst taking into consideration ecological and economic objectives” [16]. [53] aptly describes the EMS as a “(...) decision making tool that determines the operation schedule of dispatchable generation resources and (flexible) loads, by using a scheduling algorithm and information coming from DERs, energy markets (price signals), and consumers

(...”).

The main goal of an EMS is to manage facility operation in a near-optimal way. In reference to Figure 2.1 the EMS orchestrates all facilities inside the most outer circle of the Venn diagram, namely power and thermal demand, DER generation, and storage utilization under consideration of the connection to the distribution grid. To do so, the EMS communicates with the facilities. Communication is not direct but conveyed via a controller, as Figure 2.2 displays. Introducing a hierarchical communication structure helps to orchestrate different facilities in an optimized manner. Instructions for facilities are sent to the respective controller in the form of schedules as defined by the International Electrotechnical Commission (IEC) [73].

Creating schedules takes into account the current facility state, predictions, and collusion with higher level aggregators. The collusion includes a flexibility offer and unit commitment schedule in return. Processing these quantities is done by a scheduling algorithm in a way that satisfies the unit commitment under optimization for further (economic) factors as further described in Chapter 3.

The EMS acts as representative for the collective facilities as an interface to outside aggregators like the market or coordination signals from the utility operational grid operator. One quantity the EMS offers to other aggregators is flexibility. Figure 2.2 visualizes a communication concept of an EMS for an EH approach on basis of a hierarchical communication concept developed by the IEC [74]. In total, six participants take part in the communication on levels ranging from process (facilities), to field (controller), station (EMS), operation, and enterprise (aggregator/utility operational grid management), up to market level.

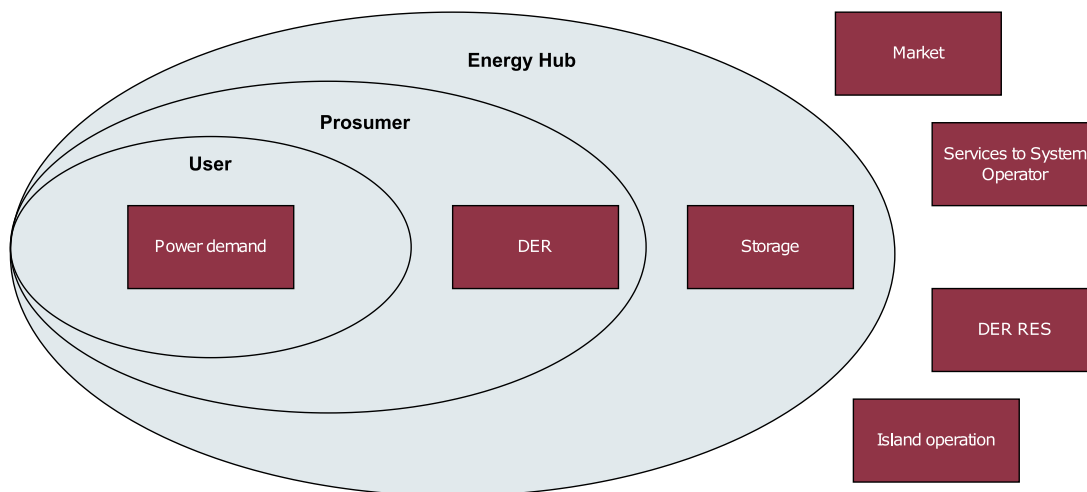


**Figure 2.1:** Venn diagram of the aggregation level, based on [53]

Typical optimizations include economic or environmental aspects. Depending on the optimization goal, different quantitative and qualitative information are needed. Typical information include price predictions for various energy carriers, demand and generation predictions, and

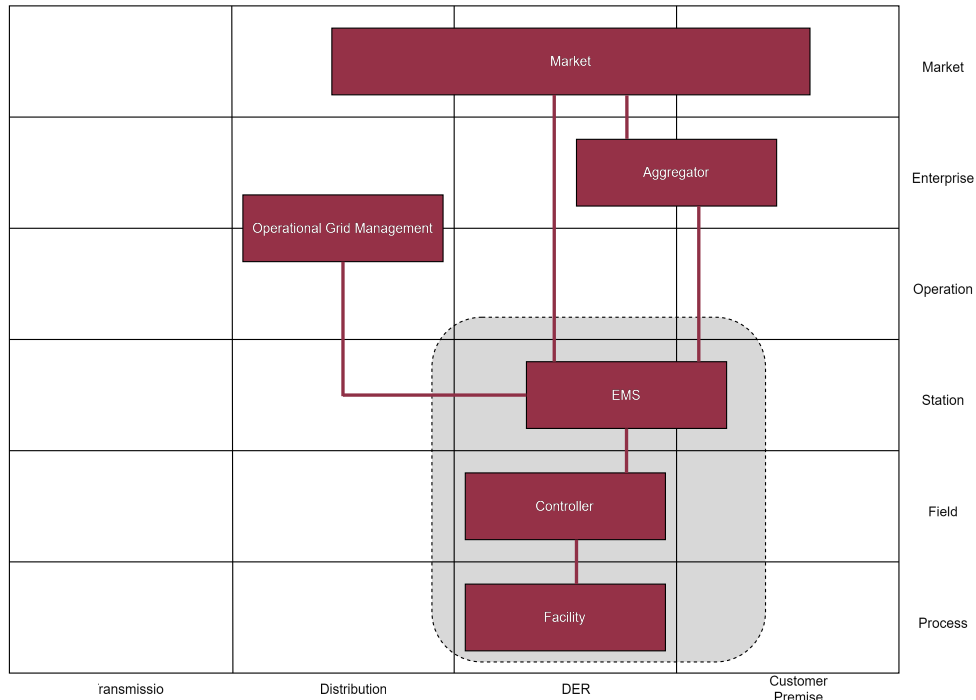


**Figure 2.2:** Hierarchical communication concept for DERs

specifications on generation and demand from superordinate aggregators. The definition of optimality is discussed in more detail in Section 2.4.

The EMS has many different tasks but, most importantly, represents the EH as a single unit to market participants on a higher hierarchy level. The EMS needs to interact with different components. Following the controller architecture, this communication has been specified in order to fit the use case depicted in Figure 2.2. The EMS has to provide communication ability with different components: the DER controller, aggregator, utility operational grid management, and the market. The communication interface with the controller must be bidirectional. First, the EMS needs to gather information about the current state from the controller. This information is then internally processed to offer power and flexibility to the aggregator. The aggregator then sells power and flexibility, which is in line with the offer on the market. The sold power information is expressed in the form of a schedule and sent to the EMS by the utility operational grid management. The EMS then processes these schedules and sends instructions to the DER controller. This, again, can be done in the form of a schedule. The scheduling concept holds the advantage that one central EMS can divide a specified schedule into several ones and pass them to different facilities through their respective controller. Also, one EMS is shown to be able to provide communication with several different controllers. Further specified communications can be established with the DER communications system, the aggregator DER and Load Management System, and the Retail Energy Market Clearinghouse. Thereby the EMS has to be able to



- calculate flexibility of the EH,
- offer flexibility,
- accept EH schedule,
- generate and solve optimization problems,
- evaluate schedule suggestions, and
- pass schedules to respective controller.

The mentioned capabilities are addressed in the implementation further described in Section 3.3 to enable the flexibility provision of an EH instance.

## 2.4 Multi Objective Optimization

The following overview of different Multi Objective Optimization (MOO) methods is based entirely on [77]. The optimization methods described are Pareto Optimization (PO), Weighted Sum (WS), and Cascaded Weighted Sum (CWS).

MOO is the optimization of different, possibly contradicting objectives. In such a case, an optimal solution is a trade-off where the improvement of one objective leads to the deterioration of another objective. These optimal solutions are called Pareto optimal solutions. A set of all Pareto optimal solutions is called Pareto Front (PF). Figure 2.3 illustrates the PF for an optimization problem with two objectives  $f_1, f_2$ . The left side shows the feasible region  $S$ , which contains all possible decision vectors  $x = (x_1, x_2)^T$ . The right side shows the feasible objective region  $Z$ . It contains objective vectors  $f = (f_1, f_2)^T$ , which are images of the decision vectors  $Z = f(x_1, x_2)$ .  $\max(f_1)$  marks the maximum value of objective one  $f_1$  accordingly,  $\max(f_2)$  marks the maximum value of objective two  $f_2$ . The ideal objective vector  $z^*$  marks the maximum values of objectives one and two and is outside the feasible objective region  $Z$ . The green line contains all Pareto optimal solutions and is called Pareto Front (PF).

In PO, initially, the PF is computed. Subsequently, the final solution is chosen by a human, who decides which solution and, therefore, which trade-off is most suitable for the problem to be solved.

Determining the PF can require high computing effort. If the area of interest is already known, calculating the PF can be omitted by using the WS or CWS. The advantages of using the WS or CWS are that they provide a single quality value and do not require human involvement to select the final solution. These properties are particularly useful when EAs are used for optimization.

The WS is given in Equation (2.13). To each objective  $f_i$  a weight  $w_i$  is assigned, representing its relative relevance in the optimization problem. The weighted objective values are then aggregated

into a single objective value  $WS(x)$ . Before calculating the WS, often a normalization is necessary to ensure that the objectives share the same scales.

$$WS(x) = \sum_{i=1}^k w_i f_i(x), x \in S \text{ where } w_i > 0 \text{ for all } i = 1, \dots, k \text{ and } \sum_{i=1}^k w_i = 1 \quad (2.13)$$

Any point of a convex PF can be reached by varying the weights. Figure 2.4a illustrates this by showing how varying the weights  $w_1, w_2$  influences the optimal solution  $P$  in a maximization problem with two objectives  $f_1, f_2$ . The optimal solution is found by moving the orange dashed line into the upper right corner of the objective region. The point where the line becomes tangential to the feasible objective region  $Z$  is the optimal solution. The slope of the orange dashed line results from the weights  $w_1$  and  $w_2$ . Increasing  $w_2$  results in a more horizontal line, while increasing  $w_1$  results in a more vertical line. The black arrows show the direction of optimization based on the weights perpendicular to the orange dashed line.

The drawback of the WS is depicted in Figure 2.4b. For a non-convex PF not every point of the PF can be reached by varying the weights. In the shown maximization problem with two objectives, the solutions between the solutions  $A$  and  $B$  cannot be reached.

The CWS mitigates the drawback of the WS by adding priorities to the weighted objectives. Initially, only the objectives within the highest priority group contribute to  $CWS(x)$ . When the objective values  $f_i(x)$  of the highest priority group reach certain thresholds  $\epsilon_i$ , the objectives of the following priority group are added to the CWS. Subsequently, the priority groups are added to the CWS. If an objective falls under the  $\epsilon_i$  threshold, the sum decreases drastically, as the objective values of the following priority groups are no longer considered.

Equation (2.14) shows the calculation of the CWS for three priority groups  $a, b, c$ , where  $a$  is the highest priority group,  $b$  is an example for any priority group, which is neither the highest nor

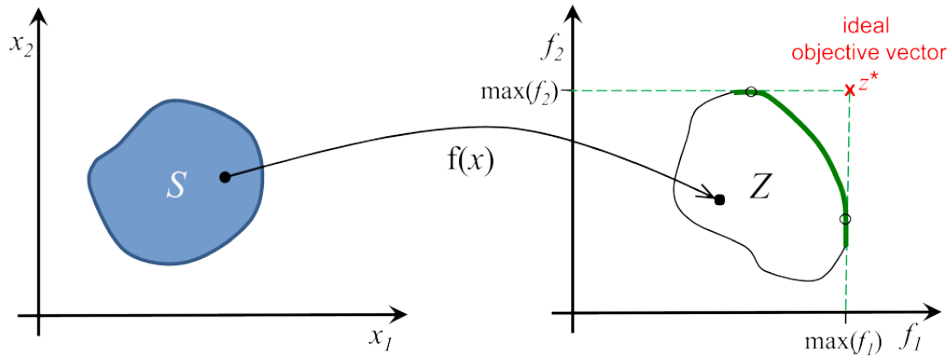


**Figure 2.3:** Example for a Pareto Front (green line) for an optimization problem with two objectives, adopted from [77]

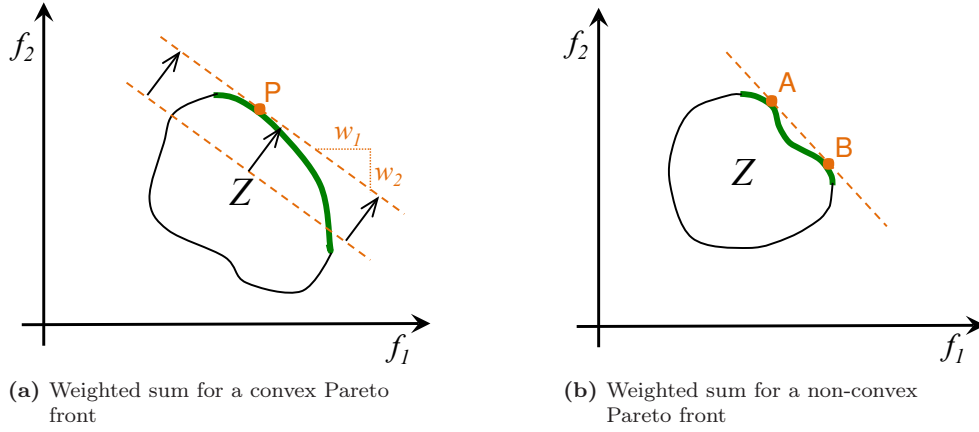


**Figure 2.4:** Weighted Sum for convex and non-convex Pareto Fronts, adopted from [77]

the lowest priority group and  $c$  is the lowest priority group. As in the WS, each objective  $f_i$  is weighted with the specified weight  $w_i$ .

**Priority a:** (highest priority)

If not all  $f_i(x) \geq \epsilon_i \forall i = 1, \dots, k$

$$CWS(x) = \sum_{i=1}^k w_i f_i(x), \quad x \in S$$

**Priority b:**  $a < b < c$

If all  $f_i(x) \geq \epsilon_i \forall i = 1, \dots, k$  and not all  $f_i(x) \geq \epsilon_i \forall i = l, \dots, m$

$$CWS(x) = \sum_{i=1}^m w_i f_i(x), \quad x \in S \quad (2.14)$$

**Priority c:** (lowest priority)

If all  $f_i(x) \geq \epsilon_i \forall i = 1, \dots, m$

$$CWS(x) = \sum_{i=1}^p w_i f_i(x), \quad x \in S$$

with  $w_i > 0$  for all  $i = 1, \dots, p$  and  $\sum_{i=1}^p w_i = 1$ .

Figure 2.5 illustrates the process of the CWS, using an optimization problem with two objectives  $f_1$  and  $f_2$  as an example. Here, objective  $f_2$  is in a higher priority group than  $f_1$ . Therefore the optimization initially aims to improve  $f_2$  only. The optimization of  $f_2$  is depicted with the red arrow. When the threshold  $\epsilon_2$  is reached, the optimization optimizes the WS of  $f_1$  and  $f_2$ . The black arrows represent the direction of optimization in the second step. As for the WS, it can be seen in Figure 2.5a that any point of a convex PF can be reached by the CWS. In Figure 2.5b, it

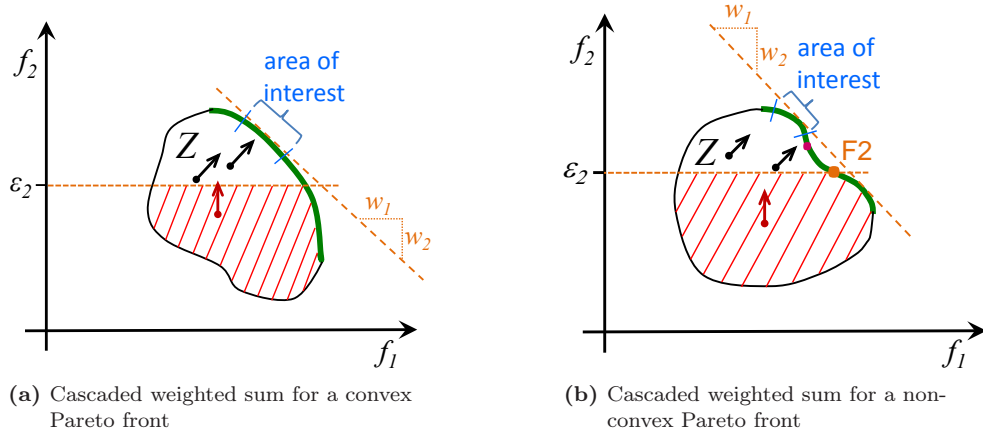


**Figure 2.5:** Cascaded weighted sum for convex and non-convex Pareto Fronts, adopted from [77]. Objective  $f_2$  is in a higher priority group than  $f_1$ ; therefore, initially, only  $f_2$  is optimized, which is illustrated with the red arrow. As soon as the threshold  $\epsilon_2$  is reached, the WS of  $f_1$  and  $f_2$  is optimized, represented by the black arrows.

is illustrated that using the CWS, it is also possible to reach an area of interest in the non-convex part of the PF.

## 2.5 Evolutionary Optimization

EAs are meta-heuristic optimization algorithms based on Darwin's evolutionary theory. There are many further meta-heuristics, such as simulated annealing, taboo search, and Particle Swarm Optimization (PSO). For the present thesis, only EAs are considered. They emerged from the evolutionary programming, genetic algorithms, and evolution strategies, which can be summarized as evolutionary computing [50]. A population of individuals is exposed to selection pressure. Each individual represents a solution to the optimization problem. Over the course of multiple generations, the solutions are adapted by applying genetic operators until a specific termination criterion is met. Figure 2.6 illustrates the schematic process of an EA. The individual steps are described below. [27]

### 2.5.1 Creating a Start Population

At the beginning of an optimization, a start population with a set amount of individuals is compiled. These individuals can be created entirely randomly or by integrating existing knowledge, e.g., using solutions of previous runs in some individuals. An individual, also called a chromosome, represents a solution in an encoded form. [27]

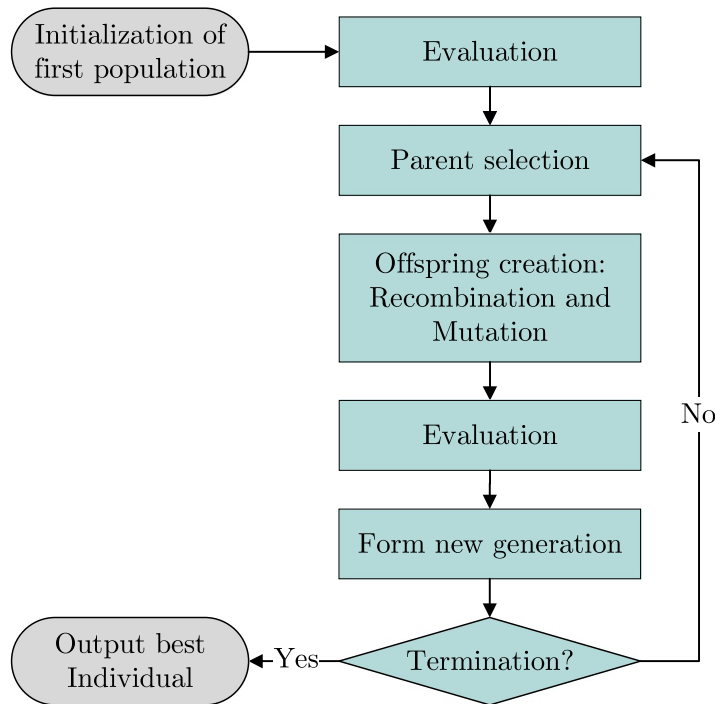
## 2.5.2 Encoding and Decoding

The gene model determines how a problem is coded into chromosomes. A chromosome is composed of genes [27], and each gene contains a set number of variables. Different types of genes can be allowed in the gene model, with the number of variables depending on the gene's type [76]. The value of a gene's variable is called an allele. The genetic information, which is the encoded form of a chromosome, is the genotype. This genotype is one individual in the decision space [38]. The decoded form and, therefore, the actual solution is called phenotype [27]. The phenotype is the acting representation of the genotype in the solution space [38].

**Table 2.2:** Exemplary chromosome for encoding a schedule for four DERs

	Gene 1	Gene 2	Gene 3	Gene 4	Gene 5	Gene 6	...	Gene n
<b>Unit ID</b>	2	1	2	4	3	1	...	3
<b>Start time</b>	3	2	1	5	2	1	...	3
<b>Duration</b>	5	1	5	2	1	4	...	6
<b>Power fraction</b>	0.2	0.3	0.6	0.4	0.5	0.2	...	0.1

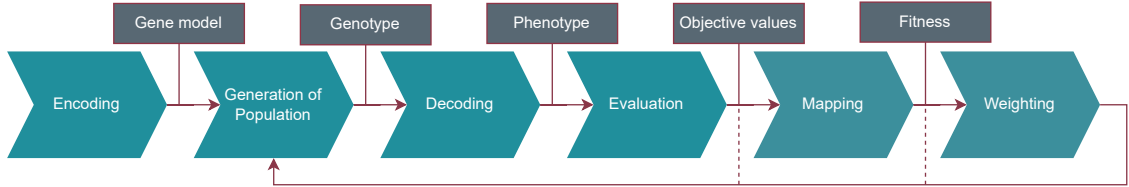
In the following, a scheduling problem comprising four DERs is used as an example for explaining encodings. The example is based on [83]. In this optimization problem, the challenge is to



**Figure 2.6:** Flowchart of an Evolutionary Algorithm, based on [27]

**Table 2.3:** Schedule resulting from decoding the chromosome shown in Table 2.2. The numbers highlighted in turquoise represent power fractions.

Time interval	1	2	3	4	5	6	7	8
Unit 1	0.2	0.2	0.2	0.2	0	0	0	0
Unit 2	0.6	0.6	0.6	0.6	0.6	0.2	0.2	0.2
Unit 3	0	0	0	0.5	0	0	0	0
Unit 4	0	0	0	0	0.4	0.4	0	0

**Figure 2.7:** Encoding and decoding within the evolutionary process

meet a power demand as accurately as possible for each time step. The problem is coded into chromosomes with genes. The gene model specifies one gene type with four variables. The first variable of each gene is the unit ID. It specifies to which unit the gene refers to. The following variables determine a time interval at which the unit operates at a specific power fraction. The time interval is set by a start time and a duration, corresponding to variables two and three. The power fraction is specified in the fourth variable. The gene model also specifies that the chromosomes contain a variable number of genes. Table 2.2 exemplarily shows a chromosome and, therefore, a genotype of a schedule of four DERs.

For the evaluation of the population, it is necessary to decode the chromosome. In decoding, every genotype is transposed into its corresponding phenotype. In this example, every chromosome is decoded into the schedule it represents. In the decoding process of the scheduling example, if an ID occurs more than once in a chromosome and the times overlap, the later gene overwrites the earlier one [83]. The resulting schedule or phenotype, thus, allows only limited conclusions to be drawn about the genotype. The general process is depicted in Figure 2.7. The dashed lines after the evaluation of the phenotype and the mapping from an objective value to a fitness symbolize that these steps only occur if the EA does not directly operate on the objective values. Furthermore, the weighting is only necessary if multiple objectives are taken into account.

The chromosome as a genotype shown in Table 2.2 is decoded into the phenotype as schedule shown in Table 2.3. The schedule of unit one corresponds to the exact decoding of gene six. Gene two, which also contains information about the first unit, is overwritten by gene six, as the time interval of gene two lies entirely within the time interval of gene six. Therefore, unit one runs from the time one to four with a power fraction of 0.2. The schedule of unit two results from decoding genes one and three, as both have the unit ID two. Here, gene three overwrites gene one partially, as the time intervals overlap partially. As a result, unit two runs from the

time one to five with a power fraction of 0.6 and from time six to eight with a power fraction of 0.2. Accordingly, the schedule of unit three results from decoding gene five, and the unit runs at time step four with a power fraction of 0.5. The schedule of unit four is only influenced by gene four. Therefore, unit four runs from time five to six with a power fraction of 0.4.

### 2.5.3 Evaluation and Fitness Functions

After decoding, the solutions are rated. In this example, for rating a schedule, the total power production of all units is calculated for each point in time, and the deviation from the target schedule is determined. The objective value of a solution or schedule is the overall deviation from the target schedule for all time steps. After determining the objective values, a fitness value is assigned to each solution [27], using mapping functions, which map objective values to fitness values [116]. In some cases the result of the considered objective function is directly used for rating the proposed solutions. This leads to the drawback that with MOOs problems, the objective functions are difficult to set in a reasonable relation. Therefore, the mapping to a fitness value is used. To create the mapping functions, it is necessary to estimate reference values or the boundary values of the objectives so that the best objective value is mapped to the maximum fitness value and the worst objective value is mapped to the minimum fitness value. A good estimation of the boundary values is essential for the well-functioning of the algorithm [70]. The influence of the boundary values is described in Section 3.4. In this case, zero deviation is the optimum and mapped to the highest fitness value. The maximum deviation is mapped to the lowest fitness value. The corresponding fitness values depend on the value range the utilized EA uses. The EA General Learning Evolutionary Algorithm and Method (GLEAM), for example, uses fitness values between 0 and 100000. Figure 2.8 shows two possible mapping functions that map deviations to fitness values.

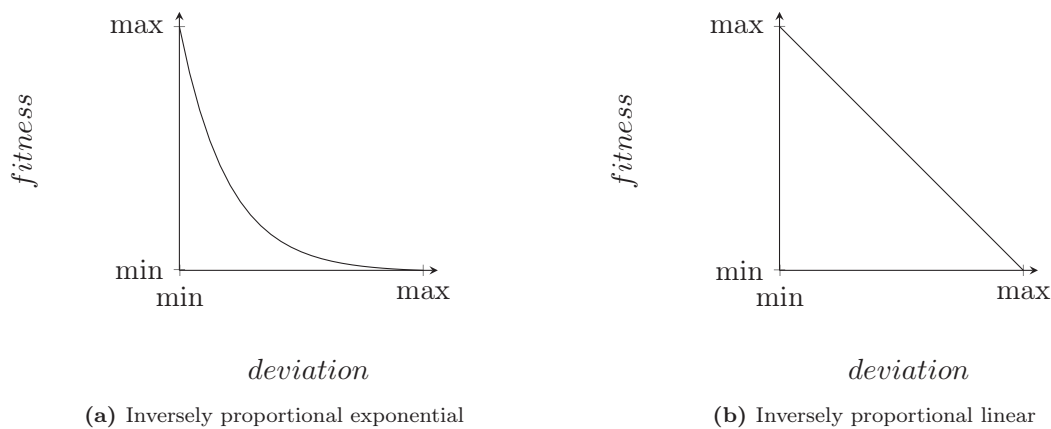


**Figure 2.8:** Examples of mapping functions

**Table 2.4:** Exemplary offspring generated with order based one point crossover

<b>Parent A</b>	Gene A.1	Gene A.2	Gene A.3	Gene A.4	Gene A.5	Gene A.6
<b>Parent B</b>	Gene B.1	Gene B.2	Gene B.3	Gene B.4	Gene B.5	Gene B.6
<b>Offspring 1</b>	Gene A.1	Gene A.2	Gene A.3	Gene A.4	Gene B.5	Gene B.6
<b>Offspring 2</b>	Gene B.1	Gene B.2	Gene B.3	Gene B.4	Gene A.5	Gene A.6

## 2.5.4 Creating Next Generation and Termination

The higher the fitness value of an individual, the higher the likelihood of being selected as a parent or to be part of the next generation [76]. After selecting parents, offspring are created by recombination and mutation [27]. Table 2.4 shows one kind of recombination, the one-point crossover. A crossover point is set randomly into the parents' chromosomes, dividing them into two parts [27]. In this example, the crossover point is set after the first four genes. The first offspring combines the first part of parent A and the second part of parent B. Accordingly, the second offspring is a combination of the first part of parent B and the second part of parent A.

To diversify the gene pool, offspring or clones of parents can be mutated. A mutation is a random change in chromosome. One way of mutation is a change in the alleles, the values of the variables of the genes [27]. In the example at hand, a possible mutation is a change in the start time of a gene. For instance, in the chromosome in Table 2.2, the start time of Gene three could be set from one to four. After the execution of genetic operations, all the individuals, namely offspring, parents, and mutants, are evaluated. Depending on the EA's acceptance rules, offspring are selected to form the next generation. A possible rule is to accept offspring only if they are better than their parents [27]. Accepting only a part of the offspring limits the number of individuals that need to be stored and evaluated.

Finally, termination criteria are checked [27]. If an individual's fitness exceeds a requested value, the best individual is issued as the solution, and the optimization process is terminated. If no individual is fit enough, further termination criteria, such as exceeding the maximum calculation time or stagnation in improvement, are checked. If no termination criterion is met, another generation is created and evaluated until a termination criterion is met. Note that the mentioned termination criteria are provided solely as examples based on [76], and alternative or supplementary criteria can also be utilized. Furthermore, termination criteria may also be checked before forming the new generation.



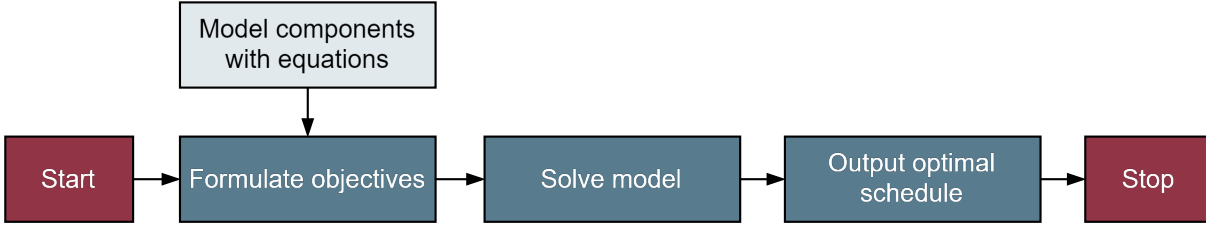


Figure 2.9: Optimization process with a MILP

## 2.6 Mixed Integer Linear and Quadratic Programming

In contrast to the EA presented in the previous section, the MILP represents an analytical approach for optimizing DERs. The MILP is a widely used and versatile form of integer programming. It extends the basic approach of Linear Programming (LP) to include integer and binary decision variables in addition to continuous variables. Unlike its LP counterpart, a MILP optimizes in addition a subset of decision variables being restricted to integer numbers, aside from linear objective functions. A further extension is described as Mixed Integer Quadratic Program (MIQP) that can handle problems containing quadratic objective functions. Describing components of an EH with linear functions might be too inaccurate or the objective function might utilize a quadratic error metric, such as the Root Mean Squared Error (RMSE). This example leads to a MIQP. The MILP uses linearized component models. These describe the relationship between the input and output of a component using linear equations. The interactions between the different components are also described by linear equations.

The general approach of the analytical optimization process is given in Figure 2.9. The general formulation is given by Equation (2.15) for a MILP

$$\min_x c^T x \quad \text{s.t.} \quad Ax \leq b \quad x, c \in \mathbb{R}^n, \quad (2.15)$$

where the vector  $c$  represents the coefficients of the objective function and matrix  $A$  the coefficients of the constraints. The vector  $b$  describes the right-hand side of the constraint inequality [20]. Equation (2.16) is the equivalent standard formulation for a MIQP with a quadratic objective function

$$\min_x \frac{1}{2} x^T Q x + c^T x \quad \text{s.t.} \quad Ax \leq b \quad x, c \in \mathbb{R}^n, \quad (2.16)$$

where  $Q$  is a symmetric matrix. [109]

Each component needs to be modelled as linear or quadratic equation. Furthermore, the objectives also must be formulated as linear or quadratic functions, according to Equation (2.15) or (2.16). To solve the equation system, commercial or open source solver are available with sufficient performance. As a popular framework for modelling a MILP or MIQP, Pyomo [33, 69] offers a wide range of solvers, e.g., Gurobi [67], a commercial solver. To assess whether an analytical or a heuristic approach for the scheduling problem of an EH is beneficial, a comparison of

of both is presented in Subsection 3.2.1 on basis of the specific optimization problem concerning the EH.

## 2.7 No Free Lunch Theorem

To decide, which algorithm is most suitable for the optimization problem of scheduling an EH, the No Free Lunch Theorem should be mentioned. According to [138], there is no optimization algorithm that outperforms another algorithm on all problem classes. More precise, when an algorithm gains in performance on one class of problems it offsets this gain by performing worse in all other problem classes. This is formulated in the following Equation (2.17) with  $P(d_m^y|f, m, a)$  as conditional probability of obtaining a sample  $d_m^y$ , which is a time-ordered set of evaluated solutions, if algorithm  $a$  is applied  $m$  times with the corresponding cost function  $f$  [54, 138]:

$$\sum_f P(d_m^y|f, m, a_1) = \sum_f P(d_m^y|f, m, a_2) \quad (2.17)$$

In [138] it is stated and proven, that for any performance measure  $\Phi(d_m^y)$  as average over all  $f$  of  $P(\Phi(d_m^y)|f, m, a)$  is independent from the chosen algorithm  $a$ . For the decision which optimization algorithm to chose for a certain class of problems this fact should be taken into account. Therefore, a comparison of two different algorithm is provided in the further course of this thesis. On one hand a classic MILP is set up for the scheduling problem and on the other hand a generic EA. As stated in the No Free Lunch Theorem, there is no best algorithm for solving every problem. But in turn, there are opportunities to enhance an optimization algorithm within one problem class by tailoring its behavior, which is presented later.

# 3 Schedule Optimization

In the following chapter, a deeper insight into the optimized scheduling is given. The problem can be defined as the scheduling of generation, storage and conversion units over a certain period of time with a defined resolution to accomplish several objectives [72]. Taking complex boundary conditions into account, this results in a large-scale non-linear optimization problem. To achieve intelligent control of the EHG, which is a specific instance of the EH concept and further described in Section 3.3, an EMS, as described in Section 2.3, is crucial. First, an overview of the general scheduling problem is provided and methods to solve this are described. Second, EHG is introduced by describing the setup of the system with a comparison of different methods and algorithms for optimization. Especially, the adaptability and scalability of the chosen method for optimization are of interest, because of the rapidly growing amount of DERs to be integrated into the grid infrastructure. Based on the work presented in [6] and further extended in [3, 2], this section is dedicated to give an answer to RQ 1: *To what extent can DERs be instrumented to provide flexibility and grid supporting service?* Finally, a method to dynamically adapt the mapping function is introduced to enhance the employed EA and address the identified limitations. This method is described in detail and evaluated in two different ways. First, the general performance of the algorithm is evaluated. Second, a positive side-effect is elaborated and described concerning the ability to adjust the weighting of multi-objective optimization.

## 3.1 Scheduling

Scheduling as a research area is motivated by the problem of allocating limited resources to activities over time [10]. It faces a virtually unlimited number of problem types. In general, a schedule is an allocation of one or more jobs to one or more machines [30]. Furthermore, this task is characterized by

- the jobs to be scheduled,
- the number and types of machines,
- possible constraints,
- and the evaluation criteria [40].

In the field of energy supply the job is to provide a certain amount of power at a specific point in time. Here, the power is one of the decision variables to be determined by a scheduling algorithm. The solution space can be restricted by constraints, which can be related to, e.g., the machine properties. The machines are the DERs to be scheduled. To find an optimal solution each schedule needs to be evaluated according to one or more evaluation criteria. This leads to either a Single Objective Optimization (SOO) or MOO problem as described in Section 2.4. The complexity of this optimization problem is studied widely and the scheduling tasks can be categorized according to [56]. According to [56, 30], scheduling of DERs is an NP-hard problem to solve because of the high dimensionality of the decision variables and the complex constraints.

It is crucial to enable the flexibility provision from DERs by optimized scheduling. Beside scheduling, the term "unit commitment" is common to describe the ability of a DER to deliver a planned amount of power and energy or to consume and convert it, respectively. The difference between Unit Commitment (UC) and the discussed scheduling is, among others, that UC only aims at the optimization of the operational costs. Scheduling, in the sense used throughout this thesis, offers the opportunity to consider various objectives while optimizing the planned operation of DERs. In the field of energy scheduling, different time constants are common to use. In case of scheduling DERs within an EH a 15 minute resolution is widely used based on the day ahead and spot market for electrical energy [48, 103, 135, 104, 98, 128]. Furthermore, flexibility for a preventive or curative congestion management is also conducted on a 15 minute basis. Additionally, the time horizon to be considered is usually 24 hours. Scheduling of EH's components can be calculated once for the coming day or repeatedly conducted for the next 24 hours to take new information about the grid infrastructure and RESs generation depending on weather conditions into account.

## 3.2 Methods for Optimized Scheduling of DERs

Various methods and algorithms are used for optimal scheduling of DERs to improve the system under consideration in terms of efficiency, performance, and further objectives. Several reviews on the optimization methods in context of the EH are given by [48, 103, 135, 104, 98, 128]. Analytical methods such as Priority List (PL), Dynamic Programming (DP), Lagrangian Relaxation (LR), LP, and Successive Linear Programming (SLP) have been employed to solve the problem since the 1960s [124]. More advanced methods such as Non-Linear Programming (NLP) and as a subclass Quadratic Programming (QP) have been developed to handle several of the faced challenges and to enhance the solutions for the UC problem. The main drawback of the aforementioned approaches is the limited capability to handle the high dimensionality and non-linearities of real-world scheduling problems. This drawback can be addressed by employing heuristic approaches. These algorithms are based on experience and rules to quickly find good solutions without performing a complete and exact search. Examples of heuristic algorithms

include Tabu Search, Simulated Annealing, and Ant Colony Optimization. In addition, PSO is gaining interest in the search for an adequate search algorithm according to [48]. This algorithm is based on the behavior of particles in nature. Each individual in the swarm (particle) has a position and velocity influenced by the best solutions found so far. Through interaction between particles, the swarm gradually converges to a near optimal solution. Furthermore, EAs belong to the category of heuristic algorithms. EAs are based on the principles of natural evolution and use genetic operations such as mutation and recombination to find optimal or near-optimal solutions, as described in Section 2.5. The main drawback of heuristic approaches is that they do not guarantee optimality. However, they can lead to near-optimal solutions in a reasonable time. Furthermore, at every iteration, they provide a valid solution that respects the boundary conditions or constraints. [31] These algorithms can be used individually or in combination to optimize the scheduling of DERs and ensure efficient resource utilization. The choice of suitable algorithm depends on the specific requirements of the system and the available data.

### 3.2.1 Comparison of MILP and EA

In [107] an EA is compared to a MILP in the context of unit commitment. It is stated that with highly-constrained use cases, the EA performs better than the presented MILP. Further applications of EAs can be found, e.g., in [119] and in the reviews conducted in [48, 128].

In the following the employed generic EA GLEAM for scheduling the DERs as components of an EH is compared to an equation-based approach. This comparison is conducted to underline the usefulness of heuristic approaches in general and EAs especially. According to [4] and as described in Section 2.6 a simplified model for the EHG and its components can be used to formulate a MILP or MIQP for the scheduling problem. The corresponding models are available as open source and further models can be found in [118]. It is stated that the simplifications are appropriate when having only a single objective function. The results show a good approximation with fast scheduling results by only taking the deviation between target schedule and scheduled electrical output of the EH, introduced in Equation 3.3, into account. However, if further objectives are considered, especially the minimization of the system operational costs as formulated in Equation 3.1 introduced in 3.3.7, the analytical approach is not able to handle the non-linearities introduced by, e.g., the electrical efficiency of the Polymer Electrolyte Membrane Electrolysis (PEM). This efficiency depends on the power fraction, the temperature and several other parameters as detailed in [142].

As depicted in Figure 3.1, the efficiency of a PEM changes with the current that is used to split  $H_2O$  into  $H_2$  and  $O_2$ . Assuming a constant voltage, the efficiency depends on the provided electrical power. For the objective function concerning the operational cost, given by Equation 3.1, this leads to a non-linear dependency between power input and  $H_2$  output and consequently to non-linear  $H_2$  generation costs. Especially at low partial load, the efficiency is highly variable.

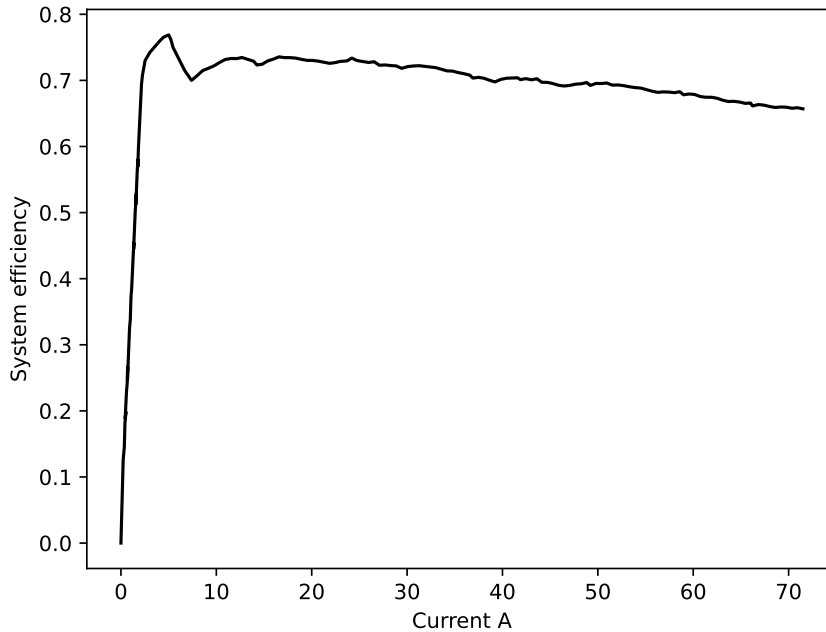


**Figure 3.1:** System efficiency of a 5 kW PEM electrolysis at partial load [142]

But also the difference between maximum efficiency ( $\approx 77\%$ ) at partial load to  $\approx 67\%$  at full load means a significant deviation in the generation costs for  $H_2$ .

However, the linear or quadratic approximation is a valid approach for optimization tasks where a fast re-calculation is necessary, e.g., within a rolling horizon optimization process. If the computing time is not the decisive factor to a certain extent, but the exact mapping of the system parameters is more important, the use of a heuristic optimization method, such as an EA, can be advantageous. Furthermore, as stated in [4], the configurability of a heuristic optimization approach is superior to that of the equation-based approach. For investigating several different EH compositions without losing accuracy the use of, e.g., an EA, is recommended.

### 3.3 The Energy Hub Gas

Parts of the following section are taken exactly from [6] and [3] and have been supplemented. First, selected EAs for optimization within the EH are compared. Then, the structure and functionality of the EHG as a representative of the EH concept is presented. As one instance of the EH concept presented in Section 2.1, the EHG is introduced. It lies a special emphasize on the provision of renewable energy carriers for hard to decarbonize sectors and applications. The general implementation is conducted according to [1] and illustrated by Figure 3.2.

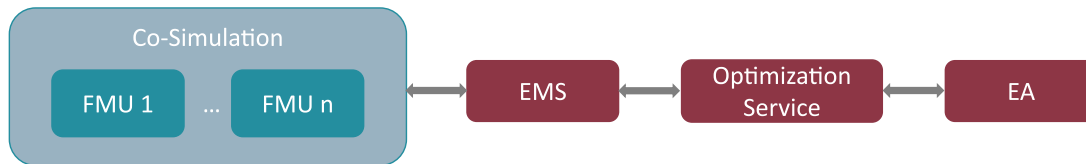


**Figure 3.2:** General simulation setup according to [1]

The different components are split into the co-simulation framework with its physical models formulated as FMUs, an EMS connected to an optimization service and the respective optimization algorithm. This modular approach allows for easy adaptation and replacement of the different components and algorithms and allows for the comparison of different approaches.

A schematic overview of the implemented system model is given in Figure 3.3. Further descriptions are provided in the following subsections, as well as a literature review of the relevant works concerning the EH concept and its implementations.

### 3.3.1 Related Work

In the following section, a brief overview of the related work in the field of co-simulation and CPES simulation is given to set the present approach for system modeling in relation to existing work.

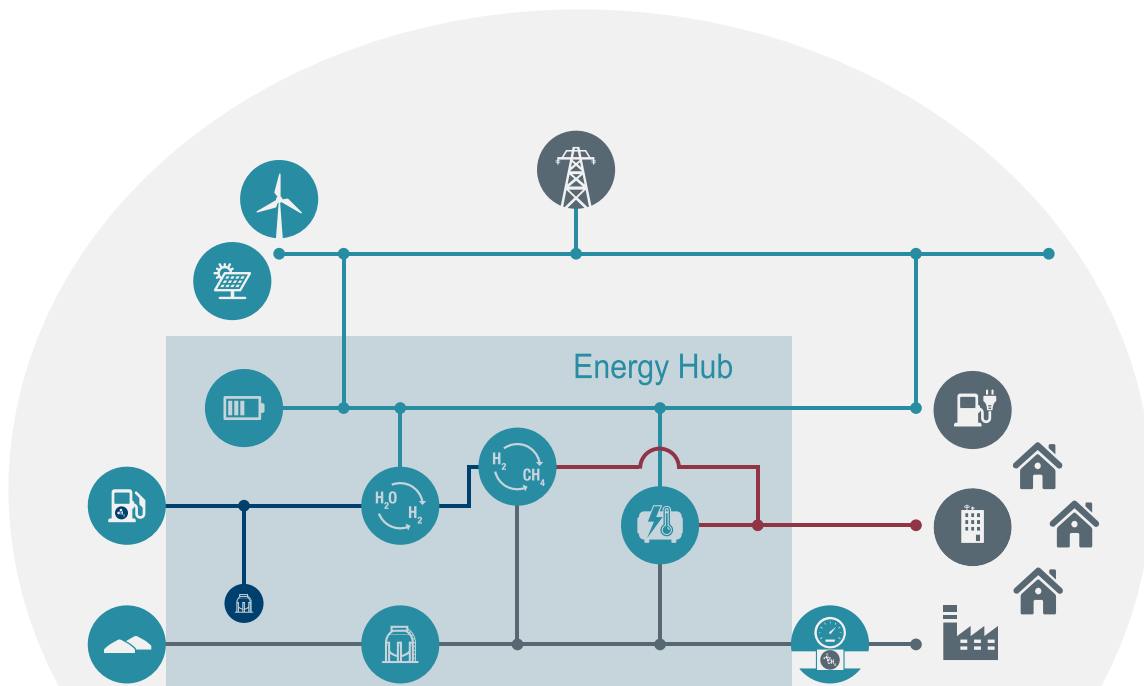


**Figure 3.3:** Energy Hub Gas Overview [6], a legend for the symbols is given in Tables 3.1 and 3.2

As further development of the approach in [5], the EHG concept utilizes a distributed system simulation model of a controllable modular set of technical plants. This system model interconnects electricity and gas supply with different final energy demand sectors (electricity, heat, fuel for mobility, chemical intermediate or commodity for industry) in a smart and flexible way, providing, e.g., utilities flexibility for grid operation. In contrast to [125], RES are considered but not included inside the EHG. [3]

Following the EH concept, RES based on weather are not controllable and thus, they cause the volatility that an EH could dampen to relieve the electricity grid.

The [presented approach] focuses on the modular design of the EH concept inspired by [59, 60, 57, 68], which allows adapting the model of the plant ecosystem to different settings of existing infrastructure and specific operational requirements. [... As suggested] in [103, 104], besides the main functionalities, the presented work considers local, sustainable mobility as fuel station hydrogen demand and connects to hydrogen pipeline infrastructure, resulting in a more diverse and realistic scenario.

In contrast to [126, 107, 42, 14, 113], for both gaseous energy carriers, the feed-in pathways are also considered and made economically feasible by introducing a compulsory green gas quota for gas suppliers [13]. The EHG participates in fulfilling this quota together with large-central upstream renewable gas feed-in and existing distributed biomethane feed-in. The controversial topics of green gas certification and "colors" for different hydrogen origins are thereby not considered and discussed as constraints. For the present work, climate-neutral gas shall be considered of non-fossil origin. Thereby, methane from the 3PM can be considered climate-neutral concerning the conversion process from hydrogen to methane. The positive correlation between low electricity prices, high renewable electricity feed-in, and the high need for feed-in management facilitates to hydrogen production with decreasing carbon footprint. Local heat demand is modeled to provide a more complete analysis of simulation data, especially regarding the level of integration and economic cost for flexibility.

The semantic description of the system and component behaviour and its extrinsic controllable interface are based on the hierarchical concept of DER modelling according to the IEC61850 standardization, especially part 7-420 with a focus on MDERs [39]. The central control logic for steering the internal plant network and allowing control, e.g., by utilities, is provided by an EMS utilizing this semantic model internally. It provides a lightweight communication interface where external control can be provided by implementing grid code behaviour in a modular fashion. The EMS covers the possible complexity of the investigated EHG instance by defining a modular plugin interface for integrating the control interfaces of, e.g., technical plants or components. It aggregates their abilities in a black-box fashion to a composed



mixed DER that is externally controllable. The provided control functionality for either TSOs or DSOs especially allows executing UC schedules on a DER[. This] can address re-dispatch 2.0 requirements for balancing generation and load[. Furthermore,] retrieving individual forecasting schedules of plants over 100 kW for planning [is possible]. Internally, the EMS uses, in contrast to [19], a multi-objective optimization method [that] converts the overall plant network schedule into an optimized set of schedules for each plant of the hub ecosystem. Thereby, the presented approach opens the opportunity to fulfill a wide range of configurable objectives to [adjust] the EHG operation to the local needs. [3]

### 3.3.2 Simulation Setup

As described in Section 2.2, the use of a co-simulation framework to investigate a multi-domain system is an advantageous approach. As a generic setup, the concept and corresponding system simulation model separate control and communication logic from the physical models of the technical plants in a modular fashion in contrast to [105]. With this, different components of the EHG system are represented either by FMUs or simulation models implemented in Python for generic control and communication behaviour. The presented implementation illustrates the advantages of this modular approach: The co-simulation framework enables the integration of different levels of details from various domains and different modeling languages. Furthermore,

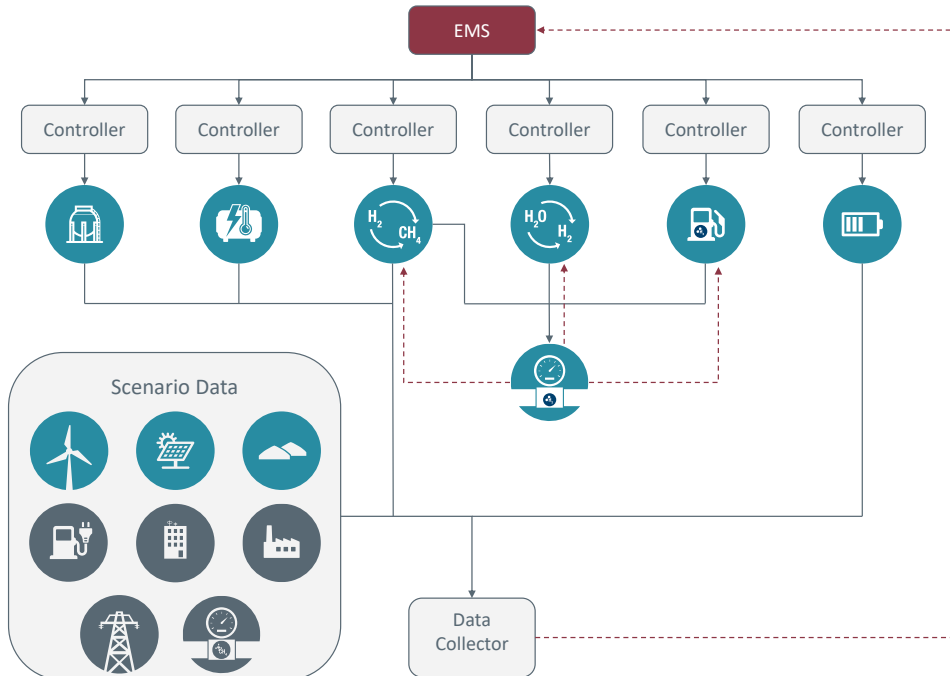


Figure 3.4: Energy Hub Gas simulation setup [6]

added features pose new sets of boundary conditions to the system and provide an opportunity to display advantages of the modular approach in both simulation setup and EMS. Finally, the modules are combined into a system model to set up a specific application environment using a distributed simulation runtime environment, which allows executing the model to perform different test cases for evaluation. To use component models from various domains and different modeling languages, a co-simulation framework needs to wrap the execution environment of the component model into a software layer that allows it to execute the model, and exchange input and output data. E.g., for executing the physical models, which were exported from Dymola according to the FMI standard [25], the co-simulation framework needs to implement a wrapper, which executes the FMU model as so called secondary models, and takes care of the data exchange between the co-simulation environment and the FMU secondary model. To connect the local co-simulation of the EHG to a distributed co-simulation with further infrastructure assets and, e.g., grid simulation, a message server is provided. As the purpose of the simulation lies within the time horizon of the operational planning, there is no need for real-time communication. The latency in the communication via a message server is therefore neglected. In contrast, the advantage of this architecture is the large amount of possible participants. Furthermore, asynchronous communication enables the distributed co-simulation to be executed independently. The general data flow of the simulation system follows the concept depicted in Figure 3.4. Blue arrows indicate direct data transmission within the same time step, whereas red dashed lines indicate an asynchronous connection, where data is transmitted in the subsequent time step. The EMS calculates schedules for all six facilities in this example and sends them to the respective controller instances. Each controller processes these schedules to a time series of single setpoint commands forwarded to the facility. A facility tries to follow these setpoints in compliance with its physical boundaries, resulting in a realistic behavioral trace of each facility. Outputs of the facilities are routed into the Data Collector, where they are finally processed and stored. [3]

Scenario data, such as RES generation, produces behavioral traces without controllers as they only react to the current simulation time and external data, e.g., weather conditions. They are modelled to provide the non-controllable energy outputs that the EHG needs to cope with and provide a holistic scenario.

Finally, the behavior of the hydrogen pipeline, which is added to the system and bidirectionally coupled with the methanation, electrolysis and H<sub>2</sub> gas station, has to be taken into account. The pipelines ensure energy conservation in the simulation system as methanation and gas station cannot consume hydrogen when the pressure of the pipeline falls under a given threshold, and respectively the electrolysis stops production when a pressure limit is surpassed. The modular, scalable, and extendable

setup allows to re-use, add, and parameterize individual component models within a system model and therefore, to easily create dedicated instances of the EHG for different application settings. This facilitates the configuration, evaluation, and usage of a specific EHG instance in different application environments and use cases. [3]



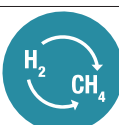



### 3.3.3 Component Models

The simulation setup in the present exemplary implementation contains component models for a PEM, a 3PM, a Combined Heat and Power Plant (CHP), a lithium-ion battery and a hydrogen supply unit for a hydrogen fuel station based on FMUs. “The FMUs are created in Dymola using Modelica. Furthermore, a methane storage implemented in Python is included. The models are based on technical parameters, e.g., nominal power. These parameters are provided in [Table 3.1] and are used for the internal optimization within the EMS.” [3] Furthermore, RESs, such as Wind Power Plants (WPPs), Photovoltaics (PVs) and Bio Gas Plants (BGPs), are included in the co-simulation system. As non-steerable demand for the different energy carriers electrical charging stations, typical households and industrial demand are modelled. Finally, the considered grid infrastructure, e.g., electrical grid and natural gas grid, provides information for the optimization process. The technical parameters for these models are given in Table 3.2.









Detailed electrochemical and thermodynamic processes are not part of the component models, but could be implemented due to the modular co-simulation framework. [...] Communication interfaces allow for communication in order to receive schedules from the EMS and to send relevant operating status to the Data Collector.

The sector coupling models CHP, PEM, and 3PM instrument key parameters for modeling conversion efficiency, systems dynamics, as well as minimum and maximum power. The conversion efficiency of the electrolysis is the ratio between specific power demand and corresponding hydrogen production [127]. The 3PM is assumed to convert hydrogen and carbon dioxide at the stoichiometric ratio of the methanation reaction [65]. The electrical efficiency of the CHP is taken from [106]. The system dynamics of CHP, PEM, and 3PM are modeled using characteristic start-up times from stand-by to full load. Information about the load status of the assets are sent to the Data Collector. The lithium-ion battery and the methane gas storage are modeled using parameters for capacity and maximum rate of charging and discharging [130]. Information about the current SOC is sent to the EMS as model output. The hydrogen supply unit is a gas buffer tank, which has to be completely loaded at certain times in order to be delivered to a gas fuel station. Charging times of the supply unit are scheduled by the EMS. [3]

**Table 3.1:** Technical parameters of the component models within the EHG

Parameter	Value	Symbol
Combined Heat and Power Plant		
Maximum power output	2 MW	
Minimal power output	0.7 MW	
Electrical efficiency	0.30 - 0.43	
Start-up time	120 s	
Polymer Electrolyte Membrane Electrolysis		
Maximum power input	1 MW	
Minimal power input	0.31 MW	
Efficiency coefficient	0 - 0.73	
Start-up time	60 s	
Three-phase Methanation		
Maximum production rate	65 kg h <sup>-1</sup>	
Minimum production rate	10 kg h <sup>-1</sup>	
Specific hydrogen demand	4 mol mol <sup>-1</sup>	
Start-up time	60 s	
Battery		
Capacity	3 MW h	
Maximum charge power	1 MW	
Maximum discharge	1 MW	
Charging efficiency	0.92	
Discharging efficiency	0.92	
Methane storage		
Capacity	1500 kg	
Maximum charge power	0.27 kg s <sup>-1</sup>	
Maximum discharge	0.27 kg s <sup>-1</sup>	
Hydrogen fuel station supply		
Maximum charge rate	1.8 kg h <sup>-1</sup>	
Time period of H <sub>2</sub> delivery	168 h	

**Table 3.2:** Technical parameters of the component models within the Scenario Data

Parameter	Value	Symbol
Wind Power Plant		
Maximum power output	2 MW	
Minimal power output	0.7 MW	
Photovoltaic		
Maximum power output	1 MW	
Bio Gas Plant		
Maximum production rate	65 kg h <sup>-1</sup>	
Minimum production rate	10 kg h <sup>-1</sup>	
Start-up time	60 s	
Charging Station		
Maximum charging power	0.15 MW	
Household Demand		
Maximum electrical demand	12.25 MW	
Maximum natural gas demand	12.2 MW	
Industrial Demand		
Maximum electrical demand	12.25 MW	
Maximum natural gas demand	12.2 MW	
Electricity Grid		
Price day ahead	Euro/MWh	
Power flow	MW	
Natural Gas Grid		
Price day ahead	Euro/MWh	
Power flow	MW	

### 3.3.4 Test Case Description

In order to use the framework described in the previous [Subsections] to answer research questions [in general], a methodical preparation of test and evaluation data for driving the simulation through use case scenarios related to research questions is required. In [137] a systematical assessment methodology is proposed that is applied to the presented EHG approach due to its holistic scope of the used energy carriers. A test environment emerges [...] by combining the specification of individual models, the scenario data<sup>1</sup>, and previously determined evaluation criteria. Within this test environment driven by the presented framework, raw data are generated to which the evaluation criteria are applied. [3]

With these results, the previously posed research question RQ 1, to what extent DERs can provide grid supporting service, and goal settings can be answered.

The separation of the individual data, models, and the framework has the advantage of allowing the flexible adaptation to a wide variety of use cases while at the same time ensuring comparability. [...] In [137] the test case description is divided into goal settings, operational strategy, system configuration, and scenario data.

As shown in Figure 3.5, the data needed for a complete simulation and evaluation cycle can be [formulated according] to the basic idea of an EHG presented in the previous [Subsection]. With the [...] input data, for example, global radiation from weather data, the simulation system converts it [...] to [...] the power generation by RES. The information [given] by the grid data is, for example the actual load without the EHG interacting. The [target schedule] is the interface for external authority, e.g., DSO or TSO, to make use of the offered flexibility from the EHG. In [this] example setting, the control value is an active power signal [split into] 15 minutes intervals according to the re-dispatch and day-ahead UC. Furthermore, the scenario data include price information for each considered energy carrier, for example, hydrogen, electricity, and natural gas. By extracting and directing the relevant information to the inputs of the EHG simulation model, respectively, the coupling matrix  $C$  from [Equation (2.1)], the raw data are calculated by the co-simulation system described in the previous [Subsection]. Each component model calculates independent results that need to be collected and analyzed. These results are summarized in the output vector  $L$  used to evaluate the results further. [3]

<sup>1</sup> Optimized Energy Hub Scheduling Using Evolutionary Algorithms - Supplementary Materials, 2024, doi: 10.35097/hubh72dd9d5mt43g

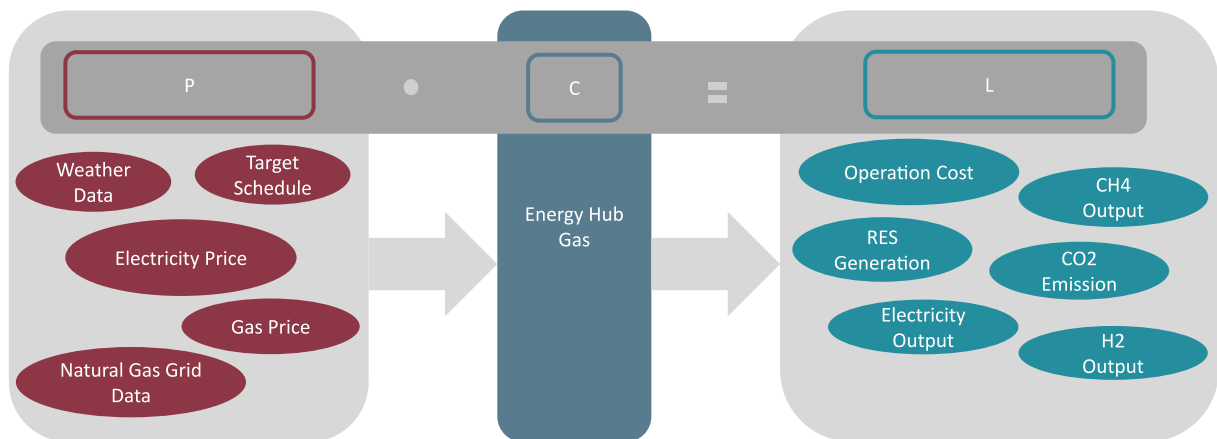


Figure 3.5: Test case data within the Energy Hub Gas system [6]

### 3.3.5 Industrial Area in Karlsruhe (Germany)

The first test case to investigate the presented system approach targets an industrial area in the south-west region of Germany[, the Campus North of the Karlsruhe Institute of Technology (KIT),] which is a characteristic region for high PV penetration. The considered time horizon [covers the year 2021]. Furthermore, the installed power of WPPs is relatively low compared to the northern part of Germany, which is considered in the second test case. In industrial areas, the load curve is dominated by a workday pattern, and the dependence on the outside air temperature is smaller. [3]

The characteristic load curve that is also used in the evaluation in Subsection 3.3.9 is depicted in Figure 3.6.

In Figure 3.7, the 20 kV electricity grid of the area of interest is illustrated, including the integrated EHG marked in red.

This leads to the test case that can be comprehensively described as follows:

**Goal setting:** Investigate how and to what extent the EHG system approach can help to reduce RE curtailment caused by feed-in management or congestion management. Thus, providing flexibility to attenuate grid variability is synonymous with integrating RES [and reducing the GHG emission]. Furthermore, the ability to provide flexibility and the amount of flexibility provided by the instantiated system model is of high interest. [... A] direct connection can be drawn to the possible substitution of fossil chemical basic molecules, e.g., methane.

**Operational strategy:** The operating strategy of the presented experimental setup aims to implement grid-serving control of the EHG with simultaneous cost-optimized use of its internal plants. The internal system structure is represented in a more abstract way and thus hidden by the EMS. Therefore, a schedule for the following

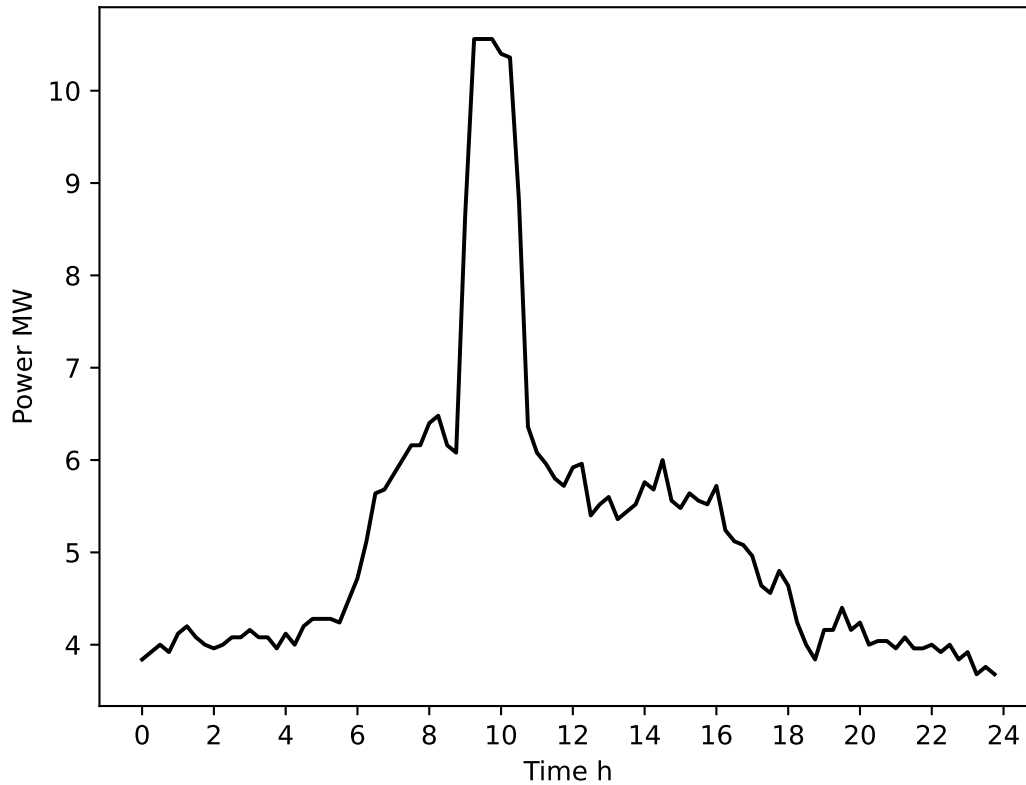


**Figure 3.6:** Load profile of an exemplary day for the industrial area for March 3<sup>rd</sup>, 2021

24 hours can be transmitted to the EMS to control the [...] EHG [in total. This schedule] is used to control the internal [DERs] in an optimized way. [...] The optimization target is on the one hand the operating costs of the EHG including expenses for CO<sub>2</sub> emissions and on the other hand the fulfillment of the external power demand by adjusting the components setpoints for their power output.

**System configuration:** The system configuration schema introduced in [Figure 3.3] consists of the EHG system model including the presented component models [(see Subsection 3.3.3)]. Furthermore, [...] the surrounding system into which the EHG model [...] is integrated, local [...] RES [...], local demand by industry, and regional mobility demand are [taken into account] by the scenario data. For TC1 the considered RES possess the following peak [megawatt (MW<sub>p</sub>)]: local PV plants with 10MW<sub>p</sub> and a single WPP with 2.5MW<sub>p</sub>.

**Scenario data:** To complete the set of information for a simulation and evaluation run, scenario data are needed. Weather data regarding solar irradiance and wind speed are used to determine renewable generated energy. These are available for TC1 as real-world data from measurements [collected] at the Campus North of the

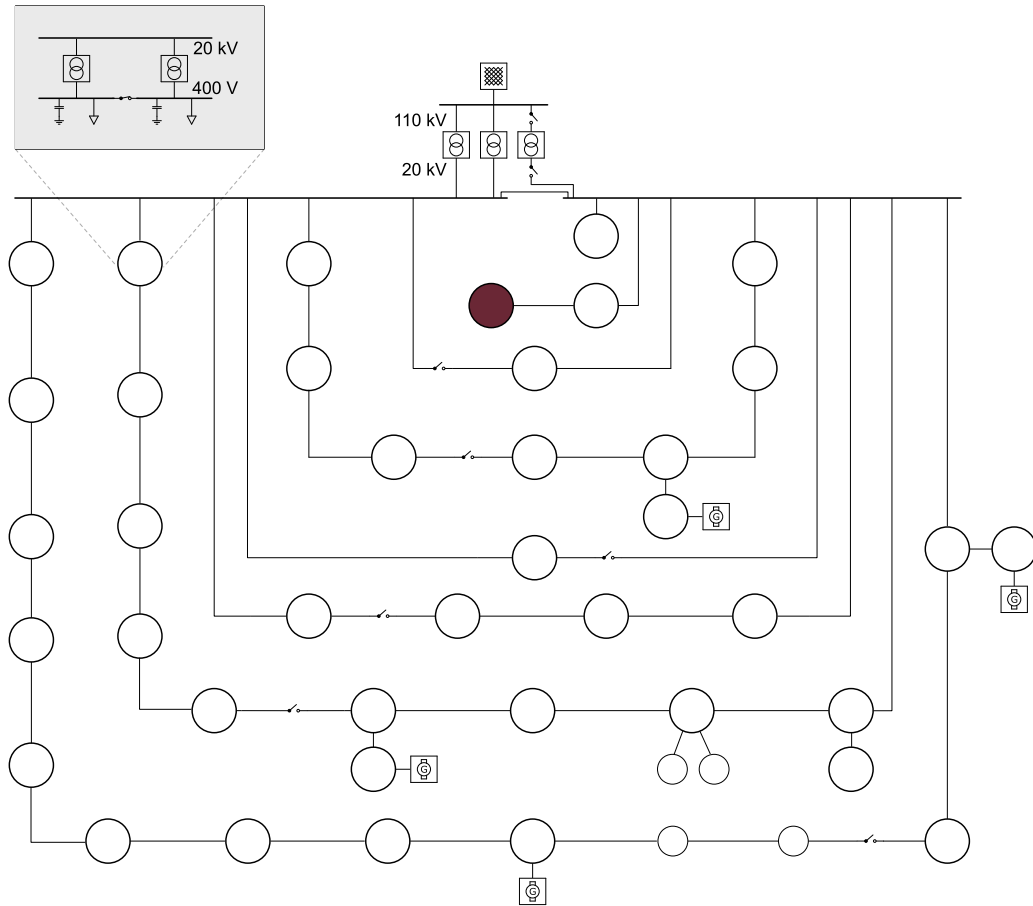


**Figure 3.7:** Single-Line Diagram of the 20 kV Grid of Campus North, KIT, where the EHG is integrated [2]

KIT. The price information for the period under consideration in 2021 has been prepared from publically available sources, e.g., Bundesnetzagentur (smard.de). The electricity prices are data from the EPEX SPOT day-ahead market. The prices for the other energy sources are average prices from 2021 and [are valid for] the entire period under consideration, as these are not traded on an intra-day market. The control signal, [which would be send by a network operator in a real-world application,] is based on a measured load series. A perfect forecast of the power flow for the next 24 hours is assumed in each case.

[3]

### 3.3.6 Industrial Area in Northern Germany

The second test case considers a location in the northern part of Germany close to the coast. This area [is characterized by] a high share of WPP generated RE in [combination] with low consumption. The amount of curtailed RE from WPP is of



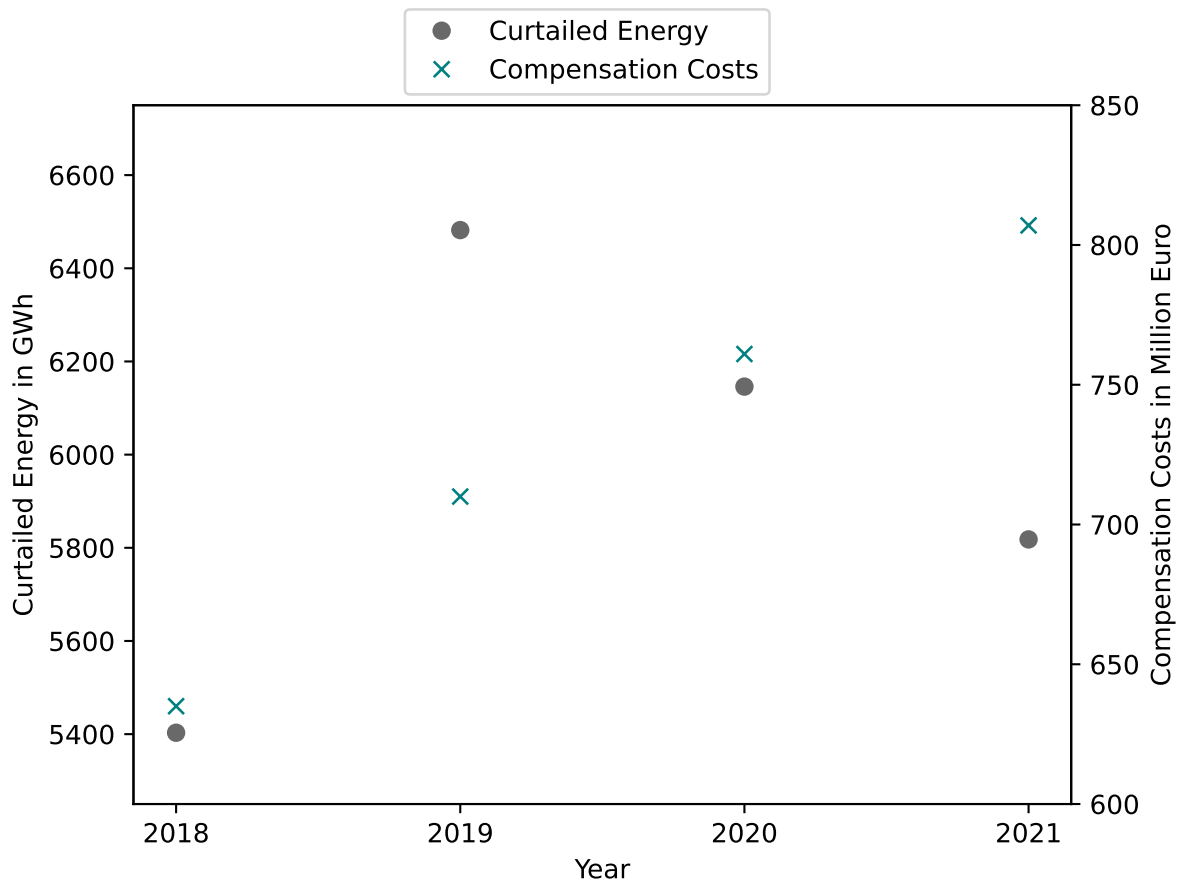


**Figure 3.8:** Curtailment in Germany and the respective compensation costs from 2018 to 2021 according to [32]

high interest for the operation of an EHG from an economic point of view, as well as for the society from an ecological point of view. [3]

The development of the curtailed energy from RESs and the compensation costs between the years 2018 and 2021 are depicted in Figure 3.8. Eventhough the curtailed energy varies between 5.400 GW h and 6.500 GW h, the corresponding compensation costs are continuously rising from nearly 650 million Euro in 2018 to over 800 million Euro in 2021. This reduction of electric energy from RES under feed-in management represents about 3% of the total generated RE [32]. Both, the lost RE and the immense cost related to feed-in management measures underline the need for flexibility provision, which the EHG can be part of.

The considered time horizon is the same as in TC1. This leads to the following test case description:

**Goal settings:** The avoidance of curtailment of RE is the primary goal since, on a coastal level [in Germany], there is significantly more generation by WPP than consumption [...]. Thus, the large transmission lines [from northern Germany to southern Germany] are to be relieved by transferring the RE to other sectors. At the

same time, the provision of renewable chemical energy sources offers an opportunity to reduce greenhouse gas emissions in different application areas.

**Operational strategy:** The operating strategy of the experimental setup presented aims to implement grid-serving control as described in TC1. With [internally generated and optimized schedules for the following 24 hours, considering the] external requests of utilities, the EMS offers flexibility to the DSO or TSO, [allowing the integration of] the fluctuating generation by RES [...]. The economic benefit of this operating strategy consists of two parts: First, selling the long-term storable energy carriers converted from RE [...]. Second, [generate] additional income [from the compensation payment the DSO or TSO must pay for curtailment under feed-in management to the RES operator]. The internal optimization target again consists of two objectives: First, the operational costs [...]. Second, the fulfillment of the external power demand [...].

**System configuration:** The system configuration for TC2 differs only in the considered RES [...]. The EHG system model including the same component models with the same rated power as in TC1 assumed to be located next to a RES farm with a PV plant with  $2.5 \text{ MW}_p$  and WPPs summarized to  $10 \text{ MW}_p$ . Furthermore, the local demand of industry and the regional mobility demands are identical to TC1.

**Scenario data:** Weather data is taken from measurements of the DWD in a 10-minute resolution. The control signal is adapted by calculating the possible renewable generation for the considered area. Furthermore, the same [price data] is used as in TC1. In addition, the same load curve of local industry is used.

[3]

### 3.3.7 Specification of the Optimization Problem

In the following subsection the general problem formulation concerning the EH scheduling problem is provided. The optimization can be conducted by regarding several objectives that can be configured upon the needs of the use case investigated. Depending on the application and perspective, the selected objective functions may complement or contradict each other. With regard to the different perspectives, the distinction between business and economic optimization should be mentioned here, for example, to illustrate with just one example that a flexibly configurable formulation of the objective functions is indeed useful. For the further course of the thesis three of the most common objectives in literature are considered: 1) system operational cost, 2) emissions, and 3) deviation from target schedule. These three objectives represent a combination of social and economic benefits and the profit of the DERs' operator. From a general perspective, both minimization for system operational cost and system emission are the same, as they punish an energy or mass flow with a price  $p_\alpha$ . Resulting in the minimization of operational cost

$$\min c_{operational} = \sum_t \sum_i \sum_\alpha P_\alpha^i(t) \cdot p_\alpha(t) \quad (3.1)$$

It is common in literature to separate the emission cost from the operational cost. The minimization of operational cost can generally be formulated as the sum over all time steps  $t$ , facilities  $i \in N$  and energy carriers  $\alpha \in \varepsilon$  as in Equation (3.1) with  $P_\alpha^i(t)$  the power flow, and  $p$  the price. In the same way the total cost of emission  $c_{CO_2}$  is formulated as sum over  $t$  for  $c_{CO_2}(t)$ , the cost of emission at each time step :

$$\begin{aligned} \min c_{CO_2} &= \sum_t c_{CO_2}(t) \\ &= \sum_t \dot{m}_{CO_2}(t) \cdot p_{CO_2}(t). \end{aligned} \quad (3.2)$$

Last, the deviation from the target schedule is integrated as RMSE in terms of

$$\min d_{rmse} = \sqrt{\frac{\sum_t^n (P_{EH}(t) - P_{target}(t))^2}{n}} \quad (3.3)$$

with  $P_{target}$  the demanded power of the target schedule provided by a grid operator and  $P_{EH}$  the total electric power flow of the system. For the EHG  $P_{EH}$  is the sum over all  $\alpha \in \varepsilon$ , considering only power flows that influence the electrical interconnection. The objective functions evaluate the generated energy and mass flow matrix and return a combined cost  $c = c_{operational} + c_{CO_2}$  in Euro, as well a value for the deviation from the target schedule  $d_{RMSE}$  in MW h.

### 3.3.8 Comparison of GLEAM and DEAP

As outlined in the Subsection 3.2.1, the application of an EA offers a range of benefits for solving the scheduling problem. For this purpose, in the following subsection two different EAs are applied and compared to identify a suitable algorithm for the further course of this thesis, namely the EA GLEAM and the Distributed Evolutionary Algorithms in Python (DEAP), a framework with several different EAs to use. Both are employed to optimize the schedules of different DERs within the context of an EH. These two frameworks have been selected because of their generic adaptability and wide range of parameterization abilities. Furthermore, both have proven in several studies that they are able to deliver good results. In addition, both frameworks offer parallelization to accelerate the optimization process. The comparison is conducted on both, a qualitative and quantitative basis. The qualitative comparison aims

**Table 3.3:** Comparison of GLEAM [75] and DEAP [43], employed settings are marked in bold

	GLEAM	DEAP
<b>General</b>		
Programming language	C	Python
Design purpose	generic with existing adaption to scheduling tasks	generic
Parallelization	BeeNestOpt.IAI [84]	SCOOP [111]
<b>Gene model</b>		
Chromosome length	adjustable, <b>120-240 (random)</b>	adjustable, <b>120-240 (random)</b>
Gene sequence	relevant for evolution and genotype-phenotype mapping	relevant only for genotype-phenotype mapping
Deme	applied, size = 8	-
segmentation	8 genes	-
Initialization	<b>random</b> , best, mix, best new	random
<b>Evolution</b>		
Mate selection	linear ranking	random
Offspring selection	always, local least, always-elitist, <b>local least elitist</b>	tournament, roulette, <b>NSGA2</b> , SPEA2, random, best, worst, tournamentDCD, double tournament
Crossover	7 pre-defined functions	13 predefined functions
Mutation	21 pre-defined functions	6 predefined functions
Maximum generation without acceptance in deme	40, adjustable	-
Maximum generation without enhancement in deme	200, adjustable	-
Stop criteria	fitness threshold	-
<b>Evaluation</b>		
Multi objectives	yes	yes
Weighting	<b>WS</b> , CWS	WS
Fitness mapping	linear, <b>exponential</b>	-

at general algorithm characteristics such as programming language, adaptability, and further parameters. The characteristics are listed in Table 3.3. The quantitative analysis compares the performance of both algorithms on the same scheduling problem, presented in the previous Subsection 3.3.7. Here, the optimization quality in terms of fitness and the calculation time are taken into account. The calculation time is compared by running the algorithm on the same machine with the same scheduling task without any parallelization method applied. The fitness can be compared as the mapping function of the objective values is identical in both implementations.

### 3.3.8.1 Qualitative Comparison

To compare the mentioned frameworks, GLEAM and DEAP, on a qualitative basis, first, the general features are described and listed in Table 3.3. Furthermore, the different gene models are described and the opportunities to modify these models within the investigated frameworks are discussed. Next, the evolutionary process including the genetic operators applied are presented in detail. Finally, the evaluation of the individuals of a generation is compared.

As listed in Table 3.3 the core algorithm of GLEAM is based on C, while DEAP and its implemented algorithms are Python code. Both algorithms are generally designed to serve a wide range of application and can therefore be categorized as generic. However, GLEAM has already been adapted to the scheduling problem and is therefore, ready to use for the problem faced in this thesis. DEAP, on the other hand, must be set up from the beginning and only provides the basic functionality of a generic EA.

Both frameworks offer a ready-to-use parallelization option. While GLEAM is extended by [84] to facilitate the parallelization options, DEAP is making use of the open source package Scalable Concurrent Operations in Python (SCOOP) [111]. GLEAM also provides a flexible application-oriented method to map

the decision variables and other degrees of freedom of the application to the genetic representation [26, 27], which is used in the [encoding] described [in Subsection 2.5.2 and adopted from [80, 83]]. The [...] framework [used] [82] is based on parallelization according to the coarse-grained or island population model [34]. Each island in turn uses a structured population based on the neighborhood or fine-grained model using a ring structure [63]. This combination of population models efficiently reduces the risk of premature convergence and allows a self-adaptive balance between breadth and depth search [64, 78]. Since the encoding used is based on dynamic length chromosomes [80, 82], the related genetic operators described in [80, 78, 26] are applied. For the island sub-population, a neighborhood size of 8 as used in most applications of GLEAM is employed [27]. [9]

As described in Subsection 2.5.2, the gene model is encoded by the use of four alleles: "Unit ID", "Start time", "Duration" and "Power fraction". This gene model is applied to both algorithms for comparing reasons. The length of each chromosome is dynamically changing between 120 and 240 genes. While the gene sequence is relevant to GLEAM for both, the evolutionary process and the genotype-phenotype mapping, to DEAP the sequence is just relevant for the genotype-phenotype mapping. For GLEAM the concept of demes, which represent isolated parts of the population, and segmetation of chromosomes is used to apply the genetic operators. Further details are given in [26].

### 3.3.8.2 Quantitative Comparison

The quantitative comparison of GLEAM and DEAP is conducted by applying both algorithms to the exact same problem instance. For the evaluation of their performance, the optimization results for an exemplary week from the year 2022 are compared. Both, the operational cost objective as well as RMSE objective which describes the approximation quality concerning the target schedule, as introduced in Subsection 3.3.7, are compared on the basis of the obtained fitness per day. DEAP is set up to use the Non-dominated Sorting Genetic Algorithm (NSGA2) [45, 47]. The parallelization options of both frameworks are neglected due to the fact that the focus of the comparison is on the optimization quality achieved after a given number of generations. The evaluation of the chromosomes provided by both algorithms is conducted by the EMS as depicted in Figure 3.2. The exponential mapping function used in GLEAM is adopted for DEAP to ensure comparability. Furthermore, the WS is parameterized with 60% RMSE objective and 40% operational cost objective. The fitness as WS per day of each optimization method is

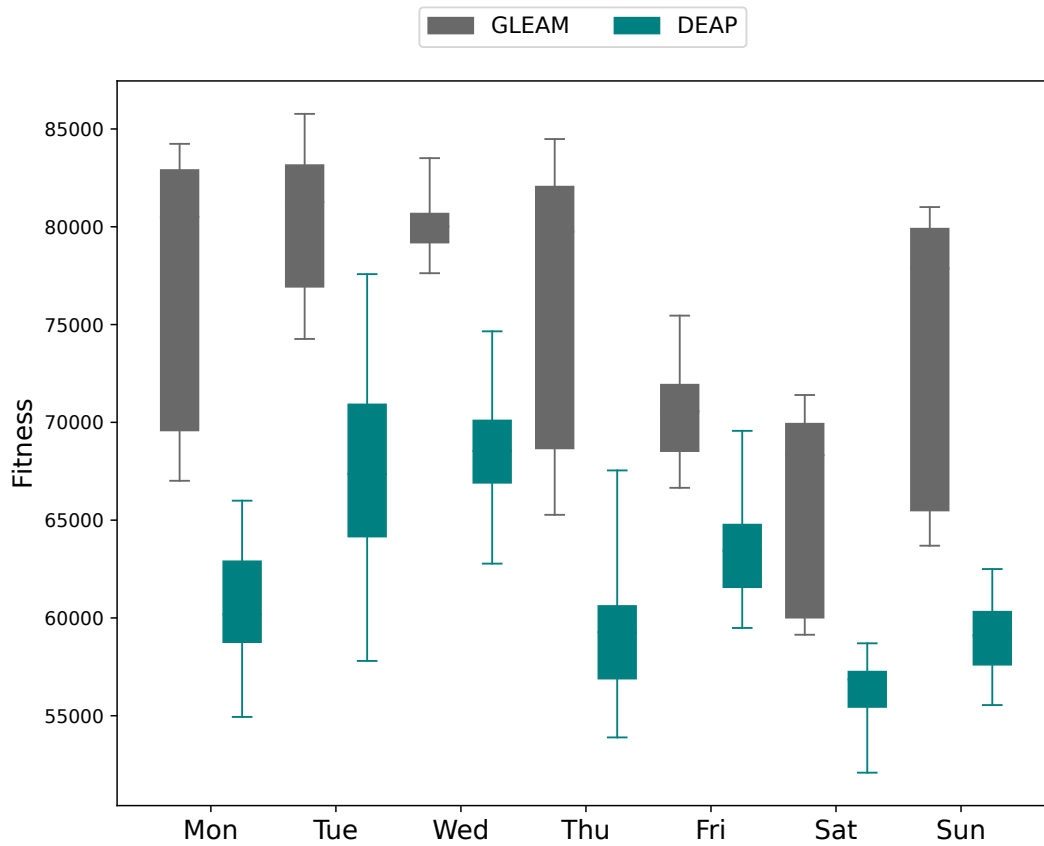


**Figure 3.9:** Boxplot of obtained fitness per day for comparing the two different heuristic algorithms GLEAM and DEAP

depicted in Figure 3.9. The upper fitness limit is set to 100000. The average fitness obtained throughout the presented week for GLEAM is 74397 and for DEAP 62068. Furthermore, GLEAM outperforms DEAP for every single day, while the differences between the days are similar except for Monday and Thursday, where GLEAM performs drastically better than DEAP.

Taking the calculation time into account, DEAP is five times faster than GLEAM. On one hand, DEAP generates less individuals to evaluate than GLEAM and on the other hand, only newly generated individuals are evaluated at DEAP instead of evaluating the complete generation as done at GLEAM. The evaluation of the entire generation is mandatory for GLEAM due to the evolutionary process using the concept of demes. The difference in the total number of individuals evaluated during evolution is caused by the differently applied genetic operators of each algorithm.

### 3.3.9 Evaluation of the Energy Hub Gas

The usefulness of the modular EHG concept is exemplarily evaluated for the two different test cases described in the previous Subsection 3.3.4. Two sets of evaluation criteria are used for the evaluation of the EHG operation: (a) In order to assess the EHG's ability to deliver flexibility in different time scales, a power spectral density analysis is performed. Short-term (minutes to a few hours) and mid-term (hours to a few days) flexibility provisions can be individually weighted and attribute different economic values to flexibility in different time scales. (b) Ecological (e.g., CO<sub>2</sub> reduction of provided final energy), economic (e.g., operational cost), and efficiency (e.g., conversion and storage energy losses) properties are assessed on the basis of the resulting power flows either with a Sankey-diagram or the analysis of exemplary load profiles. Furthermore, the attenuating effect of the EHG is evaluated by determining the percentage reduction of the difference between the minimum and maximum active power load with ( $\Delta P_{w/EH}$ ) and without ( $\Delta P_{w/oEH}$ ) the EHG interacting according to Equation (3.4) over one day. The reduction of exchanged energy in the considered grid segment is calculated to emphasize the potential for installing additional RESs, measured in nominal power, that again would increase the volatility.

[3]

$$\frac{\Delta P_{w/oEH} - \Delta P_{w/EH}}{\Delta P_{w/oEH}} = \% P_{deviation} \quad (3.4)$$

“For the evaluation of the simulation results, exemplary days are considered that show the impact of the EHG particularly clear. In addition, the entire period is evaluated in order to illustrate the grid-serving operation of the decentralized plant network.” [3] In accordance to the comparison described in Subsection 3.3.8, GLEAM is used as optimization algorithm.

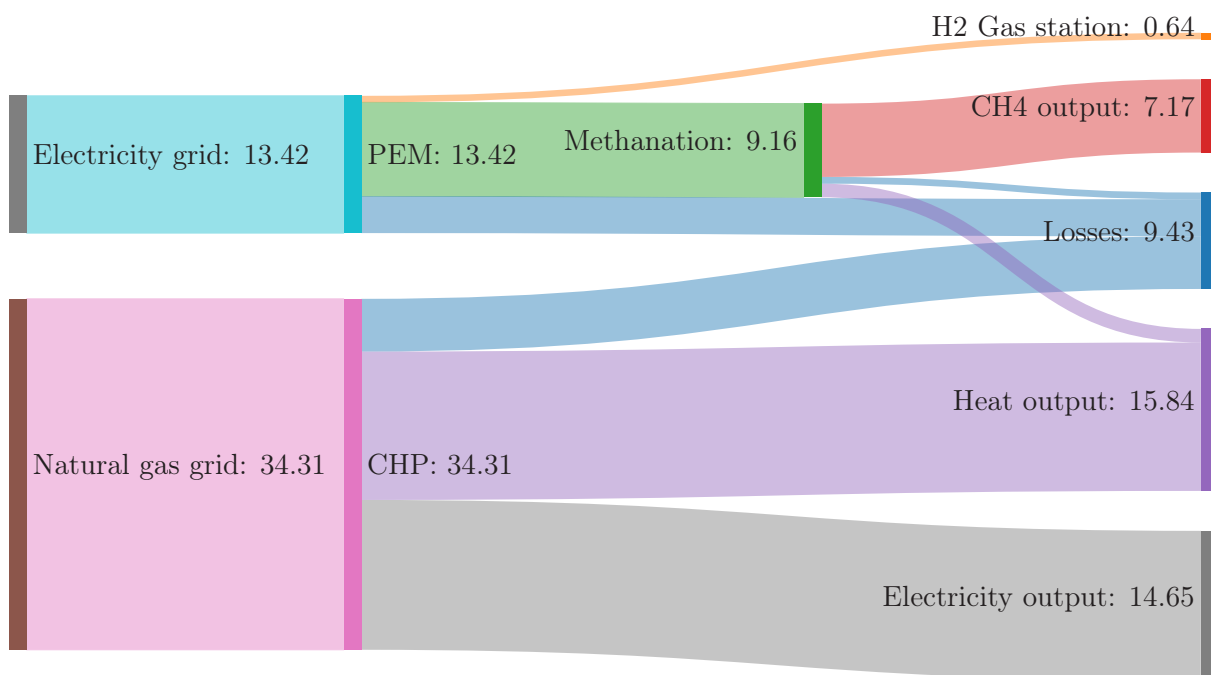
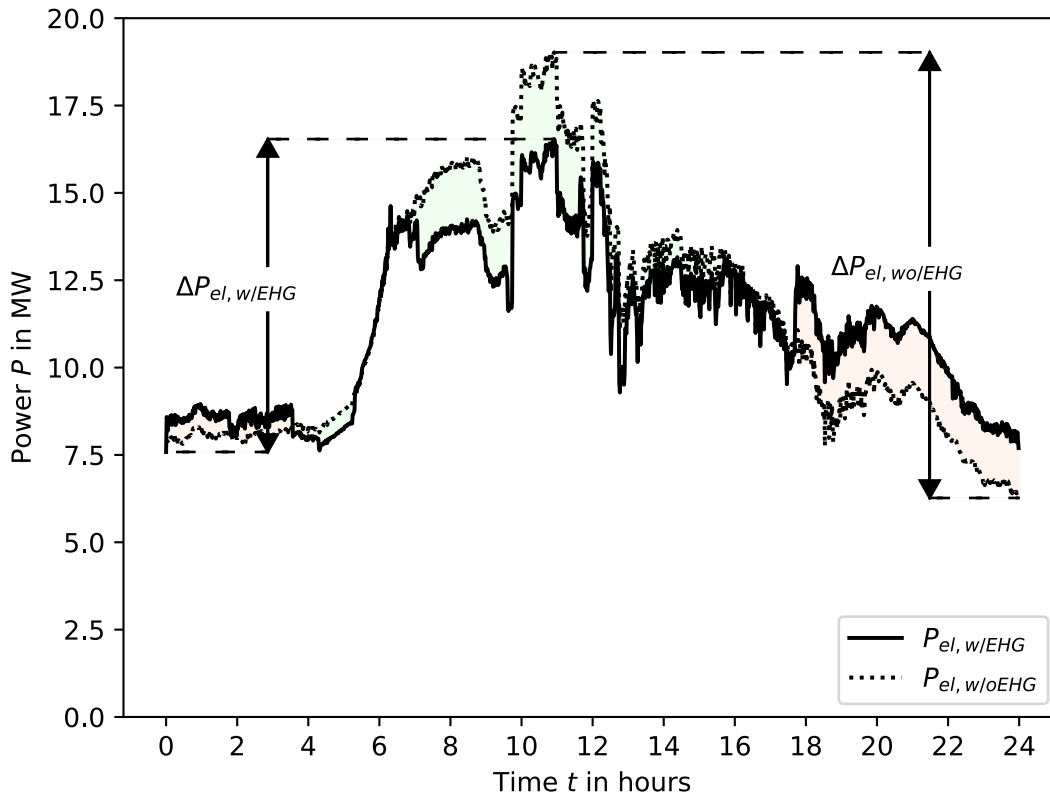


Figure 3.10: Energy flow chart in MW h for March 3<sup>rd</sup>, 2021 [3]

### 3.3.9.1 Test Case One

With TC1, the ability of the EHG to provide renewable chemical energy carriers to sectors where the processes are difficult or expensive to electrify is evaluated. The industrial area in TC1 described in the previous section with its demand for chemical energy carriers can be supplied with the energy flows shown in [Figure 3.10]. Depicted are the energy flows, including the conversion paths of the individual energy sources on March 3, 2021 including the total losses (9.4 MW h) due to conversion efficiencies. It is depicted that around 13.4 MW h of electrical energy is converted to around 9.2 MW h hydrogen that is further processed to around 7.2 MW h methane and 0.6 MW h hydrogen for the gas station. About 2.0 MW h are either used as heat energy or summed up within the total losses. By replacing about 7.2 MW h of natural gas with renewable methane, approximately 1.45 t of CO<sub>2</sub> emissions can be avoided. Most of the energy is [...] sourced from the natural gas grid and converted to electrical power and heat by the CHP. However, the fluctuation in the electrical grid can be used to [provide] other chemical energy carriers from renewable energy, for example, hydrogen. A total amount of [32.5 t] of hydrogen is produced under the grid-supporting operation conditions over the entire simulation period of [one year as reported in Table 3.4]. By selling this product as green hydrogen, ignoring possible uncertainties or [costs related] to certification, a revenue of around [186 000 EUR], according to the price of green hydrogen calculated by [11], could be achieved. [3]





**Figure 3.11:** Resulting power w/ and w/o EHG interacting at March 3<sup>rd</sup>, 2021 [3]

Taking the complete simulation into account, the average exchanged energy is reduced by 7.2% which results in a reduction of around 17.8 MWh per day for the overlaying transportation grid.

A more detailed look into the electrical energy [...] is given in [Figure 3.11]. Here, the electrical load profile at the ECP with and without the EHG interaction is shown. Negative values, which do not occur in this case, would mean backfeeding into the transmission grid level. The attenuating potential of the EHG can be quantified for the considered date by a reduction of 29.8% concerning the maximum power variation

**Table 3.4:** Summary of the results for TC1 over the complete year 2021

Parameter	Value
Average $P_{deviation}$	11.6%
Relative electrical energy exchange reduction	7.2%
Total electrical energy exchange reduction	6497 MWh
Produced $H_2$	32.5 t

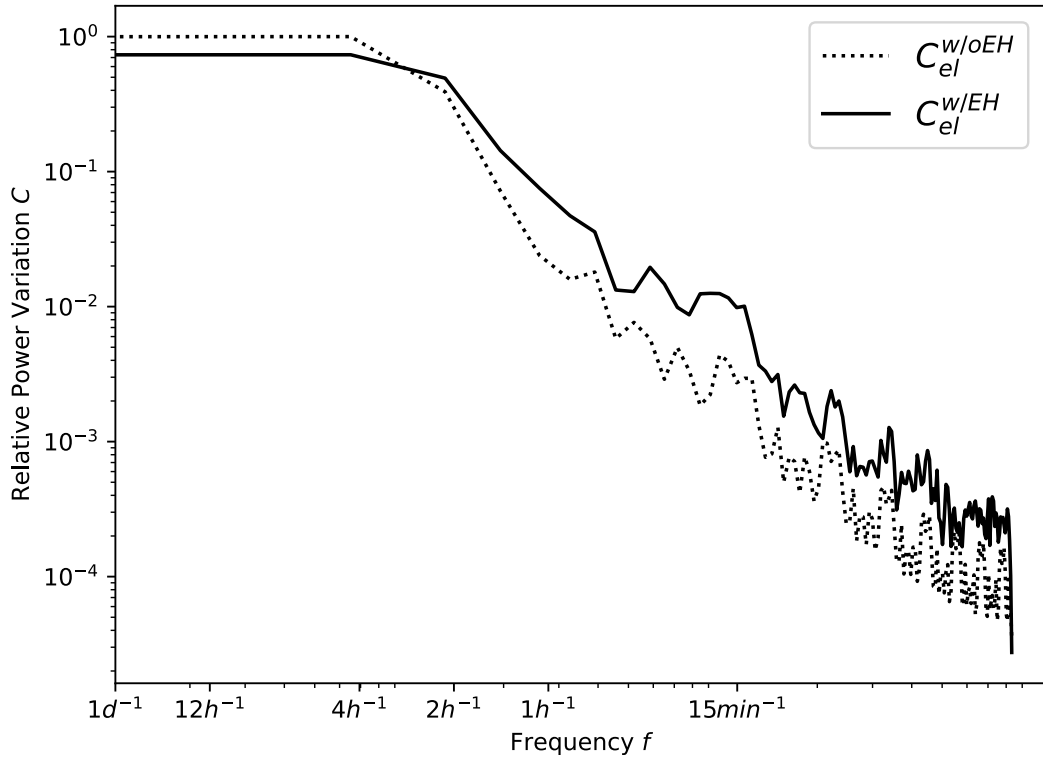


**Figure 3.12:** Power Spectral Density (PSD) of the power flow w/ and w/o the EHG on March 3<sup>rd</sup>, 2021 [3]

over the course of one day according to [Equation (3.4)]. This relieves the existing grid infrastructure and opens the possibility for additional RESs. If the entire simulation period [...] is considered, the average attenuation through the EHG is 11.6%.

To evaluate the [...] provided flexibility and hence the electricity grid supporting effort the EHG can achieve, a PSD analysis is conducted and shown in [Figure 3.12]. The relative power variation  $c$  with and without the EHG interacting is depicted over the frequency  $f$  for March 3<sup>rd</sup>, 2021. The solid line depicts the power variation with the EHG interacting. For a frequency of  $2h^{-1}$  or lower, the EHG can reduce the fluctuation. Around frequencies of  $15\text{ min}^{-1}$  the power variation is even increased which in combination indicates that the flexibility provision by the presented EHG instance is only useful for longer time periods. [3]

### 3.3.9.2 Test Case Two

In TC2 the evaluation is focused on the [goal] of relieving the grid infrastructure for increasing renewable feed-in. Therefore, an exemplary load curve from 25<sup>th</sup> of February, 2021, is evaluated and shown in [Figure 3.13]. The power flow within the considered grid segment is depicted with and without the EHG interacting. A

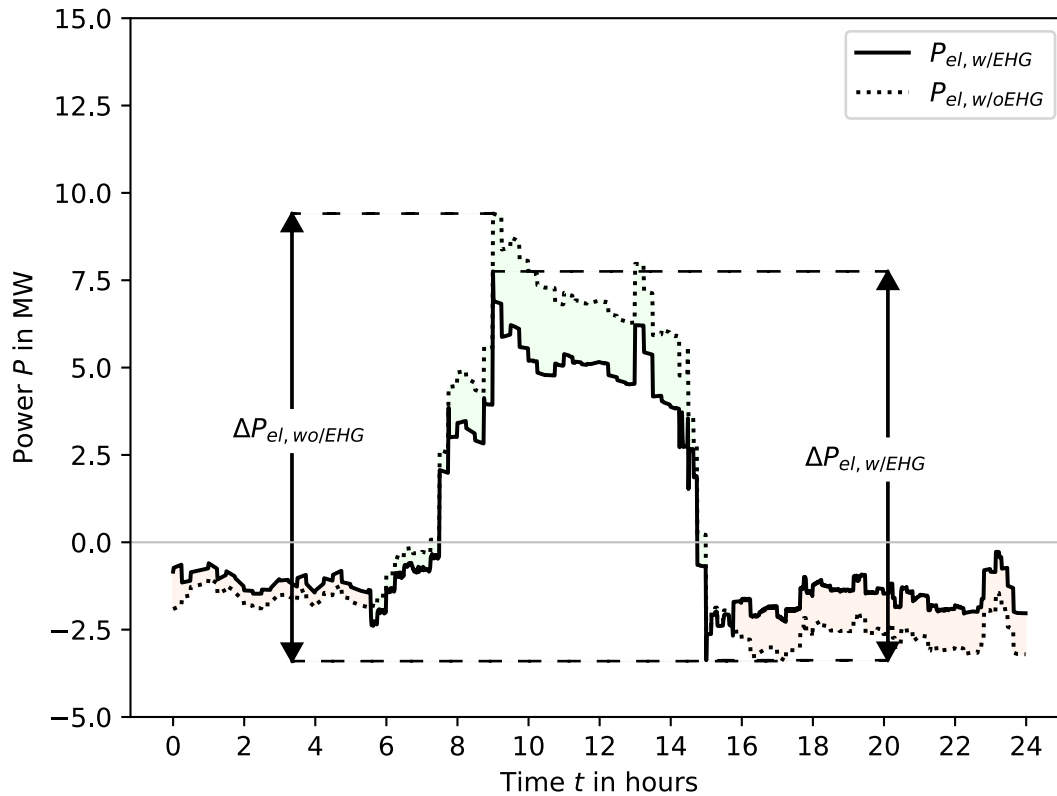


**Figure 3.13:** Resulting power w/ and w/o EHG interacting on February 25<sup>th</sup>, 2021 [3]

reduction by 13.1% is achieved concerning the difference between maximum load and maximum feed-in according to [Equation (3.4)]. [3]

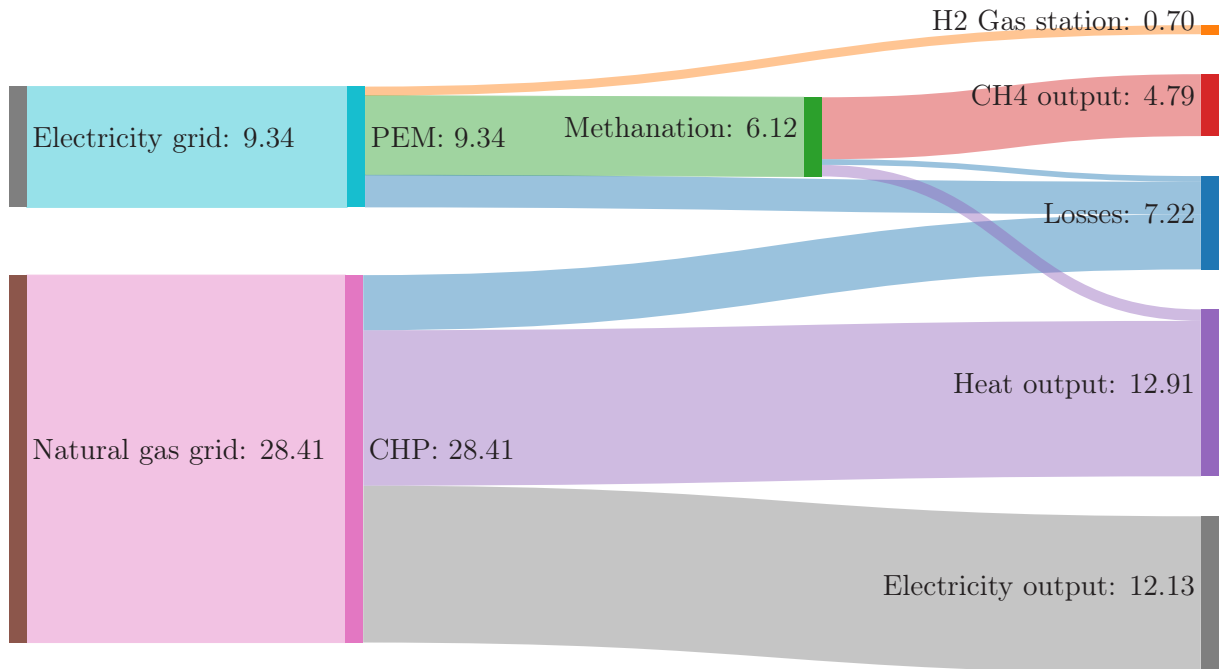
Furthermore, the energy exchanged within the evaluated day at the ECP is abated by 30.2%. The colored areas in [Figure 3.13] mark the positive (green) and negative (red) power adjustments achieved by the EHG interacting and resulting in a total reduction of 24.8 MW h within one day. The red area in [Figure 3.13] describes the additional load caused by the EHG to convert electrical power to hydrogen for either direct use or further processing within the methanation. The total additional load summarized over the evaluated day is 11.98 MW h. This reduction, in combination with the attenuated load curve, offers the opportunity to install additional RESs or integrate existing but curtailed RESs on the same scale without extending the grid infrastructure. Using the curtailed energy, there is a potential reduction in CO<sub>2</sub> emission of around [4.7 t] within the considered day according to the emission coefficients

**Table 3.5:** Summary of the results for TC2 over the complete year 2021

Parameter	Value
Average attenuation at ECP	4.9%
Relative electrical energy exchange reduction	7.7%
Total electrical energy exchange reduction	4417 MW h
Produced $H_2$	46.7 t

[(395 g/kWh) given by [52]]. Furthermore, the average compensation paid by utilities to RES operators for curtailment under feed-in management is 124 EUR/MWh according to [32], which results in additional revenues of around 1485 EUR. [3]

At the same time, the amount of green hydrogen or methane provided by the EHG by using this energy, which would be curtailed, results in additional income. The evaluation of the entire simulation period of [one year, reported in Table 3.5], shows an average reduction of power fluctuation by 4.9%. Furthermore, the average energy exchanged at the ECP is reduced by 7.7% [resulting in a total amount of 4417 MW h. The production of hydrogen accumulates to 46.7 t for the entire year.] [3]

**Figure 3.14:** Energy flow chart in MW h for February 25<sup>th</sup>, 2021 [3]

The energy depicted by the colored areas in [Figure 3.13] is converted and conditioned as shown in more details in [Figure 3.14]. Depicted are the energy flows, including the conversion paths of the individual energy sources on February 25, 2021 including

the total losses of around 7.2 MW h due to conversion [inefficiencies]. It is depicted that around 9.3 MW h of electrical energy is converted to around 6.8 MW h hydrogen that is further processed to around 4.8 MW h methane and 0.7 MW h hydrogen for the gas station. As in TC1, most of the energy is sourced from the natural gas grid (28.4 MW h) and converted to electrical power (12.1 MW h) and heat (12.9 MW h) by the CHP. [3]

To assess the [...] flexibility provision and hence the electricity grid supporting service the EHG can deliver, a PSD analysis is conducted. [Figure 3.15] shows the relative power variation  $c$  with and without the EHG interacting over the frequency  $f$  for the evaluated day. The solid line depicts the power variation with the EHG trying to follow the schedule provided by the grid operator. For a frequency of  $1h^{-1}$  or lower, the EHG can reduce the fluctuation, but within higher frequencies, there is no effect on the power variation. Although the EHG is equipped with components that technically can adjust their power in the frequency range of seconds, [in the present co-simulation framework it is not possible to make use of this to reduce the power variation]. [3]

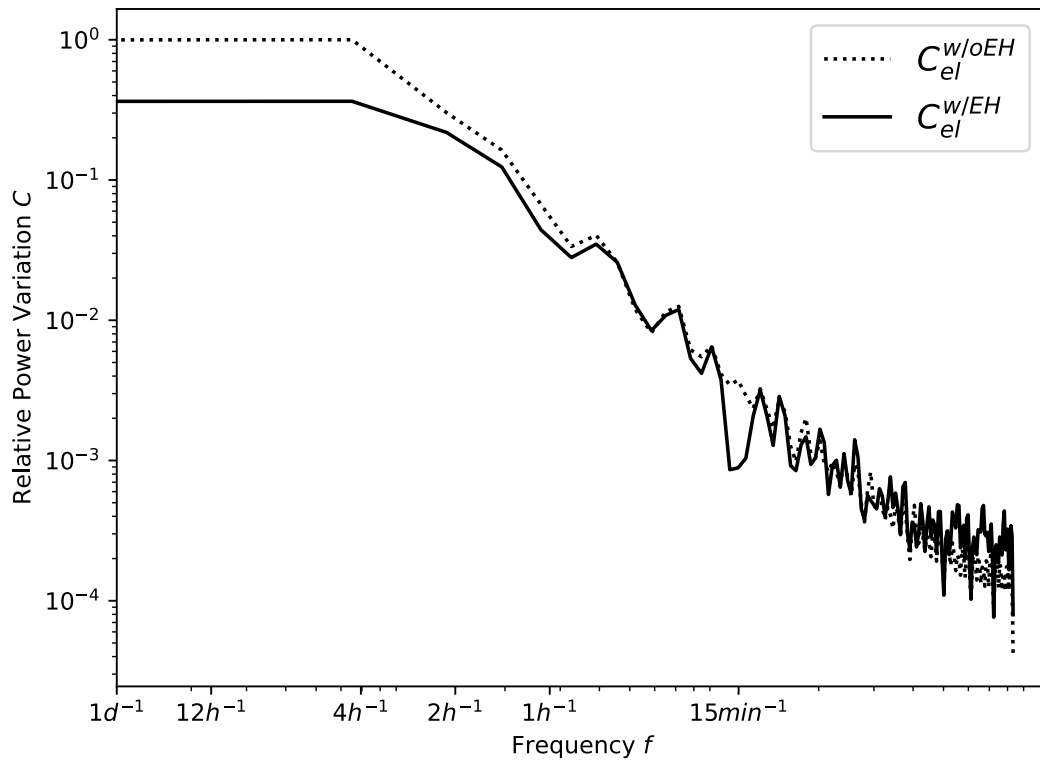


**Figure 3.15:** PSD of the power flow w/ and w/o the EHG on February 25<sup>th</sup>, 2021 [3]

## 3.4 Dynamic Fitness Mapping for EA-based Optimization

Parts of the following section are taken exactly from [8] and have been supplemented. The large number of plants, the large number of decision variables and the tracking of different objective functions represent a suitable optimization problem for EAs, as elaborated in the previous Subsection 3.2.1 and stated in [107, 83, 80, 17, 31]. “Many of the EAs employed use a normalized mapping of the objective values to corresponding fitness values to apply their particular evolution strategy in order to serve a wide range of applications and especially for the optimization of multiple objectives [27].” [8]

The functional relationship between an objective value and the fitness can be defined in different ways. A common practice is the use of an exponential function[, as depicted in [Figure 3.16].] This allows the gradient of the fitness to increase with increasing quality of the proposed solutions, in order to foster the search process of the employed EA. The disadvantage of this mapping function is that individual

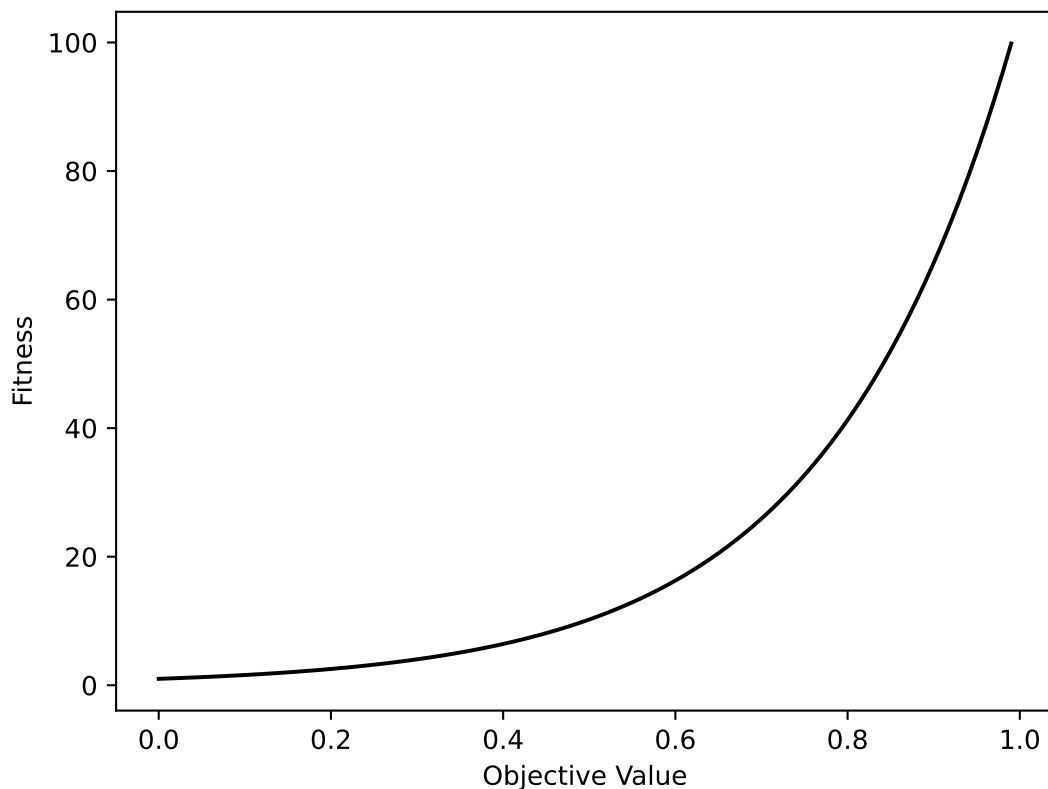


Figure 3.16: Exemplary mapping function for EAs

objective functions can be neglected in MOO tasks if they are very far from the optimum [and the gradient is rather small]. [8]

In this case, a change in the objective value results in a small gain or loss for the respective fitness. More generally speaking, the EA is less sensitive at low objective values.

Furthermore, the mapping is used to normalize different objectives to combine them within a MOO.

This mapping function and the boundary values that define the fitness range within which the proposed solutions are evaluated, play a decisive role in the search for the best possible solution within a complex search space [27]. If the boundary values for the translation into fitness are poorly chosen, it is difficult for the EA to find a good solution when searching the solution space. [8]

“Whether an objective value is neglected due to the mapping function is significantly influenced by boundary values of the defined exponential mapping function. This leads to the fact that the determination of these boundary values [is crucial].” [8] “Unfortunately, expert knowledge is required to determine these boundary values, or it may even be impossible to determine them at all in advance.” [8]

So far, there are different approaches to deal with this challenge. As a simple attempt, an average achievable value can be used, as in previous works [5, 6]. However, this neglects the different possibilities, depending on the optimization task. To address this challenge, a concept for dynamic evaluation of objective functions is presented in the [following Sections]. [8]

“In addition, in the field of [DER] scheduling, the possible boundary values change depending on the time and the given surrounding conditions. Thus, to address this challenge, a dynamic adaptation of the mapping function to the optimization task at hand is needed.” [8]

### 3.4.1 Related Work

“[... S]everal studies have addressed dynamic optimization problems using EAs.” [8] Real-world applications of EAs often face dynamic changes by nature since the objectives, some of the environmental settings or parameters may vary over time [28].

In [the] literature, the term mostly refers to optimization problems with a changing fitness landscape during evolution. Jiang et al. provide a survey of different works [81]. In the present work, the fitness landscape does not change during evolution, but between [different problem instances, respective different] optimizations of schedules for each day. This poses the problem of the dynamic calculation of the reference

values for each optimization [run]. Tracking of moving optima during evolution is not necessary.

In MOO many approaches do not explicitly calculate fitness values, but normalize objectives and choose the best individuals according to normalized and aggregated objectives. In [85], an overview of [different] MOO approaches for fitness calculation and normalization using genetic algorithms, a subcategory of EAs, is provided. Regardless of whether the objective functions are normalized or a mapping function is used, reference values are necessary. A description of how reference values are used to create mapping functions can be found in [Subsection 3.4.2].

For many optimization problems, the range of objective values, respective the boundary values, is not known before optimization [134]. Hence, boundary values are often calculated during evolution. A common approach to estimate the reference points during evolution is to use the objective values of the current population. Accordingly, the best objective values of the current population are used to create the ideal vector, and the worst objective values of non-dominated solutions are used to create the nadir [...] value vector[, that is the worst objective value vector] [70, 91].

A drawback of estimated reference values during evolution is their lack of accuracy at the beginning of the evolution [70]. Furthermore, using already found objective values for an ideal point, also referred to as an upper boundary value, can lead to too much exploitation, since it cannot be ruled out that the solutions found are in a niche with a local optimum, which leads to a false upper boundary value. Additionally, the ideal point can mislead the search, if it is close to one true ideal objective value and far from the true ideal value of another objective [70]. Another disadvantage is that reaching a certain fitness value cannot be used as a termination criterion, due to the moving boundary and fitness values. This can prolong the calculation process. To address these challenges, in the present concept, the boundary values are calculated based on predicted external influences and a simplified model of the components to be scheduled as described in [Subsection 3.4.2].

Wang et al. address the drawbacks of estimating the ideal point during evolution by adding or subtracting a dynamic variable  $\epsilon$  to the ideal point [136]. Using a minimization problem as an example, the dynamic ideal point is calculated by using the smallest objective values [of a population] and subtracting  $\epsilon$ . At the beginning of the evolution,  $\epsilon$  is set rather high. This is done since the early population's objective values are likely to be far away from the true ideal objective values and the high  $\epsilon$  maintains the population's diversity. As evolution progresses,  $\epsilon$  is set smaller since the population's objective values get closer to the true ideal point, and convergence is intended. This approach allows balancing exploration resp. diversity and exploitation resp. convergence. The method is applied to problems where the true ideal point is



not known and in comparison to problems where the true ideal point is known. The analysis shows good results when the true ideal point is not known in advance. When knowing the true ideal point, the method still performs slightly better than using the static ideal point. Since this work assumes the possibility of adjusting the evaluation of the objective values at its runtime, it is not easy to apply to certain EAs, as for example GLEAM<sup>2</sup> [26].

In [94], Liu et al. propose a method for calculating reference points, especially the ideal point in a preceding evolution. They divide the optimization process into different stages. [In the first stage], the MOO is divided into  $n$  SOO problems, where  $n$  corresponds to the number of objectives. Then for every SOO problem, an optimization is performed using an EA. The best values obtained in these SOOs are then used to create the ideal point. In the following stages, the MOO is performed by the EA with the previously calculated ideal point. In empirical tests, the proposed method achieved good results. A drawback of the optimization in several stages is the additional computational effort, which is addressed in the present work by a single stage optimization approach.

Zhou and Jiao introduce a method for calculating reference values before evolution for cloud workflow scheduling [144]. The objectives in Zhou's work are minimizing makespan and cost. Therefore, the ideal vector consists of the minimal makespan and the minimal cost. Accordingly, the worst vector contains the maximal makespan and cost. In the present work, the minimum makespan is estimated by scheduling all tasks on the fastest resources. Analogously, the minimum cost is estimated by scheduling all tasks on the cheapest resources. The maximum makespan is estimated by scheduling all tasks on one resource. The maximum cost is estimated by scheduling all tasks on the most expensive resource. The approach leads to good results based on the diversity of the population at the beginning of the evolution and the convergence when approaching the estimated ideal point. This approach is adjusted in the present thesis to the needs of scheduling DERs within an EH to fulfill different contradicting objectives. [8]

### 3.4.2 Concept of Dynamic Mapping

In the following section, the conceptual approach is presented followed by a detailed description of the boundary value determination.

[It is assumed that] the employed EA maps each objective value to a fitness value and this mapping cannot be changed during the optimization process. Furthermore, the

<sup>2</sup> <https://github.com/KIT-IAI/Gleam>

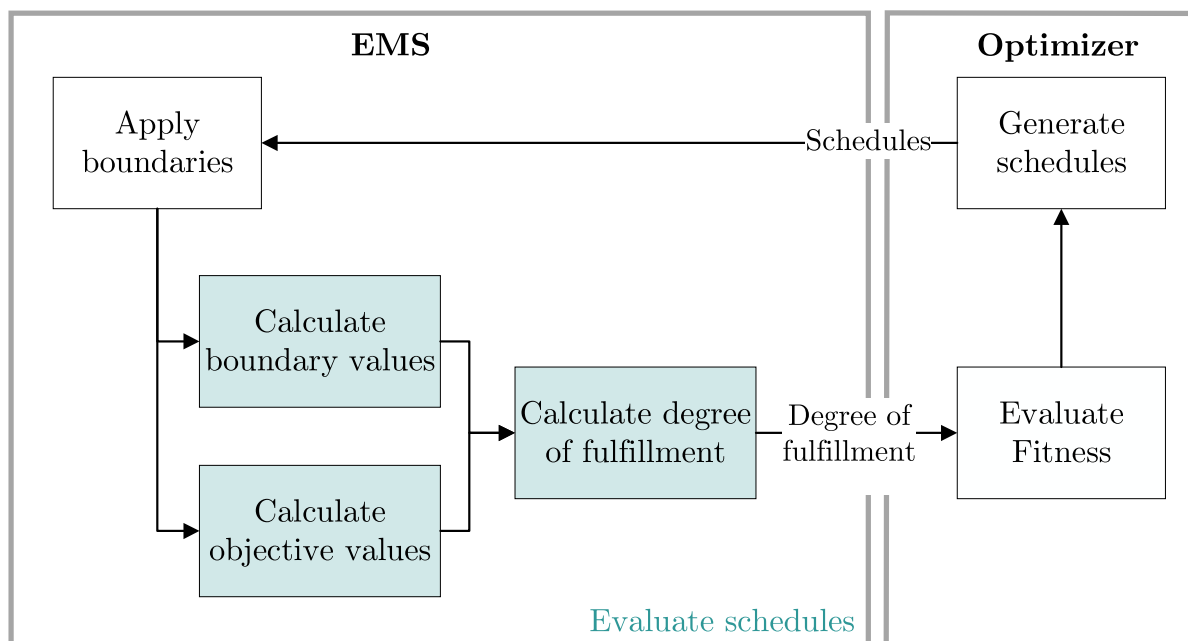


**Figure 3.17:** Process overview of the evaluation within the EMS and further mapping of DOF to fitness within the optimizer [8]

prediction of external influences, e.g., prices, is considered to be perfect as finding an appropriate forecasting method is out of scope for this [thesis]. [8]

### 3.4.2.1 Conceptual Approach

In order to obtain the full functionality of the evolutionary optimizer, e.g., GLEAM, multiple objective functions, and the respective mapping functions have to be adapted to the boundary values caused by external influences. This adaptation is necessary for each problem instance in the case of daily scheduling of DERs, since the external influences, e.g., prices for energy, can change over time. This process is depicted in [Figure 3.17]. Within the EMS box (top left corner in [Figure 3.17]), the technical boundaries of the underlying physical simulation models are applied to the schedule suggestions from the optimizer. Based on a forecast for the day to be optimized, the boundary values for each each objective are calculated. These boundary values are a theoretical [maximum and minimum] for each objective function. These values are to be understood as [upper and lower bounds] for the current optimization task. Instead of the direct absolute result of the objective function evaluation, the DOF as the relative value is submitted to the optimizer to be mapped to a respective fitness value. For this purpose, the schedule suggestions are evaluated based on the objective functions, and the DOF is determined by setting the evaluation result in relation to the adjusted boundary values of the objective functions. The mapping to

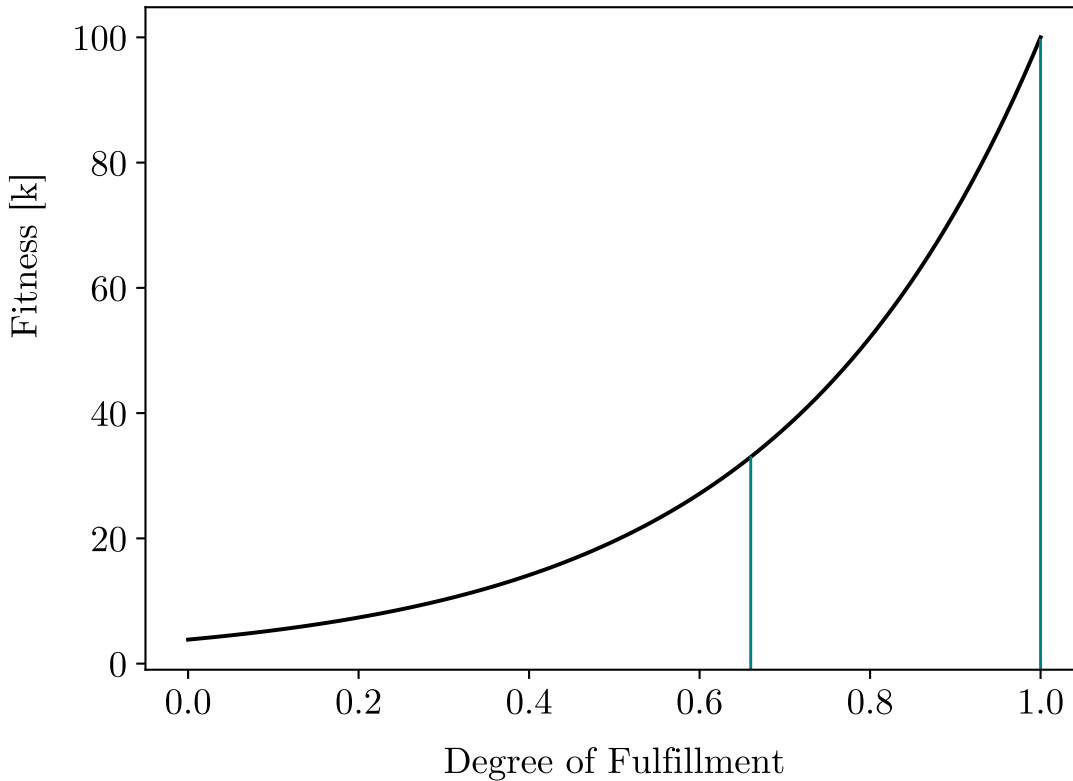


**Figure 3.18:** Mapping function between DOF and fitness [8]

the fitness within the employed EA can therefore be determined statically because the DOF is calculated dynamically in accordance with the boundary values, as depicted in [Figure 3.18]. In this figure, the fitness assigned to a certain DOF is plotted. From this point, the mapping within the EA is dynamically adaptable because of the aforementioned use of the calculated DOF inside the EMS. [8]

### 3.4.2.2 Boundary Values

The determination of the boundary values used in the present concept to calculate the DOF spans the solution space for each objective function to be searched by the EA. For this purpose, forecasts of the external influences are used, such as price information. The components of the EHG are first divided into conversion and storage plants according to the concept presented in [57], since different technical characteristics require adapted calculations. For example, the SOC of a storage facility is

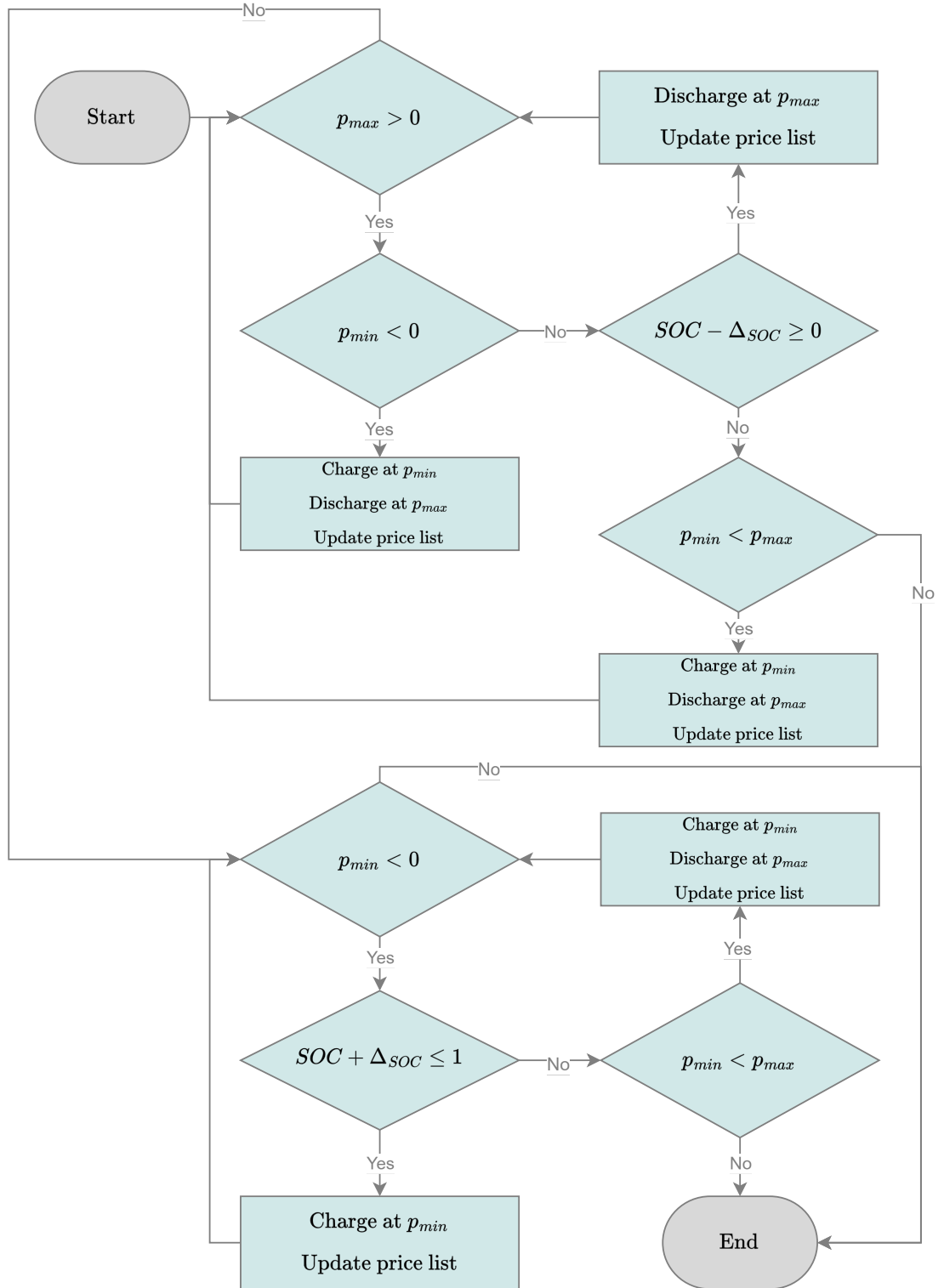


**Figure 3.19:** Process of determining the boundary values on the example of storage units with  $p_{min}$  and  $p_{max}$  as minimum and maximum price of a sorted price list [8]

relevant for the calculation of its maximum achievable profit. By taking the nominal values of each conversion and storage plant into account for the calculation of the boundary values, a simple model of the respective plant is formulated and subsequently evaluated [with] the time-dependent price and power information. These simplified models are used to estimate the best and worst case for each optimization task and each objective separately. The exemplary calculation methodology for a storage is shown in the flowchart in [Figure 3.19]. In this figure, a storage facility is discharged at the maximum price for electricity and charged again at the minimum price. Furthermore, the SOC is taken into account to determine the capacity for charging or discharging the storage. To calculate the energy to be charged or discharged, referred to as  $\Delta_{SOC}$  in [Figure 3.19], the nominal power is multiplied by the duration of the considered time step, e.g., 15 minutes. The calculation method for conversion plants is simplified since only the nominal power and the price information of the used energy sources have to be taken into account. [8]

### 3.4.3 Evaluation of the Dynamic Objective Mapping Function

In the following, first, the evaluation environment is described. Second, an analysis is conducted to demonstrate the enhanced parameterization ability of the EA's weights between different objectives with the presented concept. Finally, the results of the applied concept are presented in comparison to a Base Case without the dynamic objective mapping. [8]

#### 3.4.3.1 Evaluation Environment

The evaluation environment is adopted from [6], and the used test case data, e.g., price information as forecast and a target value for the electrical output of the EHG, is taken for the year 2019. As in [6] and already introduced in [Section 3.3], the system consists of three parts: First, the EMS that is responsible for the evaluation of the proposed schedules. Second, the optimizer, i.e., GLEAM as a representative of an EA that suggests schedules for the EHG, maps the evaluation results to a normalized fitness value and conducts the evolution process according to [83, 27]. Finally, the simulation environment that calculates the results based on the physical models of the EHG's components[, given] the final schedule that has been found during the optimization process [...]. The considered objective functions are the total operational cost, further referred to as "cost objective", and the deviation between a given target [schedule] for the electrical output of the EHG and the scheduled electrical output of the EHG, calculated as [RMSE]. The target [schedule] is meant to be a control signal of an external authority, e.g., a DSO or TSO, to retrieve flexibility of the EHG. The

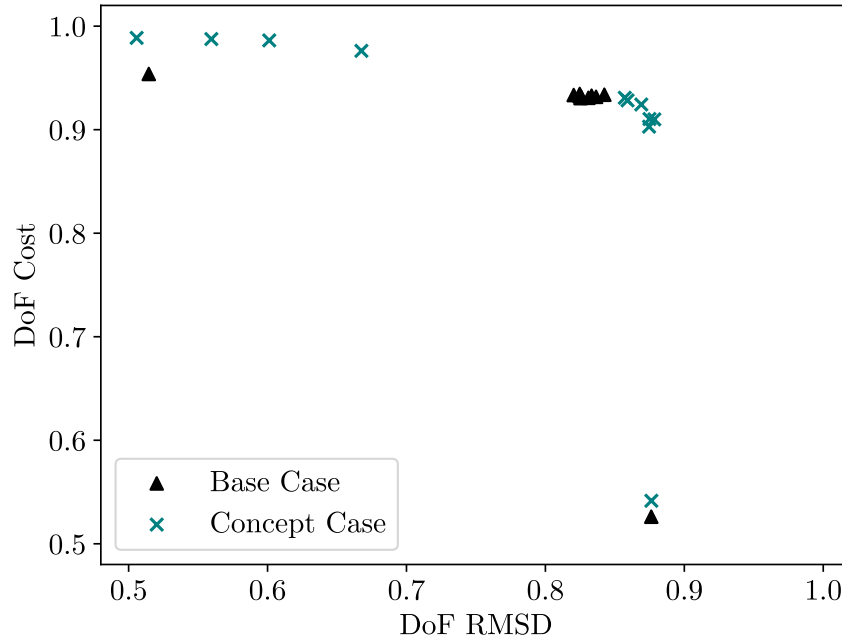


**Figure 3.20:** DOF results sensitivity analysis for a single day [8]

better this target [schedule] can be approximated by the scheduling optimization, and subsequently by the EHG itself, the more grid supporting service can be provided by the EHG. [8]

### 3.4.3.2 Parameterization Analysis

To analyze the ability of the used EA to weight different objectives within a MOO according to its parameterization, as described in [Subsection 3.4.2], two experiments are conducted. First, the Base Case with fixed boundary values for the evaluation of the objective functions is investigated with step-wise changed weights of two objectives, i.e., cost and [RMSE]. Second, the presented concept is applied, and again the weights of both objectives are iterated to obtain the PF [as described in Section 2.4]. [Figure 3.20] shows the respective results for the scheduling of an exemplary day, while the Base Case is expressed also in DOFs even though during the optimization process the absolute boundary values are used for evaluation of the schedule suggestions. The weights of both objectives are varied from 0% to 100% in steps of 10%. The Base Case results show clearly that the parameterization of weights has no influence on the search of the EA except for the experiments, which consider only one objective by weighting one objective either with 0% or 100%. The improved mapping through the introduction of the DOF enables the targeted parameterization of the

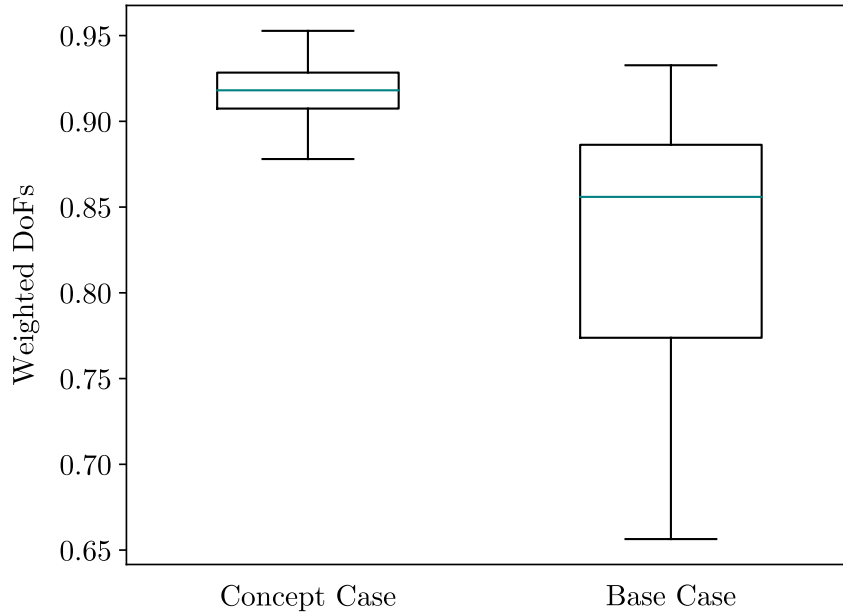


**Figure 3.21:** Boxplot of the simulated year 2019: in comparison the applied EA concept and the Base Case [8]

optimization based on the different weightings of the respective objective functions, as it is depicted by the results of the Concept Case in [Figure 3.20]. As a further result of this analysis, an estimation for the cost of flexibility can be found in the difference of the DOF for the cost objective between the weightings of 0% and 100% in the Concept Case. With an objective weighting of 100% on the cost objective, the DOF reaches nearly one, while 100% weighting on the [RMSE] decreases the DOF of the cost objective to approximately 0.55. This means that around 45% of the maximum possible revenue for the considered day is spent on the provision of flexibility by weighting this objective with 100%. [8]

### 3.4.3.3 Comparison of Base Case and Concept Case

As an overall evaluation of the concept, [Figure 3.21] shows the results of the achieved DOFs for the Base Case and the Concept Case for the year 2019. Again, [for the sake of comparability], the DOFs for the Base Case is determined afterwards [...]. The [RMSE] objective is weighted with 60% and the cost objective with 40%, respectively. This weighting is applied as a result of the previously mentioned parameterization analysis in [Subsubsection 3.4.3.2]. The average DOF at the Concept Case is 10.2% higher than the Base Case and leads to significantly smaller [variance] around the median. This results in more uniform and better optimization solutions. [8]





# 4 Adaptive Schedule Optimization

The following chapter is dedicated to find an approach answering the RQ 2: *Which (dis-) advantage can a dynamization of EA based optimized scheduling provide to enhance flexibility provision by DERs* and RQ 3: *To what extend can a ML model improve the dynamization of EA based scheduling?* For this purpose, in a first step the general opportunity to dynamically adapt the time resolution at finding a suitable and near optimal solution schedule to follow a given target schedule is investigated. Furthermore, this chapter addresses the outlined challenges from previous Section 3.3 on the basis of the general knowledge about the effectiveness of dynamically allocating the computational effort of an optimization algorithm, as elaborated to answer RQ 2. An answer to RQ 3 is given in a second step, by applying ML methods to predict the optimization quality. This approach is evaluated with two different EAs employed for the optimization problem. This Chapter is based on the works [6, 9].

## 4.1 Problem Statement

As introduced in Chapter 1 and further detailed in Subsection 3.3.7, scheduling of DERs is a difficult task, especially when considering multiple objectives.

For the scheduling of DERs within an EH, an EMS is needed [53]. By using a multi-objective heuristic optimization algorithm like [an EA, as elaborated in Subsection 3.2.1], the EMS calculates appropriate schedules for the sub-plants of an EH that can meet a third-party control demand of, e.g., a power network operator and additionally respect internal optimization criteria and boundary conditions. It then uses these schedules to coordinate the internal power flow between dispatchable generation units and loads. In the current concepts of EHs, several problems of finding a near optimal solution for internal schedules that also meets the external control demand are unsolved. For example, as stated in [5] [and further described in Subsection 3.3.9], simulation results show that an EH using an EA can have difficulties optimizing schedules that cover a load with high variability. Moreover, analyzing the flexibility provision in those cases shows that the used EA optimization solution could not reduce the relative power variation of the specified load in frequencies above  $[1h^{-1}$  and, therefore, provides] no flexibility in higher frequencies. [7]

In the context of scheduling DERs, it is common to use a fixed time interval length of, e.g., 15 minutes. This results in a homogeneous distribution of decision variables over the optimized time horizon. Doing so, differences in the difficulty of finding adequate solutions for individual parts of the optimized time frame are neglected in general. To overcome this difficulty, a general approach that focuses the computational effort on the challenging areas within the search space is introduced in the following Section 4.2. This approach yields a two-step optimization that requires additional calculation time. This increase in calculation time is addressed in the further course in Section 4.3 by applying ML to predict in advance the quality of the schedules proposed by the EA optimization. The associated computational effort is directed on the basis of the forecast delivered by the trained ML model.

## 4.2 Basic Approach

In the following section, parts are exactly taken from [7] and have been supplemented, a basic approach to dynamically allocate the decision variables of an EA according to the complexity of the search space is introduced. An improvement of the optimization results can be achieved in many different ways: One obvious approach is to increase the parameters for exploration and exploitation which are, in terms of an EA, the population size and the number of generations as explained in Section 2.5. Changing these parameters can improve the optimization quality with a trade-off of more calculation time and is therefore a good benchmark to compare with the results of testing the new optimization approach presented in Subsection 4.2.2. Analyzing the EA settings with the optimization process described in Section 3.3 shows how much impact the population size and generations have on the optimization results as well as how the calculation time changes with it. Table 4.1 shows the results of the meet demand function and the calculation time in hours for each optimization as well as the average of both values over all optimizations. The tests are done with 50 generations and population sizes of [50, 100, 200, 800, 1000] as well as for [100, 150] generations and population sizes of [50, 100, 150]. Every setting is tested only once and a test with the same setting will have a different result due to the randomness of EA's. For a robust representation of the performance of the EA with these settings, more tests are needed. But, due to the computing time, it is not easily affordable and tendencies are sufficient for the evaluation of the approaches in the further course of the thesis. It must also be mentioned that the evaluations are executed on a local machine.

Nevertheless, the results show that with 50 generations an increase in the population size does not always lead to an improvement in the RMSE objective result. Additionally, it shows that after a population size of 200, no significant improvement can be noticed. For 100 generations the RMSE performance did also not improve from a population size of 50 to 100. An increase in the number of generations results in nearly all tests to an improvement except for optimization run 1 and 7 for the change of [100gen, 50pop] to [150gen, 50pop]. Comparing the values for [50gen,

200pop] with [150gen, 50pop] shows that with the same calculation time and setting [150gen, 50pop] an average increase of the RMSE result of 0.35 is achieved. Inspecting the results of the individual optimization runs which correspond to different days clearly show that optimization run 1, 6 and 7 are performing always much better than for the other days.

In conclusion, an increase in the number of generations resulted in a better RMSE value than an increase in the population size in comparison to the calculation time. This shows that a high population size is not always needed for an acceptable exploration of the search space, but instead, the exploitation of problem domain oriented search strategies have high potential for improvements of the RMSE objective. Also the test results show a clear difference of optimization complexity between different days.

**Table 4.1:** EA settings tests with different population sizes and numbers of generations

Optimization run		1	2	3	4	5	6	7	Average
50pop	RMSE [MWh]	0.44	2.39	2.68	2.95	3.18	1.43	0.67	1.96
	Calc. time [h]	0:08	0:08	0:08	0:08	0:09	0:08	0:08	0:08
100pop	RMSE [MWh]	0.70	2.95	2.88	2.79	3.14	1.35	0.66	2.07
	Calc. time [h]	0:13	0:14	0:15	0:15	0:15	0:14	0:13	0:14
50gen 200pop	RMSE [MWh]	0.58	2.41	2.37	2.25	2.58	0.95	0.61	1.68
	Calc. time [h]	0:28	0:30	0:30	0:30	0:31	0:28	0:26	0:29
800pop	RMSE [MWh]	0.45	2.33	2.24	2.10	2.48	0.91	0.49	<b>1.57</b>
	Calc. time [h]	2:40	3:07	3:06	3:19	3:34	2:44	2:40	3:01
1000pop	RMSE [MWh]	0.45	2.27	2.46	2.11	2.67	0.90	0.46	1.62
	Calc. time [h]	3:42	4:35	4:48	4:22	5:02	3:51	3:39	4:17
50pop	RMSE [MWh]	0.36	2.00	2.16	2.50	2.36	0.80	0.48	1.52
	Calc. time [h]	0:17	0:17	0:18	0:17	0:20	0:17	0:17	0:17
100gen 100pop	RMSE [MWh]	0.33	2.28	2.13	2.37	2.47	0.79	0.47	1.55
	Calc. time [h]	0:27	0:35	0:44	0:37	0:34	0:29	0:31	0:33
150pop	RMSE [MWh]	0.38	1.99	2.26	1.82	2.57	0.65	0.46	<b>1.45</b>
	Calc. time [h]	0:45	1:02	0:58	0:58	1:01	0:48	0:45	0:53
50pop	RMSE [MWh]	0.54	1.92	1.99	1.65	1.99	0.69	0.55	1.33
	Calc. time [h]	0:25	0:27	0:26	0:28	0:34	0:27	0:27	0:28
150gen 100pop	RMSE [MWh]	0.26	1.95	1.70	1.48	2.04	0.60	0.36	<b>1.20</b>
	Calc. time [h]	0:47	1:00	0:54	1:07	1:20	0:50	0:49	0:58
150pop	RMSE [MWh]	0.29	1.89	1.65	1.71	2.13	0.55	0.37	1.23
	Calc. time [h]	1:30	1:38	1:41	1:37	1:33	1:26	1:07	1:30

### 4.2.1 Related Work

The proposed adaptive optimization approach makes use of time steps of varying length, that is, different time scales.

In current research, several concepts using more than one timescale are discussed, e.g., multi-timescale coordinated optimized scheduling in [139], multi-timescale rolling optimal dispatch in [115], timescale adaptive dispatch in [90] and multi-timescale model predictive control in [37], which are grouped in the present thesis under the term multi-timescale scheduling. The basic idea is using multiple timescales for calculating the optimal unit commitment of various energy resources [88]. Multi-timescales are mainly used in the literature for solving problems regarding uncertainties in the optimization, e.g., in [18, 115, 90], separating optimization for economic and operational factors, e.g., in [141, 140, 37], improving the control in energy systems or shifting deferrable loads in [100]. In this context, a rolling optimization approach is often used, allowing different look-ahead periods to combine short-term and long-term benefits [89]. In the following, different multi-timescale scheduling approaches are described to distinguish them from the present work. [7]

In [139], a hierarchical optimization approach with three different timescales is used to schedule a combined system of RES, thermal generator, hydro pumped storage, and batteries. The first timescale is a day-ahead scheduling for thermal units based on a 24 h ahead forecast. For optimizing the dispatch of hydro-pumped unit power outputs, a second scheduling is proposed in which a day-ahead schedule as well as a 1 h ahead forecast are used. On the smallest time scale of 15 minutes, the aforementioned schedules are taken into account to obtain an optimal battery system schedule. [7]

But in summary, each time scale is used with a fixed interval length.

In [18], an approach for an integrated multi-timescale optimization of a coupled multi-type energy supply similar to an EH is presented. Regarding multi-timescale operation, a day-ahead schedule takes the uncertainty of RES generation into account. Additionally, real-time dispatch for storage, combined cooling and heat power, and ice storage air conditioners is used to react to fluctuations in RES and demand.

In [115], a multi-timescale rolling optimal dispatch framework is developed to cope with the impact of uncertainty in load on hybrid micro-grids at timescales of day-ahead and intraday. For the day-ahead scheduling, a distributed robust optimization model considering uncertainties in source-load power is used [with a fixed interval length of 1 h]. While performing the intraday rolling optimization with a fixed 15 min resolution, a relaxed penalty cost for the final state of charge is added to ensure cyclic regulation of the energy storage.

In [90], the selection of the timescale is based on a threshold which is defined by a confidence interval. The optimization addresses the scheduling of a RES on an island and has to deal with very high uncertainties. When the prediction error exceeds the available reserve, the energy system can become unstable. Therefore, the timescale is dynamically selected to stay within the confidence interval.

A multi-timescale economic scheduling strategy for a virtual power plant is presented in [141]. Their goal is to unlock the potential of a large quantity of DL by participating in the wholesale energy and reserve market. A day-ahead bidding and real-time operation are used for the multi-timescale scheduling. With the proposed strategy, efficient management of a large number of DL can be realized while reducing energy management complexity and increasing overall cost-effectiveness.

A multi-timescale coordinated optimization of an EH is proposed in [37]. It includes a global optimization of day-ahead economic dispatch, a local intraday model predictive control with 15 minute timescale and a minimization of the total adjustment amount of all controllable devices every 5 minutes.

The authors of [140] propose a multi-timescale model for regionally integrated energy systems. The multi-timescale aspect is used on two levels in the model. On the first level, it is applied to differentiate between day-ahead and intraday scheduling. For day-ahead scheduling, the objective is to minimize costs in scheduling the energy system. The intraday scheduling uses a rolling [horizon] optimization which is divided into three different control sub-layers. They achieve a balance of supply and demand in the system and can also restrain the fluctuation of renewable energy and load in the intraday scheduling.

In [143], the main goal is to coordinate the substation on-load tap changer operation on an hourly time scale [in the context of smart distribution grids. This is conducted in a power network with PV inverters and battery storage on a 15 minute interval basis].

The usage of multi-timescale scheduling in the context of deferrable appliances in a smart home is proposed in [100]. The appliances are categorized into two groups. While one group can be shifted on an hourly scale within a day, the second group can be additionally shifted between days.

With the main focus on managing uncertainties in the demand and power generation of RES, multiple methods are applied. In [18], several fixed timescales are used for the optimization, and specific facilities are assigned to one of these. Additionally, in [139, 115] the timescales are optimized in hierarchical order so that finer timescales use the result of a coarser timescale optimization as an input. In [90], the timescales are dynamically chosen. Another approach is presented in [141, 140, 37] using a

day-ahead timescale with focus on economic and intraday timescales for operational aspects. [140] introduces –as a multi-timescale approach– an intraday rolling optimization for control, and is applied with a special focus on battery systems in [143]. Finally, [100] applies different timescales to shift deferrable loads.

However, in the aforementioned related work, there is no approach that uses different timescales to apply adaptive time segments for scheduling flexibility provided by DERs on a day-ahead scale. The method presented in [Section 4.2] uses different timescales within the same schedule to solve the problem of optimizing schedules for an EH to follow a target schedule with different DERs included. In other words, all DERs are considered in the day-ahead scheduling without distinction of specifically related timescales. Timescales are therefore applied using adaptive time segments which are chosen based on the deviation to the target schedule. Furthermore, the EA implemented for evaluation of the present method relies on [27, 82, 83]. [7]

## 4.2.2 Concept

The goal of the present method is to improve the EH operation to enhance the flexibility provision of the EH and reduce the total power exchange of the EH at its electrical connection point. The total power exchange results from the superposition of the calculated schedules provided for each subsystem to meet a third-party target [schedule]. The main task of the optimizer, such as EA – beside other objectives like economic cost – is to minimize the difference between the power output of the EH  $P_{EH}(t)$  and the third-party target [schedule]  $P_{target}(t)$  for all time segments according to [Equation (3.3)]. [7]

“The general idea of [the] method for solving the problem described is to concentrate the computational effort of the EA on specific time segments where there is high variability in the given target [schedule].” [7] “Optimizing a complete schedule with an EA in higher time resolution but with the same computational effort does not necessarily lead to an improvement of the optimization as only a larger search space is inspected.” [7] This is due to the fact that the number of decision variables increases with the temporal resolution of a schedule. “The present method allows an EA to generate schedules with more control point changes for those segments than for others to achieve a better approximation.” [7] By allocating more control points in a certain time segment, the computational effort to find a solution in this specific time segment is scaled. According to the time resolution considered for this segment, the focus is to shift the computational effort to time segments that are more difficult to optimize.

[On the other hand], this approach can also be used vice versa. If there is little to no fluctuation within a time segment, there is no need to provide more than one schedule

entry for this segment. The computational effort is [made] adaptable for each time segment. Time resolution determines the number of entries in the schedule and, therefore, also the number of possible solutions to approximate the target [schedule] for the power output of an EH.

[7]

The time resolution in the optimized schedules can be inspected from two perspectives, the use case and the optimization algorithm, namely the EA in combination with the EMS. In the perspective of the use case, the time resolution determines how fast an EH can respond to changes in the target [schedule]. For example, if the demand changes in 15 minute intervals and the schedule only provides control steps every 30 minutes, the EH is not able to respond to changes below 30 minutes. The use case benefits only from a higher time resolution as long as it is not more granular than the input data. Looking at the EA calculation time or the number of populations analyzed is another perspective. An EA uses genetic operators, which are based on random changes in the solutions to find new and better solutions over multiple generations. In general, scheduling DERs is an NP-hard problem, and therefore, when applying an EA, the goal could not be to find the best possible solution but only a good approximation in timely manner using the available computing resources. The more fine-granular the time scale for schedules is defined, the larger the search space which directly results in higher computation time for finding an appropriate solution.

[7]

The proposed method makes use of the general process described in Section 2.5, and especially of the translation from a chromosome to a schedule.

The value of the power output of a subsystem in a certain scheduling interval, as well as the start time and duration are not interpreted by the EA itself, but by the EMS. In the employed EA, a schedule (chromosome) is represented by a chain of set points (genes) which are interpreted as a schedule with a certain number of time intervals. The set point value is a unitless number between -1 and 1. "Duration" and "Start Time" can be interpreted as relative values, whereas the "Start Time" is the index of the corresponding schedule segment. It is one main duty of the EMS to transform the contextless information within the chromosomes to their technical interpretation context. Thereby, translating the unitless and relative values to their absolute values, e.g., the real power output of a technical sub-system will be calculated by the EMS based on the relative value given by the optimizer and configuration parameters specifying how to interpret this number for the given subsystem. The same transformation will be applied for the scheduling interval by translating index values into start times and durations into time intervals. A second important duty of the EMS is then to calculate objective functions and to verify the boundary conditions. [7]

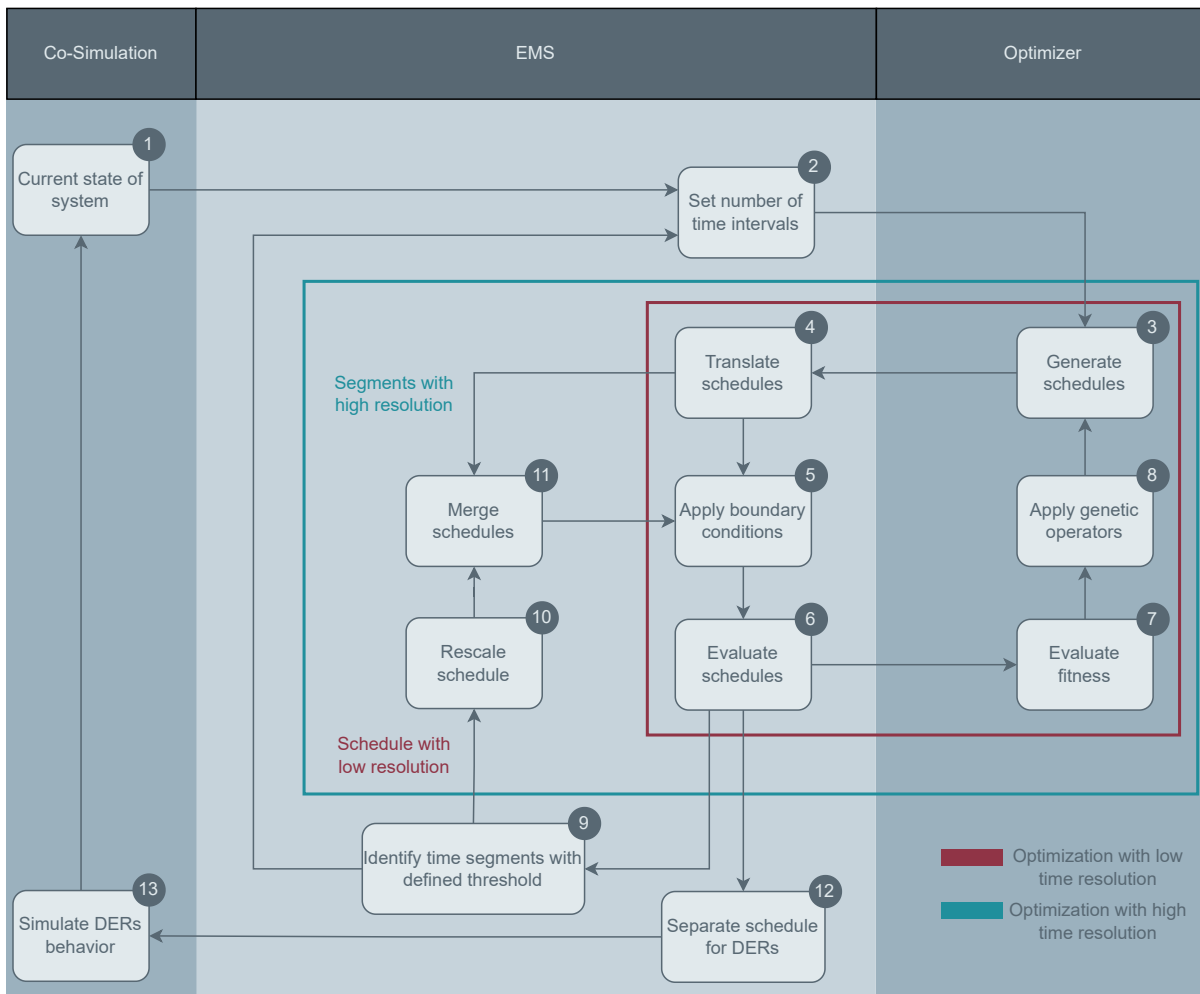


Figure 4.1: Adaptive optimization process overview [7]

The complete optimization process, including the implemented use case, is depicted in [Figure 4.1]. First, the current state of the system under concern is determined either via the system simulation (1) or, in a real-world application via sensor data of real DERs, to initialize a new optimization run with low time resolution (2). Then, the first optimization is executed (red box, 3-8). The optimizer performs a loop where the EA first generates new populations (3) by applying genetic operators to the (initial) populations (8). The schedules are then sent to the EMS, which translates them into the technical context (4) and then evaluates the schedules (6) by first calculating and checking the boundary conditions (5) and then calculating the objective functions. With the results from the evaluation from the EMS a new fitness value is calculated in (7) by the optimizer. If the fitness value is too low, the optimizer performs the next generation cycle. If the fitness threshold configured [as termination criterion, according to Subsection 2.5.4,] is reached, the optimization run ends and the found schedules are translated into the technical context [(12)] and are



then send to the simulation [(13)]. The simulation will apply the schedules to the system model, which calculates the resulting behavior of the EH at its connection point to the external network [as described in Section 3.3]. These values can then be compared to the given target [schedule] curve to calculate how well the internal schedules approximate the target [schedule]. In this first optimization run using a low time resolution, the EA has less options to respond to changes in the target [schedule]. Giving only one set point for a larger time interval that approximates the given target [schedule well] is unlikely. Hence, after the first optimization run, an analysis of the approximation quality is performed where the time segments [that do not provide a good approximation are identified] (9). [7]

Then, a new optimization run (green box) that uses a higher time resolution for the determined time segments is initialized, which means additional decision variables are introduced for this time segments. When this optimization run finishes, the schedule parts with lower time resolution are rescaled to the resolution of the new optimized parts (10) and then merged (11). Finally, one merged schedule with high and low time resolution parts is build to be evaluated in (6) after another check for boundary conditions in (5).

To apply this approach, a method is needed to identify time segments that could not be adequately approximated with the lower time resolution. The [refined] time resolution is defined for the segments according to their variability and approximation error. One approach is by sequentially executing two optimization processes as depicted in [Figure 4.1]. Suitable criteria for classifying time segments for a second optimization need to be defined. [... O]ne possible criterion is the absolute error [ $d_{abs}(T_s)$ ] of time segments  $T_s$ , which is the difference between the proposed schedule and the target schedule] calculated according to [Equation 4.1]. [7]

$$d_{abs}(T_s) = \sum_{t_s \in T_s} |P_{target}^{EH}(t_s) - P^{EH}(t_s)| \quad (4.1)$$

On the basis of a configurable threshold for  $d_{abs}(T_s)$ , time segments are identified and optimized with higher time resolution.

These shortened time segments replace the respective longer, low time resolution segments. This replacement is conducted by the EMS. Afterwards, the adapted time segments are optimized with higher resolution in a second optimization run. The evaluation in this second optimization run is done for the complete schedule and not only for the identified segments. By evaluating the entire schedule with different time resolutions feasibility of the schedule is guaranteed.

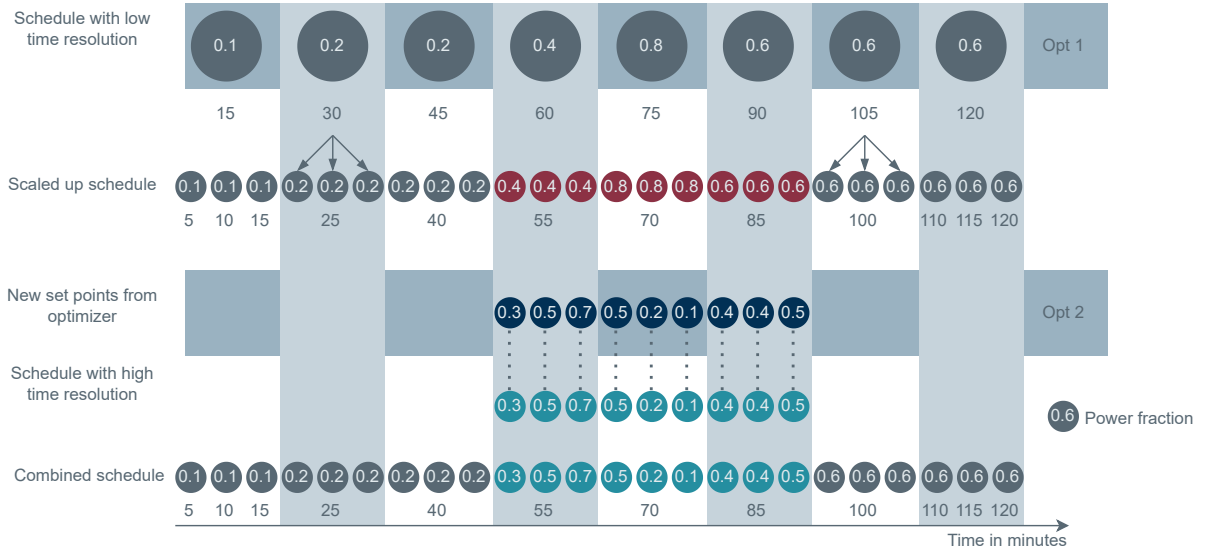


Figure 4.2: Combining schedules with different time resolution [7]

### 4.2.3 Evaluation of the Basic Approach

To assess whether the previously presented approach is a viable method to improve the ability of an EH to follow a target [schedule and answering the RQ 2], an evaluation is [conducted] using a concrete use case. The evaluation setup includes a specification of the evaluation environment with a test scenario, as well as an implementation of the approach. Furthermore, a precise definition of the evaluation criteria used to analyze the test results is needed. [7]

The evaluation environment is based on previous work described in [5] and [82, 83, 27]. The co-simulation environment from [5], presented in Section 3.3, is used with the combination of DERs depicted in Figure 3.3. The EA used for scheduling the EH is the GLEAM from [27] in combination with the EMS from [5]. The decisive criterion is the RMSE  $d_{RMSE}$  calculated according to Equation 3.3. Furthermore, the calculation time for the complete process is evaluated and compared.

The settings for the EA are as follows: The maximum amount of generations is 100 and considered as termination criterion. The start population size is 50 individuals. Both parameters are identified from the experiment results given by Table 4.1 considering the trade-off between optimization quality and calculation time:

A drastically reduced population size produces low quality solutions, whereas a population size bigger than 50 does not lead to significantly better results. Further configurations, e.g., mutation and crossover, are adopted from [78]. In the first optimization process, the simulation and optimization time resolution is 15 minutes,

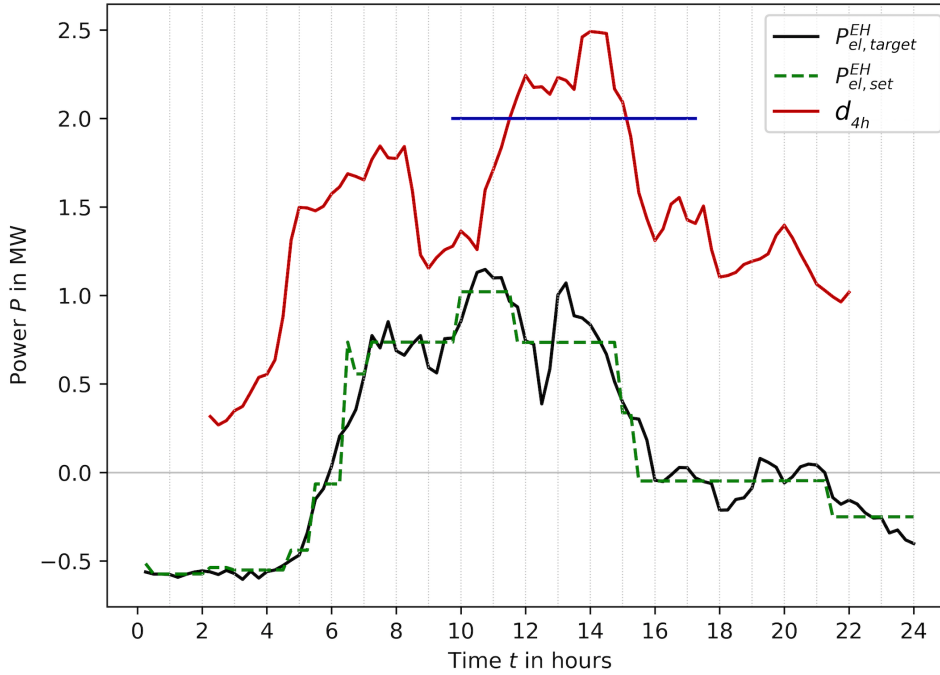


**Figure 4.3:** Optimization result with low time resolution for an example day [7]

which corresponds to 96 intervals in the schedule. The [...] optimization time resolution in the second optimization process is [...] 5 minutes[, only for the identified time intervals]. The number of intervals for [the second] optimization is calculated after the time segments are identified. The optimization time horizon [in total] is one day and seven days are evaluated. The number of optimization runs that can be tested in the second optimization process depends on the time segments identified for each day. The criterion used to identify time segments is the absolute deviation between the target schedule and the proposed schedule computed from [Equation (4.1)] for a rolling period of 4 hours [as  $d_{4h}$ ]. [7]

The threshold to identify a time segment for the second optimization run is set to 2 MW h. This threshold has been tested in advance.

## 4.2.4 Results

The results of the first optimization runs for an exemplary day of the evaluated week are shown in [Figure 4.3]. According to the criterion described above, the time segment identified for a second optimization with higher time resolution is marked by the solid blue line at 2 MW between 9.75 h and 17.25 h. The RMSE after [the] first simulation run accumulates to 2.0 MW h with a total calculation time of 17 min. For the identified time segment of 7.5 h a second optimization with 90 intervals is

conducted. The combined schedule is shown in [Figure 4.4]. Blue dotted lines mark the time segment where the second schedule is inserted. By evaluating the merged schedule, only solutions with continuous transition at the edges of the identified time segments are valid. In the example shown in [Figure 4.4], the RMSE is reduced by 15.5% to 1.69 MW h. The average improvement for the evaluated week is 11 %, while the computation time increases up to three times [due to the additional optimization processes]. [7]

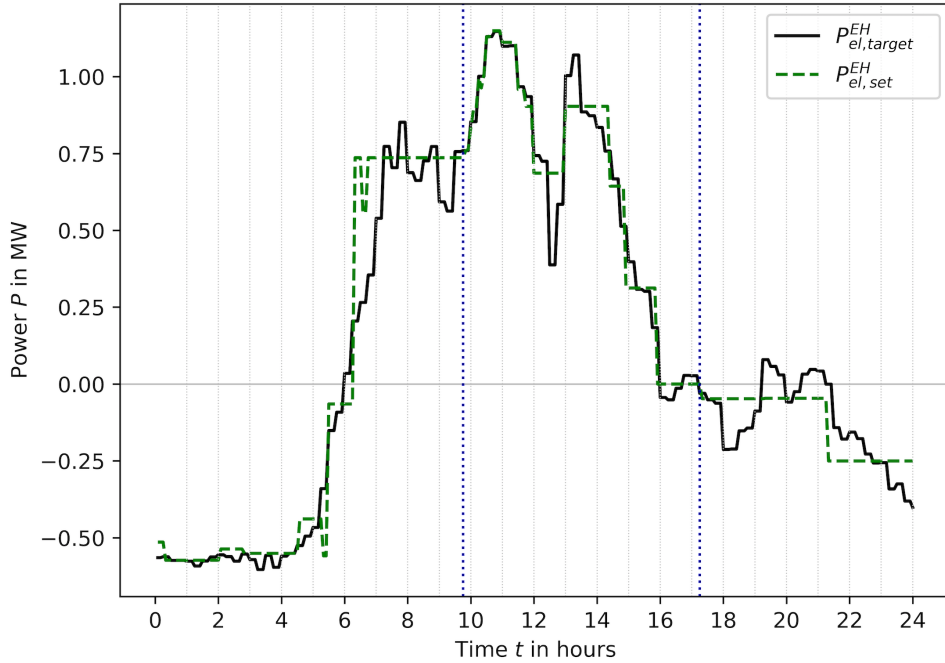


Figure 4.4: Combined schedule for an example day [7]

### 4.3 Hybrid Evolutionary Algorithm for Scheduling Energy Hubs

In the following section the drawback of a two-step optimization approach as presented in the previous Section 4.2 are addressed by applying ML methods. This approach is described in detail and evaluated to answer RQ 3: *To what extent can a ML model improve the dynamization of EA based scheduling?* First, the related work dealing with multi-timescale scheduling is discussed to emphasize the novelty of the concept presented in Subsection 4.3.2. Second, several different forecasting algorithms are evaluated on two different EAs to underline that this approach is agnostic concerning the underlying employed EA. This Section is based on the concept presented in [9].

### 4.3.1 Related Work

All the works on the topic of multi-timescale scheduling for optimal control of DERs mentioned in Subsection 4.2.1 use discrete and equal length time step sizes within each timescale. The approach introduced in the present thesis differs from these previous works in this point by adjusting individual time interval lengths according to the respective predicted optimization quality. To the best of the author's knowledge, no previous work has presented such an approach.

In [92] a dynamic multi-objective EA is proposed to handle an optimization problem with time-variant PF. It is stated, that the algorithm detects environmental changes and identifies the similarities to historical changes, which based on response strategies are applied. One strategy is differential prediction based on previous populations, if no similar change in the PF is detected. The other strategy is a memory-based approach to react to the change in the PF. A mix between existing solutions and randomly generated ones is used to alleviate the effect of the strategies. A different approach to address the dynamic interval multi-objective optimization problem is presented in [61]. The basic idea is to decompose the decision variables and group them into two different groups according to their similarity. Then these two groups are optimized by two different sub-populations. The evolutionary process is driven by two different strategies: one is based in the intensity of change in the PF and the other is a random mutation strategy. Furthermore, a summary of the main dynamic evolutionary optimization methods is given by [108] and general overview is presented by [28]. This approaches directly effect the generation of individuals during the evolutionary process in contrast to the concept presented in the following Subsection 4.3.2.

A different approach to reduce the complexity in the optimization process to use an equation-based algorithm is presented in [121] by substituting similar time intervals. Hence, the amount of decision variables can be reduced if similar intervals can be determined. In [120], this approach is extended by a systematic method for the identification of promising initial time intervals that can be aggregated. This leads to a further reduction in the decision variables. This approach is the inversion of the concept presented in the following section.

In the literature, some research works, e.g., [44, 46, 22, 21] have proposed different algorithms and techniques to deal with complex search spaces of EAs. While [44] and [46] alter the genetic operators or the optimization problem itself to reduce the complexity, [22] and [21] instrument a Variational Autoencoder (VAE)

to generate a new and simple search space from a complex and discontinuous one, aiming at reducing the problem dimensionality. The authors of [22] and [21] proposed a method with three steps to create a better search space by mapping a difficult search space to a learned latent representation that is easier to be explored by an EA. [9]

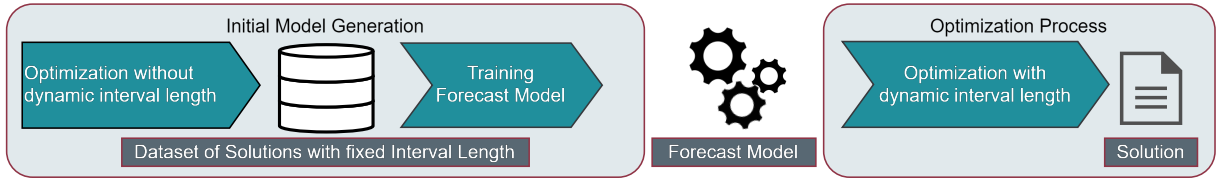


**Figure 4.5:** General concept overview. The approach consists of two phases: First, initial model generation using a database of solutions with a fixed interval length and second, a dynamic time interval optimization for each day, based on the results of the trained forecasting model. [9]

The steps of this method can be summarized as follows: First, a dataset is generated with random solutions to the optimization problem that meets some additional criterion, e.g., a range limit or correlated variables as chained inequality. These random solutions are obtained from a simple optimizer such as a simple genetic algorithm. Second, a VAE is employed to learn the representations of the original search space and facilitate it by generating a new and simple one with the learned latent representations. Finally, a genetic algorithm is used to solve the optimization problem with the help of the newly generated search space, considering the objective function and further criteria. The results of both works show that using VAE to reduce the complexity of a search space can improve the overall performance of an EA in terms of solution quality and computational efforts required to reach such a solution.

To dynamically parameterize the chromosome interpretation of the used optimizer for directing its computational effort to difficult regions in the search space, the present work uses a forecast of the quality of the optimization solution. This quality is interpreted as the absolute error between the target schedule and the actual EH output power for each point in time and is therefore a time series. Time series forecasts are commonly applied in the context of renewable energy systems [12] and a variety of time series forecasting methods exist [114, 23, 36, 93, 35, 132, 131]. Such time series forecasts are often used as input for a given optimization [12], and have even been applied to optimally determine the input parameters of an optimization problem [51]. However, to the best of our knowledge, no previous work has used time series forecasts of the quality of an optimization solution for the purpose of parameterizing the interpretation of the used optimizer dynamically.

### 4.3.2 Concept

“The general concept is depicted in [Figure 4.5]. An initial forecasting model is trained based on a data set [that is previously] generated by the optimization process with fixed time interval length.” [9] This initial training is only necessary once to generate the forecasting model which is described in detail in Subsection 4.3.7.

With the results produced by the generated model, the schedule optimization with dynamic interval length is conducted. The starting point of the [...] scheduling process[, depicted in Figure 4.6], is the initialization of a start population within the

EA, e.g., GLEAM. As further described in [Subsection 4.3.4], the list of chromosomes is interpreted as raw schedules. Each of these raw schedules is processed within the interval length assignment to define the exact timestamp for each power fraction from the previously ordered ascending interval numbers. Details of the interval length assignment process are described in [Subsection 4.3.5]. To [ensure] the validity of a schedule, the boundary conditions, i.e. ramp rate, SOC, etc., are enforced within the EMS or an equivalent calculation service with domain knowledge. A more detailed description is given in Subsection 4.3.6. As a result of this evaluation process, each chromosome, i.e. schedule, is listed with its respective result concerning the evaluated objectives. This list of results for the entire generation is [returned] to the EA to map them to a weighted fitness value. After checking the termination criteria, the EA either determines the final schedule or continues the evolution process. Within the evolutionary process, genetic operators are applied according to the fitness of each individual. Details of this process are given in [80, 78, 26]. [9]

### 4.3.3 Population Generation and Coding

[Regarding the] optimized scheduling of DERs, a population generated by the EA consists of a set of chromosomes, which represent the respective schedule proposals. Within each generation, each chromosome contains a list of genes, and each gene is represented by different decision variables that are equivalent to alleles. In the context of scheduling DERs, the respective alleles are Unit ID, Start Time, Duration, and Power Fraction [9],

as shown exemplarily in Figure 4.6 with the *Chromosome List*. Slightly different from the process in the loop, depicted in Figure 4.6, is the first generation. This initial population can be built in many different ways, as stated in [26, 27]. In the presented approach “a random distributed initial population is used.” [9]

### 4.3.4 Chromosome Interpretation

“[... T]he interpretation of the proposed chromosomes as schedules is [a crucial step]. Depending on the implemented gene model of the EA, this offers a wide range of applications and interpretation space.” [9] As described in Subsection 4.3.3 a gene consists of four alleles. This modeling has been adopted from [80] and can be used with further EAs beyond GLEAM.

The *Unit ID* refers to a defined component of the respective EH. The *Start Time* determines the interval from which the *Power Fraction* as a set point is valid for the respective *Unit ID*. The *Duration* defines how long the *Power Fraction* is set in terms of interval counts. Each chromosome consists of a list with  $n$  genes that are

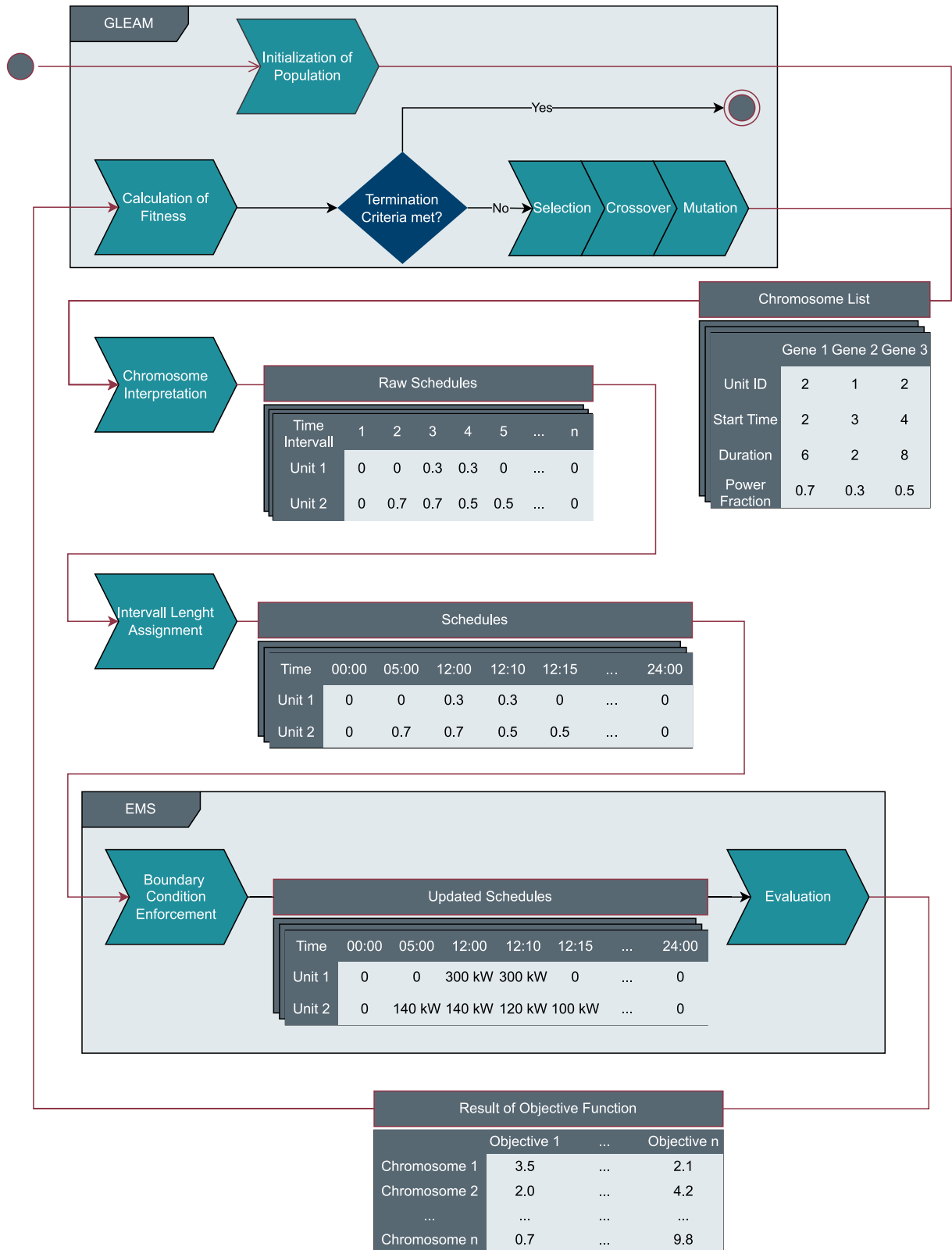


Figure 4.6: Optimization process using results of forecasting model for the *Interval Length Assignment*



interpreted as a schedule. The transformation from a chromosome to a raw schedule is adopted from [83]. To build the *Raw Schedule* [depicted in Figure 4.6] from a single chromosome of the *Chromosome List*, shown in Figure 4.6], the chromosome interpretation reads the listed genes one after the other. In this process, the preceding gene is overwritten by the following one if they carry information for the same time interval and component. Finally, a list of raw schedules is handed over to the following interval length assignment process. In each raw schedule from this list, each component has a power fraction representing a setpoint during a time interval further described in the subsequent step. [9]

### 4.3.5 Interval Length Assignment

The main contribution of the present concept is to focus the computational effort of the optimization on the time ranges that are difficult to approximate. This is undertaken by varying the length of the intervals as described in [Section 4.1]. From the previously only ordered setpoints per DER of each schedule proposal, a concrete point in time is determined in the interval length assignment based on the predicted quality of the approximation by the optimizer. The better the approximation predicted, the longer the time intervals, and vice versa. [9]

Through this, the EA is assigned a particularly large number of alleles for variation in the time intervals in which an approximation to the target schedule is considered to be particularly difficult. “The original number of intervals is kept equal, but the length of each interval is dependent on the predicted quality.” [9] In other words, the length of the interval is determined dynamically.

*Applying Forecast Result to Time Interval Length Assignment.*

[From] the forecast, the deviation between target schedule and predicted power output of the considered EH instance is computed. To [convert] this result into the respective time interval length for the evaluation of the proposed schedules, the relative error  $\hat{\mathcal{E}}_{\text{opt, rel}}(n)$  per time interval  $n$  is determined by dividing the predicted error  $\hat{\mathcal{E}}_{\text{opt}}(n)$  for time interval  $n$  by the sum of the predicted error over the complete day [as shown in Equation (4.2)]. In accordance with the standard time interval length for a unit commitment of 15 minutes the total number of intervals per day  $n$  is exemplarily 96. [9]

$$\hat{\mathcal{E}}_{\text{opt, rel}}(n) = \frac{\hat{\mathcal{E}}_{\text{opt}}(n)}{\sum_{n=1}^{96} \hat{\mathcal{E}}_{\text{opt}}(n)} \quad (4.2)$$

The relative error distribution  $\hat{\mathcal{E}}_{\text{opt, rel}}$  should be equal to the new interval length distribution over time. [For this reason], the relative error per time interval is multiplied by the total number of setpoints (96) to redefine the number of setpoints per interval. This is summed up and plotted over time. To determine the new time interval length per setpoint, the inverse function of the previously described plot is calculated. As a result, a list of 96 entries with [exact points in time] is determined. This time information is used in the interval length assignment to prepare schedules for the evaluation within the EMS. [9]

An exemplary forecast result is depicted in Figure 4.7 with  $\hat{\mathcal{E}}_{\text{opt, rel}}(n)$  and the corresponding interval length assignment plotted over the intervals  $n$ .

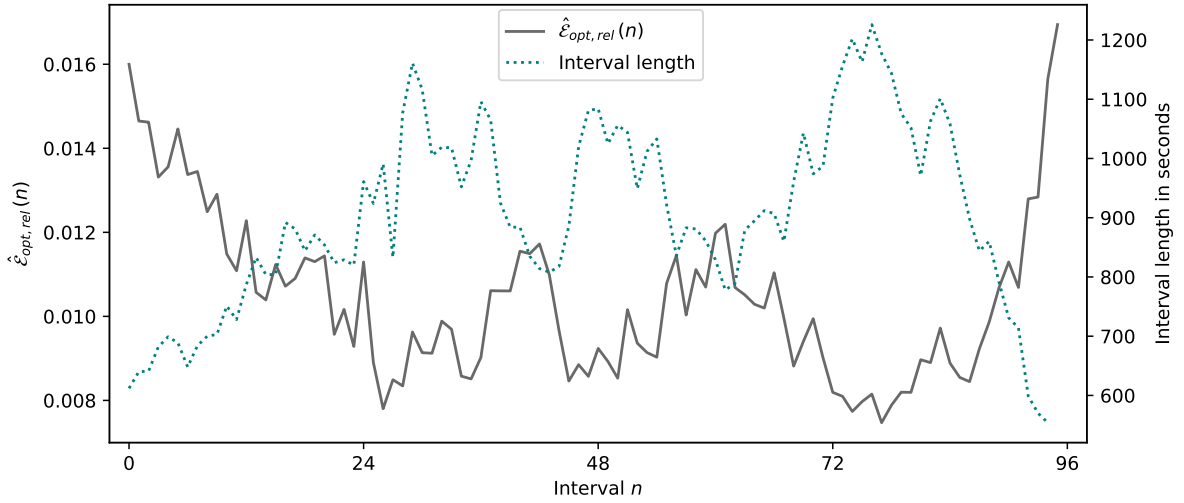


**Figure 4.7:** Exemplary determination of the interval lengths depending on the relative predicted error  $\hat{\mathcal{E}}_{\text{opt}}(n)$

### 4.3.6 Boundary Condition Enforcement and Evaluation

“Before the schedules can be evaluated, the technical boundary conditions of the underlying physical models must be checked, and, if necessary, the respective power fractions must be adjusted and updated schedules generated.” [9] During this process, in addition to the rates of change, the current SOC of a storage facility is monitored, and the technical possibility of implementing the proposed schedule is checked. For this purpose, the verifying instance, i.e., the EMS, has the corresponding information about the underlying models. After the boundary condition enforcement, the evaluation of the objective functions is conducted. These can be one or several different objectives which are evaluated. “The result for each schedule proposal and each objective is summarized in a list of results that are handed back to the EA for translation into fitness values per schedule proposal.” [9]

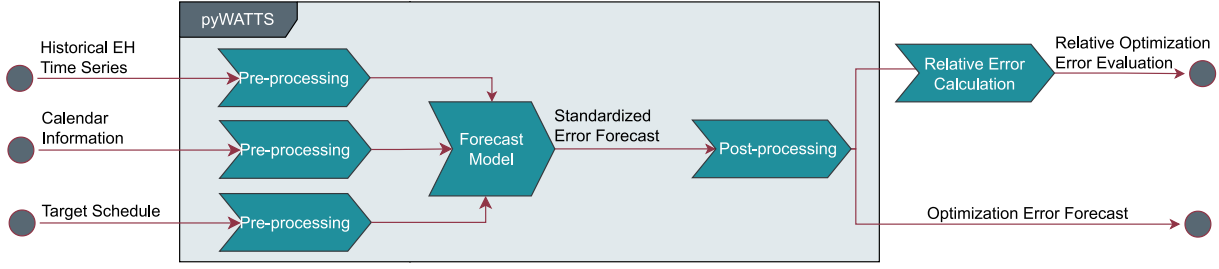


**Figure 4.8:** An overview of the approach used to forecast the optimization error. After pre-processing the input time series, the optimization error time series is forecasted and scaled in the post-processing step. From the optimization error forecast, the relative optimization error time series is calculated for the evaluation of the forecast quality.

### 4.3.7 Forecast Methods

The prediction of the optimization quality for the next 24 hours provides the basis for the interval length assignment. Since there is a monotonic relationship between the fitness value of the EA and the error between the target schedule and the actual EH power time series, that is, a larger error leads to less fitness, this error is used as a proxy for optimization quality. To forecast this error, the approach shown in Figure 4.8 is used and implemented as a pyWATTS [71] pipeline. In this section, the forecasting approach with the pre- and post-processing is described in detail, before discussing the evaluation criteria and the ML methods applied.

The optimization error time series  $\mathcal{E}_{\text{opt}}$  is defined as

$$\mathcal{E}_{\text{opt}}(t) = |\mathcal{P}_{\text{EH}}(t) - \mathcal{P}_{\text{Target}}(t)|, \quad (4.3)$$

where  $\mathcal{P}_{\text{EH}}$  is the power time series of the EH and  $\mathcal{P}_{\text{Target}}$  the target schedule time series. Additionally, the forecasts are evaluated in terms of the relative optimization error ( $\mathcal{E}_{\text{opt, rel}}(n)$ , see Equation (4.2)) and multiple ML methods are applied to generate the forecast.

Before the input time series are used in the forecasting model, pre-processing is needed. An overview of the pre-processing steps is given in Table 4.2. In pre-processing, first the numerical input time series are resampled to a resolution of fifteen minutes before standardizing them to move the mean to zero and scale the time series to a variance of one. Furthermore, important features are extracted from the calendar information, such as the day of the week and month of the year. To retain temporal similarity, the hour of the day, day of the week, and month of the year are extracted and encoded with Sine and Cosine.

Since the resulting optimization error forecast is also standardized, this forecast is post-processed in the inverse way to obtain the original scale. Therefore, the final forecast is the predicted optimization target error in the same scale as the input time series and is used directly to calculate the interval length assignment.

**Table 4.2:** An overview of the input time series used to forecast the EH power time series and the applied pre-processing applied to each of these time series

Input Time Series	Description	Pre-processing
Historical EH Time Series	Historical real world power values of the EH	<b>Resampling, Standardization</b>
Calendar Information	Calendar Information specifying the forecast period	<b>Feature Extraction:</b> Sine and cosine encoded hour of the day, day of the week, and month of the year. Boolean indicating whether it is a workday or not
Target Schedule Time Series	Target power values for the forecast period	<b>Resampling, Standardization</b>

To forecast the  $\mathcal{E}_{\text{opt}}$  time series multiple forecasting methods are considered. Each of these methods receives the same input data and directly forecasts the next 24 hours of the  $\mathcal{E}_{\text{opt}}$  time series, with a resolution of 15 minutes. This multi-horizon forecast approach results in each method having an output dimension of 96. Data for the entire year 2021 are used for training the models and evaluation of the models is conducted with data for the entire year 2022. The prediction is made using the target schedule and mean historical  $\mathcal{E}_{\text{opt}}$  values from 30 simulation runs to create a robust prediction for the error.

For benchmarking purposes, additionally a perfect forecast is considered. It is used to explore the maximum benefit of the proposed dynamic interval assignment and is not available in practical application. As the name suggests, this perfect forecast uses the true values as a forecast. In this case, the true values, which slightly differ due to the randomness of the used EA, are the mean optimization error calculated from the 30 simulation runs used for training. As simple forecasting methods, a Random Forest (RF) regression [131] and a K-Nearest Neighbors (KNN) regression [23] are considered, which are implemented using the default hyper-parameters from sci-kit learn [112]. Furthermore, a simple Feed Forward Neural Network (NN) [132] with six hidden layers consisting of 256, 210, 150, 80, 64, and 52 neurons respectively, is implemented with sci-kit learn [112]. To include a simple state-of-the-art method, an XGBoost regression [36] is implemented with default hyper-parameters using the XGBoost library<sup>1</sup>. Finally, to include state-of-the-art forecasting methods, the Neural Hierarchical Interpolation for Time Series Forecasting (N-HITS) [35], and Temporal Fusion Transformer (TFT) [93], both implemented with default hyper-parameters via the PyTorch Forecasting library<sup>2</sup>, are considered.

<sup>1</sup> <https://xgboost.readthedocs.io/en/stable/>

<sup>2</sup> <https://pytorch-forecasting.readthedocs.io/en/stable/>

In this section, [the] novel approach for scheduling DERs using an EA with dynamic genotype-phenotype mapping based on [ML techniques] is presented. This approach focuses on the interpretation of the proposed solution of the employed EA [rather than the EA itself]. Hence, the approach is adaptable to any EA for optimized scheduling applications that uses an external evaluation service for the calculation of [the objective functions of the proposed chromosomes]. [9]

### 4.3.8 Evaluation Criteria

As described in Section 4.3.5, the computational effort of the optimization is directed through the assignment of varying interval lengths. This interval length assignment is calculated based on the relative optimization error defined in Equation (4.2). As a result, the forecast of the optimization quality should ideally perform well with regard to the relative optimization error. More specifically, it is more important that the forecast accurately predicts the relative optimization error for a certain point in time than the actual optimization error. For example, a forecast that does not predict the true optimization error but mimics the relative error exactly would also be useful for the optimization problem. Therefore, to evaluate the performance of the forecasts in terms of the relative optimization error, first the relative optimization error time series is calculated according to Equation (4.2). Then the quality of the forecast based on this relative optimization error time series is evaluated.

### 4.3.9 Evaluation of the Hybrid Optimization

The approach described in Subsection 4.3.2 is implemented for an evaluation of the concept and the proposed forecasting methods. In this subsection, the evaluation is presented by first introducing the evaluation environment, including a definition of the use case and the evaluation criteria to assess whether the approach enhances the flexibility provision of an EH. Furthermore, the evaluation comprises the forecast of the optimization quality and the optimization results with a dynamic interval length assignment.

#### 4.3.9.1 Evaluation Environment

The evaluation environment is based on previous work [7] as described in Chapter 3 and the relevant data for the use case are taken from real-world data from the years 2021 and 2022, according to [6]. More specifically, the electrical load profile of an industrial area for the mentioned period is used for defining the target schedule depicted in Figure 4.9, which would be provided by a DSO or TSO in a real-world application for flexibility retrieval. The target schedule aims to dampen the power flow variation at the substation to enable further RESs installation and integration.

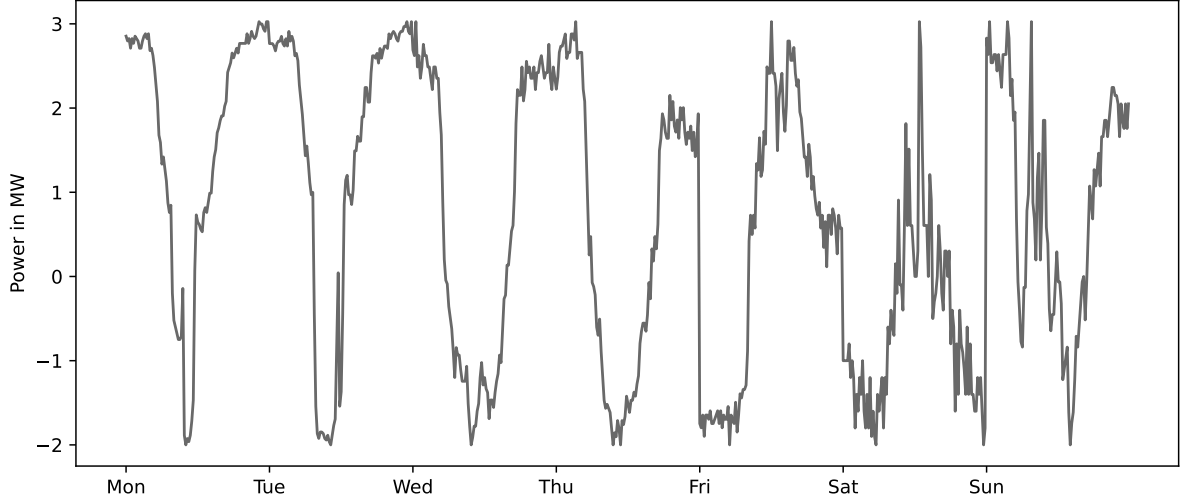


**Figure 4.9:** Target schedule to be approximated from the EH for the evaluated exemplary week

Two different EAs are employed to solve the optimization problem. On one hand GLEAM is used with the general configurations of a limit of 50 generations and a population size of 100. These settings have been tested and explored in advance and proved to produce sufficiently good results as shown in Section 4.2 with Table 4.1 and consistent with the findings in [66]. Further settings concerning the genetic operators are adopted from [26, 78, 79]. On the other hand the framework DEAP is implemented with NSGA2 as algorithm. DEAP with NSGA2 is set up with the same configuration as GLEAM regarding the population size and the amount of generations. As presented in the comparison of both algorithms in Subsection 3.3.8 the genetic operators differ slightly. The concept, presented in Subsection 4.3.2, is applied to both algorithms to investigate whether the hybrid optimization approach is algorithm specific or generally applicable. Although the optimization is implemented as a multi-objective optimization, the evaluation of the presented approach concentrates on the objective of approximating the given target schedule for the electrical output of the EH. Hence, as evaluation criteria, two different aspects are taken into account. First, the general quality of the approximation by the optimized scheduling is assessed by calculating the RMSE, the resulting  $DOF_{RMSE}$  according to [8] and as described in Section 3.4, and its fitness representation within GLEAM. The corresponding objective function is given by Equation (4.4). Taking the  $DOF_{RMSE}$  into account for the evaluation, the approach is compared to the theoretical upper and lower boundaries, as described in [8] and Section 3.4. The second objective, the operational costs expressed as  $DOF_{Cost}$ , is evaluated in Subsection 4.3.10.3.

$$\min d_{RMSE} = \sqrt{\frac{\sum_{n=1}^{96} ((\mathcal{P}_{EH}(n) - \mathcal{P}_{Target}(n)) * \Delta t(n))^2}{96}} \quad (4.4)$$

**Table 4.3:** An overview of the MAE and RMSE, as evaluation metric for the optimization target error  $\hat{\mathcal{E}}_{\text{opt, rel}}$ , calculated over the forecast period for each of the considered forecasting models and the different optimization algorithms on the test data set. The best values for each metric are highlighted in bold.

Model	GLEAM		DEAP	
	RMSE	MAE	RMSE	MAE
RF	<b>0.007066</b>	<b>0.005608</b>	<b>0.005031</b>	<b>0.003923</b>
NN	0.008377	0.006711	0.005992	0.004659
XGBoost	0.007199	0.005672	0.005523	0.004259
N-HITS	0.008855	0.007135	0.006272	0.004816
TFT	0.009319	0.007400	0.007152	0.005467

Second, the influence of the forecast quality is determined by comparing two different forecast models (RF and TFT model) to a perfect forecast as ground truth and the base case without dynamic interval length assignment.

#### 4.3.9.2 Forecast of the Optimization Quality

To decide which forecasting model to use for the interval length assignment, first, the quality of the forecasts for the optimization error time series is evaluated. This is conducted by calculating the Mean Absolute Error (MAE) and RMSE for each forecasting model presented in Table 4.3 on  $\hat{\mathcal{E}}_{\text{opt, rel}}$ .

With regards to MAE and RMSE, it is observed that the RF performs best, both for GLEAM and DEAP. XGBoost performs comparably well. Furthermore, the N-Hits and the NN perform similarly to each other. The TFT performs noticeably worse in comparison to every other forecasting model. While the ranking of the prediction models within a training dataset is the same, it should be noted that the prediction quality of the models trained on the DEAP data is significantly better overall.

To further evaluate the approach, two forecasting models used to determine the dynamic interval length assignment are applied and further evaluated. First, the RF model is selected as the best forecasting model. Second, to investigate whether a poor forecast is also beneficial, the TFT is applied as the worst forecasting model. Combined with the benchmark perfect forecast, this selection includes a range of forecasts with varying performance and allows to evaluate the benefit of the approach accurately.

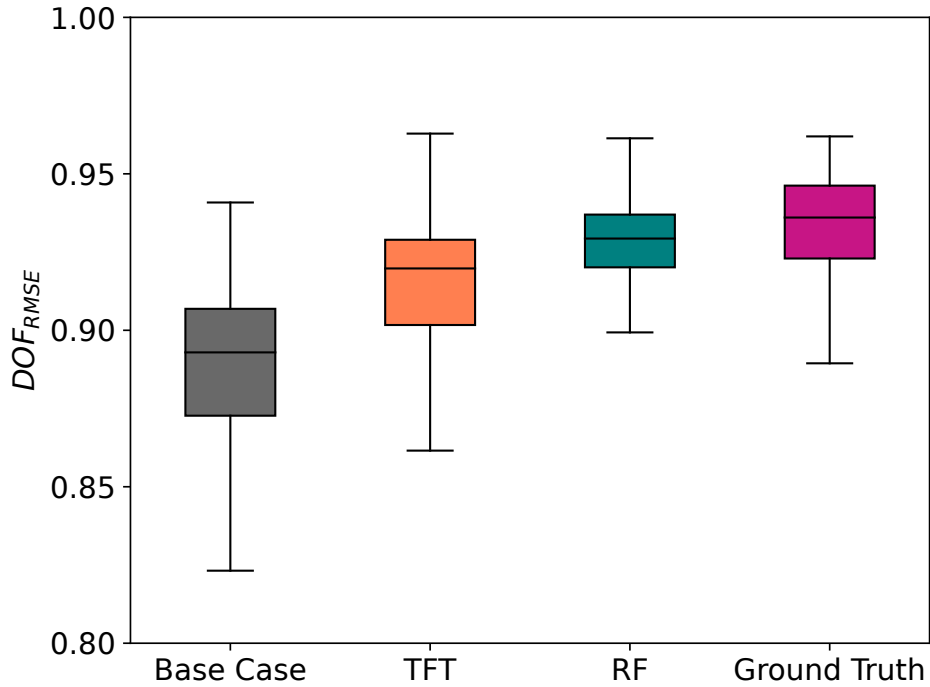


**Figure 4.10:** Boxplot of mean  $DOF_{RMSE}$  values for each considered case calculated over the complete week. The Base Case performs worse, whilst the Ground Truth results in the highest  $DOF_{RMSE}$ . Using the two forecasting models in the interval length assignment increases the  $DOF_{RMSE}$  compared to the Base Case.

### 4.3.10 Results with GLEAM

To evaluate the approach, an exemplary week in 2022 is considered. This week is characterized by a typical load profile for an industrial area, which is the basis for the target schedule to approximate. In total, four different cases are compared in the evaluation. First, a fixed-time interval optimization is performed for each day of the week to generate a *Base Case*, i.e. optimized schedules for the EH as they would be generating according to previous work. Second, a *Ground Truth* forecast is created that is based on previous optimization results that are also used for the evaluation of the forecasting models. This Ground Truth is then used for the time interval length assignment and is included to show the maximum potential of the approach. Third, the forecasts from the trained RF for the interval length assignment, and fourth, the forecasts from the trained TFT are used.

Given these four cases and the exemplary week, first the average performance over this week is evaluated before considering the performance for each day individually. In the following, the results of these two evaluations are reported.



#### 4.3.10.1 Weekly Performance

The mean  $DOF_{RMSE}$  of each considered case (Base Case, RF, TFT and Ground Truth) for a full week is depicted in Figure 4.10. The mean  $DOF_{RMSE}$  of the Base Case over 30 repetitions of the week, resulting in 210 optimizations, is 88.9%. Using the forecast results of the RF model, the mean  $DOF_{RMSE}$  is 4.4% higher at 92.8%. Furthermore, the mean  $DOF_{RMSE}$  obtained with the TFT model is 91.3% and 2.7% higher than the Base Case. Finally, using the Ground Truth results in a mean  $DOF_{RMSE}$  of 93.2%, which is increased by 4.8% compared to the Base Case. Interestingly, the variance of the  $DOF_{RMSE}$  values is similar for all cases except for the RF, where a noticeably smaller range of values over the optimizations is observed. Taking the improvement of the optimization quality by using the perfect forecast as a benchmark, the RF model achieves 92% of the maximum, and the TFT model reaches 56% respectively.

Regarding the significance of the differences in mean  $DOF_{RMSE}$ , one must first note that according to the D'Agostino-Pearson test for normality [41], the results suggest a normal distribution for all four cases (p-values  $\ll 1\%$ ). Therefore, the parametric statistical t-test according to [49] is utilized to compare the result's distribution of the Base Case and the three cases using the dynamic interval length assignment. All three tests carried out show with sufficient confidence (p-values  $\ll 1\%$ ), that the  $DOF_{RMSE}$  of the cases with dynamic interval length assignment are better than those of the Base Case.

#### 4.3.10.2 Daily Performance

In Figure 4.11, the daily  $DOF_{RMSE}$  from three cases (Base Case, RF, and TFT) are compared across the week considered in 2022. Furthermore, the associated evaluation metric (MAE and RMSE) for each day for the two considered forecasting models are plotted. On the basis of this plot, three key observations can be made. First, the dynamic interval length optimization improves the  $DOF_{RMSE}$  for each day when using the RF model and for each day except Monday when using the TFT model. Second, there is a large variation in the  $DOF_{RMSE}$  across the days for all cases considered. However, this variation is most noticeable in the Base Case and least noticeable when using the RF for the interval length assignment. Third, a general correlation between the evaluation metrics of the forecasting model (MAE and RMSE) and the  $DOF_{RMSE}$ , respectively the fitness, improvement when using the corresponding forecasting model for the interval length assignment can be observed. Specifically, the performance of the TFT is noticeably worse than that of the RF on Monday, resulting in a worse  $DOF_{RMSE}$ . A similar result is seen on Thursday and Friday, where the TFT also performs worse. On Tuesday and Wednesday, the performance of both forecasting models is similar, resulting in a similar  $DOF_{RMSE}$ . However, this correlation cannot be confirmed for the weekend. On Saturday and Sunday, the TFT performs worse than the RF according to the evaluation metrics, but the resulting  $DOF_{RMSE}$  is similar or higher.

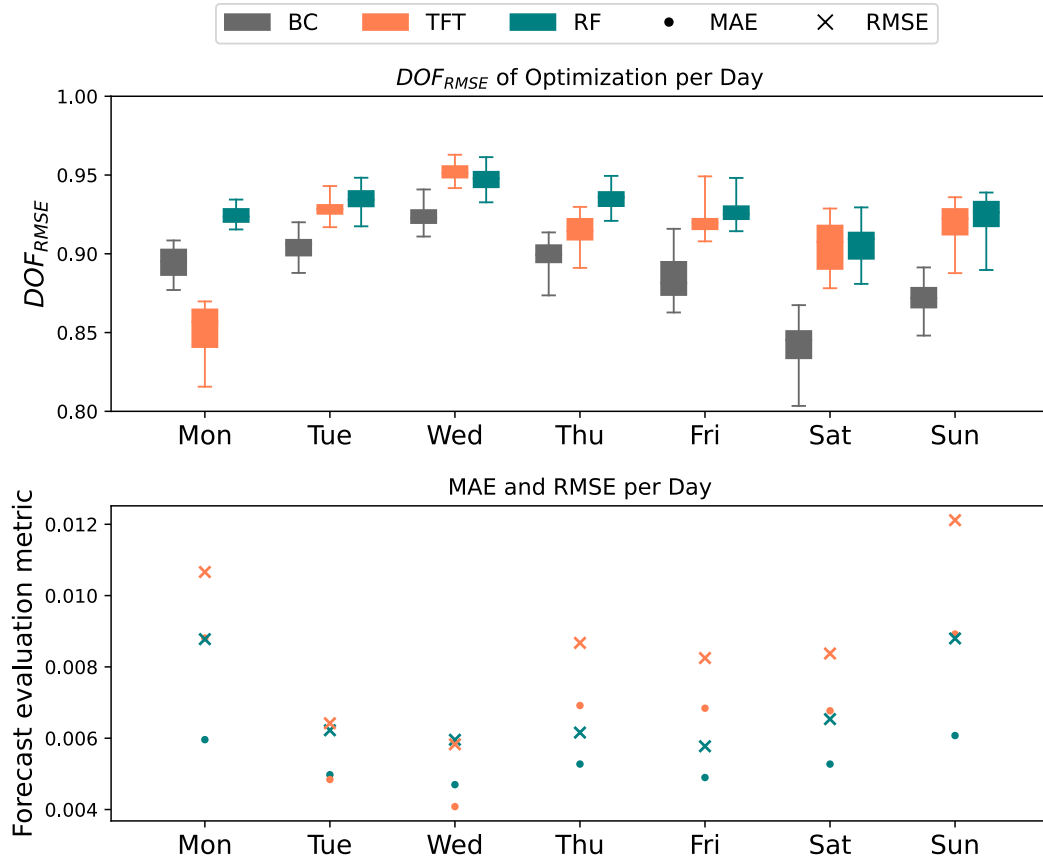


**Figure 4.11:** A comparison of the daily  $DOF_{RMSE}$  and the associated forecast evaluation metric (MAE or RMSE) for each day in the considered week. The  $DOF_{RMSE}$  of the Base Case (BC) is plotted along with the results using the dynamic interval length optimization based on the RF and TFT. The results show a large variation in  $DOF_{RMSE}$  across the days and a general correlation between the evaluation metrics and the obtained  $DOF_{RMSE}$ .

#### 4.3.10.3 Effect on Operational Cost Objective

The interval length assignment, described in Subsection 4.3.2, is based only on the forecast of the optimization quality considering the RMSE objective. To evaluate whether this approach effects also the second objective, the minimization of the operational costs, Figure 4.12 shows the respective optimization results for the considered week for the operational cost objective expressed as  $DOF_{Cost}$  for costs calculated according to the procedure introduced in Section 3.4. The optimization process always considers both objectives with the concept of WS as described in Section 2.4. The RMSE objective is weighted with 60% while the operational cost objective is weighted with the remaining 40%. The optimization results are reported separately to clearly distinguish the influence of the present approach on each objective. The mean  $DOF_{Cost}$  is for

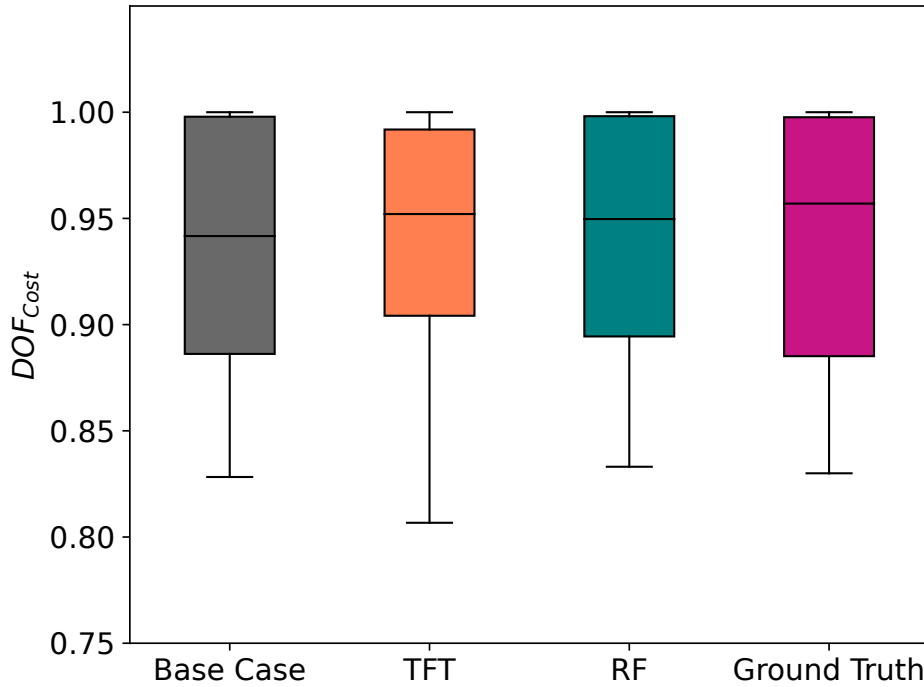


**Figure 4.12:** Boxplot of the  $DOF_{Cost}$  considering the operational cost objective to outline that the dynamic interval length assignment has no effect on this objective

all four cases similar around 95%. Furthermore, the variance only reports a marginal difference between the cases.

### 4.3.11 Results with DEAP

A second evaluation is conducted with DEAP and NSGA2 as employed EA. The same exemplary week in 2022 is considered as with GLEAM in the previous Subsection 4.3.10, but the training data set is now produced by DEAP with NSGA2 instead of GLEAM. Also, four different cases are compared in the evaluation. First, a fixed-time interval optimization is performed for each day of the week for the *Base Case*. Then, the *Ground Truth* based on previous optimization results, a newly trained RF model, and a TFT on the basis of the same training procedure with training data for the year 2021 as described in Subsection 4.3.7 is used for the time interval assignment. The evaluation is conducted according to the results obtained with GLEAM and therefore, first, the average performance over the entire week is reported, followed by a daily evaluation.

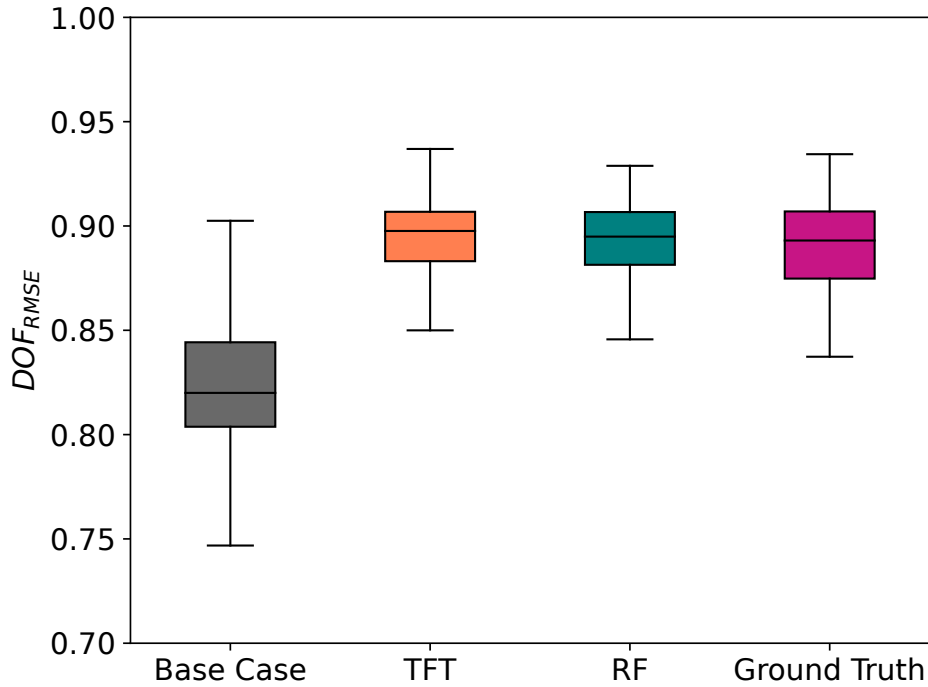


**Figure 4.13:** Boxplot of mean  $DOF_{RMSE}$  values for each considered case calculated over the complete week with DEAP. The Base Case performs worse, whilst using the two forecasting models and the perfect forecast in the interval length assignment increases the  $DOF_{RMSE}$  compared to the Base Case.

#### 4.3.11.1 Weekly Performance

The mean  $DOF_{RMSE}$  of each considered case (Base Case, RF, TFT and Ground Truth) for a full week is depicted in Figure 4.13. The mean  $DOF_{RMSE}$  of the Base Case over 30 repetitions of the week, resulting in 210 optimizations, is 82.3%. Using the forecast results of the RF model, the mean  $DOF_{RMSE}$  is 8.6% higher at 89.4%. Furthermore, the mean  $DOF_{RMSE}$  obtained with the TFT model is 89.3% and 8.5% higher than the Base Case. Finally, using the Ground Truth results in a mean  $DOF_{RMSE}$  of 88.9%, which is increased by 8.0% compared to the Base Case. Hence, the full potential for enhancement of the  $DOF_{RMSE}$ , represented by the Ground Truth, is already reached by the considered models.

Analogous to the statistical analysis of the results obtained with GLEAM, the same test on normality is conducted. The prediction results suggest a normal distribution according to the D'Agostino-Pearson test [41]. The following parametric t-test according to [49] confirms with sufficient confidence (p-values  $\ll 1\%$ ) the advantage of the dynamic time interval length assignment over the Base Case.

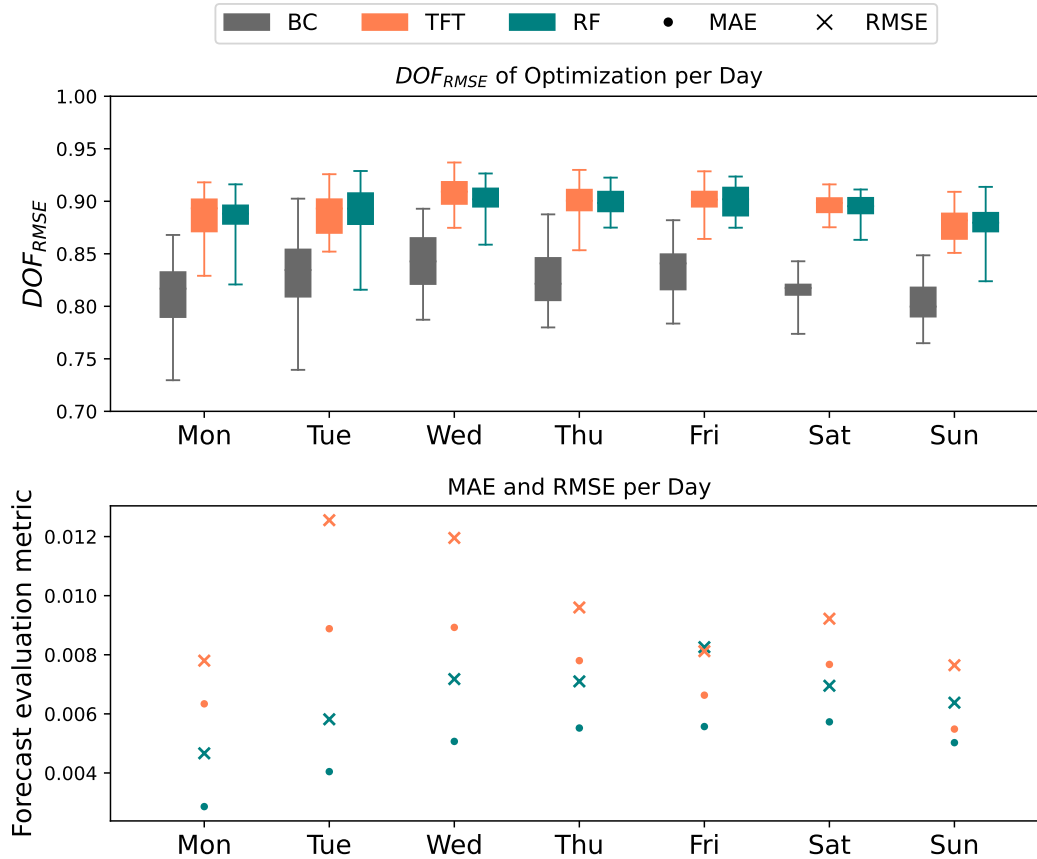


**Figure 4.14:** A comparison of the daily  $DOF_{RMSE}$  and the associated forecast evaluation metric (MAE or RMSE) for each day in the considered week. The  $DOF_{RMSE}$  of the Base Case (BC) is plotted along with the results using the dynamic interval length optimization based on the RF and TFT. The results show a large variation in  $DOF_{RMSE}$  across the days and a general correlation between the evaluation metrics and the obtained  $DOF_{RMSE}$ .

#### 4.3.11.2 Daily Performance

In Figure 4.14, the daily DOF from the two models (RF and TFT) are compared to the Base Case across the week considered in 2022. Furthermore, the associated evaluation metric (MAE and RMSE) for each day for the two considered forecasting models are plotted. Both models improve the  $DOF_{RMSE}$  for each day in the week. The mean  $DOF_{RMSE}$  in the Base Case ranges from around 80% to 85%. The daily performance for both, the RF and the TFT model is nearly the same and ranges from around 88% to 92%, while the highest  $DOF_{RMSE}$  is reached on Wednesday for all three cases. Besides the general performance enhancement, the variance per day is significantly smaller using the dynamic time intervals based on the forecast models.

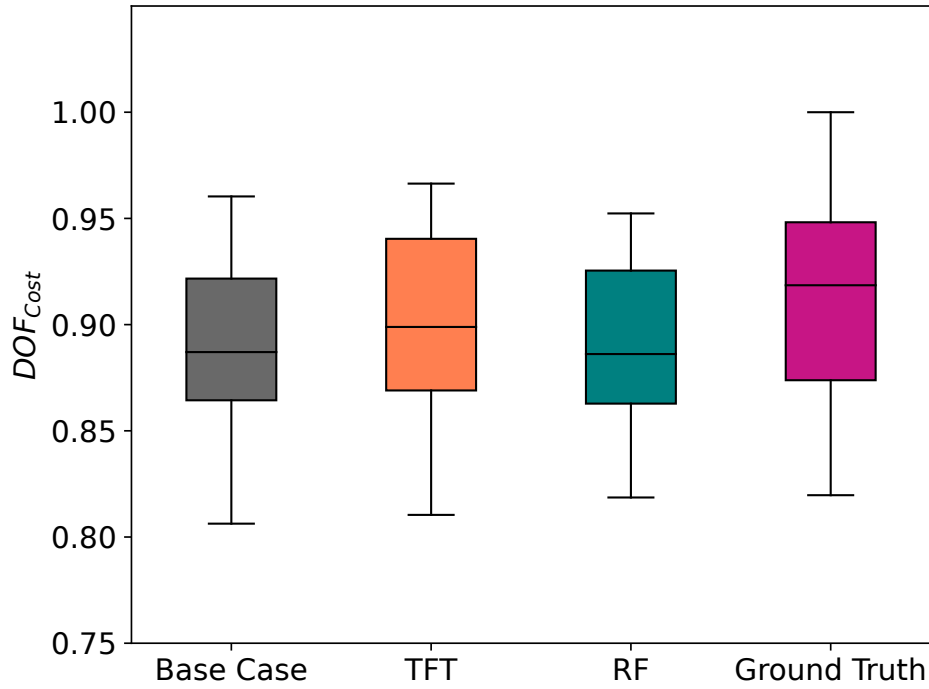


**Figure 4.15:** Boxplot of the  $DOF_{Cost}$  considering the operational cost objective to outline that the dynamic interval length assignment has no effect on this objective

#### 4.3.11.3 Effect on Operational Cost Objective

According to the evaluation of the results obtained with GLEAM the effect of the interval length assignment on the operational cost minimization objective is analyzed also for DEAP. Figure 4.15 shows the respective optimization results for the operational cost objective expressed as  $DOF_{Cost}$ . The mean  $DOF_{Cost}$  is for all four cases similar around 90%. Furthermore, only a marginal difference in the variance between the cases is observable.

# 5 Discussion

In the following chapter, the presented concepts and consecutive obtained evaluation results are further discussed to outline the main benefits as well as the drawbacks. First, in Section 5.1, the key benefits and limitations of the co-simulation approach are outlined. Second, the results of the main contribution are discussed in Section 5.2 to provide detailed insights and a critical examination.

## 5.1 Energy Hub Gas

The results of the simulations of the co-simulation model in Section 3.3 already show the positive effect that an EHG can have on the surrounding electrical grid area in two different test cases. Due to the dampened power peaks in the electrical grid caused by the EHG, additional capacities are available to integrate volatile renewable generation. However, some limiting factors must be taken into account when assessing the provision of flexibility by the EHG. Firstly, it should be noted that only one instance of the EHG was considered in the simulation results of the two different test cases presented. Comparing the results of both test cases leads to the conclusion that the usefulness of an EHG highly depends on its composition and the corresponding objectives of its application. While in TC1 the average attenuation for the complete simulation period results in a reduction of the difference between minimum and maximum active power load by 11.6%, in TC2 only 4.9% can be reduced. A possible reason for this deviation may be the significantly higher share of WPPs generated RE in TC2. However, the aforementioned modularity offers the possibility of investigating customized system compositions for a wide variety of applications. A corresponding design optimization for the optimal system composition is useful and required for this. The presented EHG instance is tailored to meet the demand of both presented industrial areas in south-west Germany as well as the coastal area in northern Germany.

Furthermore, the evaluation of the results is limited to the operating costs. An overall assessment and a comparison with an alternative solution, e.g., a classic grid expansion, can only be meaningfully evaluated with a total cost calculation. On the positive side, however, it must be emphasized that a corresponding EHG is available much more quickly than is the case with a grid expansion due to the lengthy planning and approval processes. This fact compensates a possible disadvantage at the total cost comparison in the way to fasten the required energy transition.

However, the current legal situation does not make it clear which stakeholder is eligible to operate an EHG. Apart from operators of larger industrial areas with diverse energy demands and the incentive to reduce the power price to be paid through peak capping, the current legal situation prohibits, for example, a grid operator from operating an EHG. In addition, the possible revenue from compensations to be paid for feed-in management measures needs to be further defined. In order to incentive a DSO or TSO to activate the flexibility provision by an EHG instead of making use of feed-in management and thereby curtailing RESs, a corresponding cost saving must be achieved for grid operators, so that the assumption of full compensation of the grid operator's costs as revenue for the EHG operator must be viewed critically. Furthermore, the trading of flexibility for the electricity grid is not uniformly regulated. Several approaches and demonstration sites are under development in recent research. Although there is a balancing energy market, this requires pre-qualification, which excludes the EHG in its current form, due to its dimensioning. The objective of the EHG also does not correspond to the provision of balancing energy. The use of the EHG is more in line with the new regulation of Section 14 of the Energy Industry Act or a low-threshold flexibility market. However, these economic and legal considerations are outside the scope of the thesis, as they need expert knowledge.

In addition to the positive effects on the electricity grid, the EHG establishes the connection to other energy sectors with its sector coupling components. In the context of the results presented, the focus is placed on relieving the electricity grid. The gas and heating grids are considered in a simplified manner. However, the proposed architecture would also allow the gas and heating infrastructure to be integrated in detail alongside the electricity grid. By varying the considered technologies (modularity) and certain plant sizes either by scale-up (scalability) or numbering-up (modularity), the effects of different system network configurations on the grid infrastructure can be adjusted. Furthermore, chemical energy carriers like  $H_2$  or  $CH_4$  provided by the EHG can be considered RE by the assumption that only surplus energy generated locally by RESs is converted. In fact, the true  $CO_2$  footprint of these energy carriers cannot be clearly determined as long as the electricity grid includes energy generated by conventional power plants. However, this simplification is also due to the lack of a legal framework and a detailed certification analysis is outside the scope of this work.

## 5.2 Hybrid Optimization

The evaluation shows the prospects of this approach. However, there are numerous points worth discussing further. In this section, first these results are discussed in more detail before highlighting some key aspects regarding the forecasts of the optimization quality. Finally, the limitations and benefits of the approach are discussed.



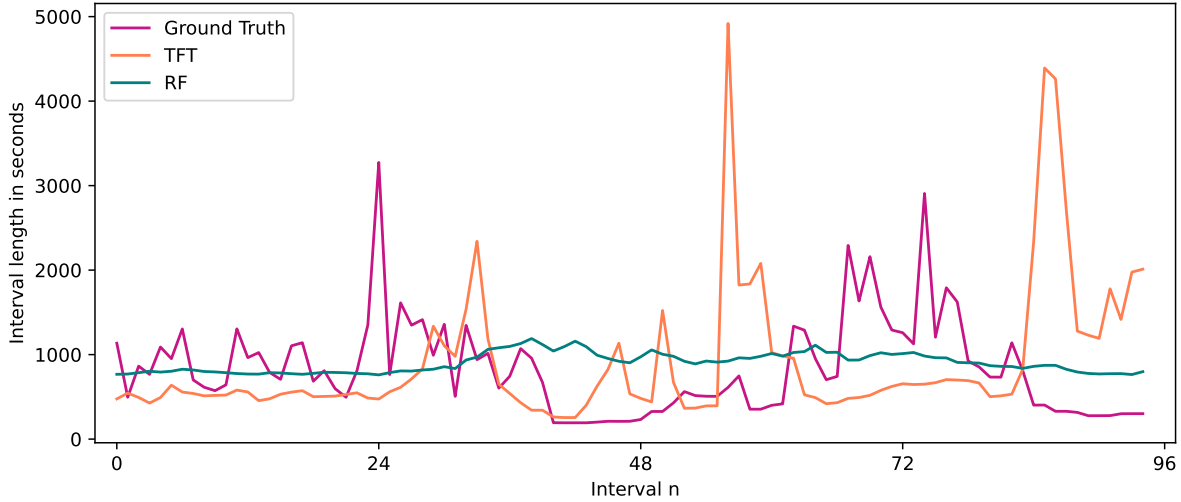


**Figure 5.1:** Interval lengths of the different forecasting models RF, TFT and the Ground Truth for Sunday, April 10<sup>th</sup>, 2022

### 5.2.1 Insights from Results

With regard to the results, four important aspects are discussed in more detail. First, the results obtained in Subsection 4.3.10 and Subsection 4.3.11 show that the proposed approach can be used to enhance the optimization results of an EA and thus obtain a better approximation of the underlying power output of an EH to a target schedule. This results in a quantitative better flexibility provision by an EH and the underlying DERs. From a qualitative point of view, the better approximation of the optimization to the target schedule results in a more reliable flexibility provision. The quantitative aspect of the improvement is expressed by the higher  $DOF_{RMSE}$  achieved. Second, the presented approach improves not only the mean optimization results, but also reduces the variance in the  $DOF_{RMSE}$  results. This effect is more obvious in the results obtained with DEAP than in those from GLEAM. This could be due to the fact that the achieved optimization results of DEAP are poorer and the forecast quality is significantly better, so that the concept can reach its full potential.

Third, when the optimization forecast improves, this generally results in an improvement in the reached  $DOF_{RMSE}$ . However, fourth, this correlation does not carry over to weekends when using GLEAM. One possible explanation for this lack of correlation is the difference in the weekend target schedule, as observed in Figure 4.9. Due to this differing target schedule, the TFT is possibly directing the computational power to a particularly difficult region on weekends, even though its performance across the entire week is worse. This is underlined by the interval lengths assigned to each interval as depicted in Figure 5.1. Three peaks in the interval length determined based on the TFT model lead to shorter intervals throughout the remaining intervals, which means higher computational effort.

With DEAP the correlation between forecast quality and  $DOF_{RMSE}$  is more difficult to analyze. While the optimization over the considered week on average improves proportional to forecast quality, the daily performance of the forecast is not directly reflected in the  $DOF_{RMSE}$ . Therefore, it is important to further analyze the performance of the forecast and its ability to identify complex regions. This is underlined by a detailed analysis in the following Subsection 5.2.2.

Finally, it can be stated, that the dynamic interval length assignment has no effect on the operational cost objective. Neither with GLEAM nor with DEAP a significant influence can be found in the  $DOF_{Cost}$ . This may be due to the fact that the prices for energy carriers fluctuate much more slowly than the target schedule does.

## 5.2.2 Forecast of Optimization Quality

Although the results are promising, the forecasts have not been explicitly designed to meet the dynamic interval length calculation requirements: For this dynamic interval length calculation, the forecasts should be designed to accurately predict the shape of the optimization error, independent of the scale. This is due to the relative optimization error (see Equation (4.2)) used when determining the dynamic interval length. Currently, all forecasting models are trained with quality-based metrics, such as MAE and RMSE, and an accurate forecast according to these metrics may not be optimal regarding the shape. Therefore, it would be interesting to investigate whether forecasts explicitly considering shape metrics in the training process improve the results.

Furthermore, the predictions of the optimization quality are based on a single simulation run for a complete year compared to the perfect forecast, which is calculated as the mean of 30 simulation runs. However, the promising results of the forecasts suggest that the considered forecasting methods are robust and that multiple simulation runs are not required. Nevertheless, also considering basing the forecasts on multiple simulation runs to investigate whether this further increases the accuracy and robust nature of the forecasts is of interest.

Comparing the forecast quality, listed in Table 4.3 and the enhancement of the  $DOF_{RMSE}$  based on the applied forecasting model to the interval length assignment between both algorithms for the complete week, depicted in Figures 4.10 and 4.13, it shows that  $\hat{\mathcal{E}}_{\text{opt, rel}}$  is better predicted with the RF model trained on DEAP than on GLEAM results. This correlates with a higher improvement in the  $DOF_{RMSE}$  for DEAP in comparison to GLEAM. This correlation is similar for the TFT model. Furthermore, a comparison between both models (RF and TFT) for each algorithm also supports the correlation between the forecast error on  $\hat{\mathcal{E}}_{\text{opt, rel}}$ , either expressed as MAE or RMSE, to the improvement of the resulting  $DOF_{RMSE}$ . Additionally, the improvement of the  $DOF_{RMSE}$  with DEAP and both RF and TFT as forecast models is similar to the Ground Truth. A possible explanation for this is that the forecasting performance is good enough to realize the approach's full potential.

### 5.2.3 Limitations and Benefits

The first limitation of the approach is that it requires an initial training dataset. As a result, when no prior data are available, i.e., the "cold start" problem, it is currently impossible to directly apply the approach. A second limitation of the approach is that only one objective (RMSE) is considered for the dynamical interpretation of chromosomes, due to the focus on flexibility provision. Consequently, the positive effect of the approach is concentrated on the same objective without any influence on other objectives. A further limitation of the approach is that it currently does not consider uncertainty. Therefore, it would be interesting to include uncertainty in the approach, perhaps similar to Appino et al. [15] and González-Ordiano et al. [62]. To address this problem the present approach could be implemented in a rolling horizon optimization process. This allows the consideration of changing target schedules according to updated forecasts of RESs generation and load in order to enhance the flexibility provision by the EHG.

The main benefit of the approach is the general performance, which leads to an improvement of the optimization results. Up to 8.6% increase in  $DOF_{RMSE}$  is reached when using the RF model for DEAP. Furthermore, the implemented forecasting models, i.e., RF and TFT, show sufficiently good results by enhancing optimization results either with GLEAM or DEAP. This enhancement leads to a significant improvement of the flexibility provision by the underlying EHG, which follows the target schedule more closely. "Thereby, the concept of guiding the computational effort of the EA on difficult time segments helps to improve the results." [9] Another key benefit is the computational effort. "After the forecasting model is trained once, no additional computational effort is needed to improve the optimization results. This is achieved by intelligently allocating the computational effort [...] based on the optimization quality prediction." [9] However, the additional computational effort required to create the training data and train the forecasting model should be worthwhile in terms of the application. Furthermore, the evaluation suggests that simple forecasting methods with default hyper-parameters and simple input features are sufficient to improve optimization quality. Finally, the transferability of the approach needs to be discussed. There are two different perspectives on transferability: First, to interchange already trained forecasting models from one EA to another. Second, once a forecasting model is trained, the considered EH instance could be changed. Generally, it is shown that the approach is able to improve the optimization results for two different EAs using the same chromosome encoding. But it is necessary to train the forecasting models on previous data provided by the respective EA. Tests to interchange the forecasting models failed. A concept for transfer learning could address this aspect. Furthermore, in the present thesis, the trained models are applied only to the same instance of the EHG, which provided the training data set. For the mentioned cold start problem, it would be interesting to apply a trained forecasting model on a different instance of the EH concept.



## 6 Conclusion

The present work shows the methodological setup and implementation of an EH that operates independently of any specific co-simulation framework in a modular fashion with the opportunity to flexibly adapt the EH to the requirements of a use case. The investigated concept offers grid supporting services and can help with the integration of RES feed-in (electricity). Furthermore, it serves as a regional gateway for renewable energy carriers (molecules). Scalability and modularity are essential features for expanding the model in the future. They allow the application of the EH approach across diverse scenarios and infrastructure setups. Using the modular concept of the co-simulation setup and configuration, two test cases were investigated using different goal settings, surrounding generation, and demand structures. The results demonstrate the positive effect that an EHG can achieve, providing an answer to RQ 1. By relieving the power grid, new RESs can be built and integrated, and the curtailment of already existing RESs can be reduced. The results indicate that bidirectional coupling of, e.g., the gas and electricity grids offers flexibility to the power grid, reducing power flow volatility. Consequently, fewer infrastructure measures are needed in order to integrate further RESs, which in turn results in a total CO<sub>2</sub> reduction for the electricity generation mix.

The performance of the employed optimization method is decisive for the applicability of the mentioned results. Further optimization improvement will further improve flexibility provision in terms of reliability and achievable energy quantities. EAs are a viable approach for this complex scheduling problem, as shown in this thesis and several previous works. However, some generic EAs require the mapping of objective values to fitness values. This mapping can heavily influence the evolutionary process, and the choice of a suitable mapping function is an ongoing challenge. Hence, the present work introduces a concept to dynamically evaluate the objectives to parameterize the boundaries of the mapping function. This is conducted on the basis of forecasts for the relevant influences, e.g., energy prices. As the evaluation of the concept shows qualitatively, expert knowledge is no longer required to parameterize the considered mapping function. Furthermore, test cases show a quantitative significant improvement in the found solutions by the tested EA. Solutions using the described concept of dynamic mapping exceed the DOFs that was achieved without the concept applied by 10.2%. As a positive side effect, the concept has made the weighting between different objectives more controllable. The relation between the weights of operational costs and flexibility provision by following a given target schedule can now be investigated in depth. One direction could be determining the costs for providing flexibility by following an external target schedule.

This thesis further examines the impact and application of varying time resolutions in schedule optimization in the context of the EH concept to answer RQ 2. It introduces a novel approach using adaptive time segments for EA-based schedule optimization, alongside a method to pinpoint time segments that would benefit from different time resolutions. Initially, a schedule is generated with a low time resolution; then, the results guide the identification of segments requiring higher resolution optimization. These specific segments are subsequently recalculated at a higher time resolution. Tests on various time resolutions in the optimization process, along with the new method, were conducted and analyzed. Findings indicate that higher time resolutions across an entire schedule do not always enhance performance. However, focusing higher resolution on specific time segments leads to better optimization results. The average deviation between the EH's electrical output and the target schedule is reduced by 11%, which results in a more reliable flexibility provision. The study also demonstrates that similar outcomes in deviation and processing time can be achieved with different EA parameter settings. Thus, this research highlights that scheduling an EH with adaptive time segments and varying time resolutions can enhance the flexibility that an EH can offer.

By introducing a forecast of the optimization results, the previously shown method can be further enhanced. The forecast results direct the computational effort of the applied EA to time segments that are difficult to approximate. Thus, no additional computational effort is needed after an initial model training in order to find better solutions within a single optimization run. By applying ML models to perform optimization result predictions, once trained, the generated forecasting model can be used to direct the computational effort of the EA towards time segments that are difficult to approximate. Consequently, the strategy eliminates the need for additional computational resources to find better solutions. With the evaluation of two forecasting models used to determine dynamic interval length assignments, an answer to RQ 3 is given. When using the RF model, the improvement of the  $DOF_{RMSE}$  of the optimization is 4.4% on average for GLEAM and 8.6% for DEAP. The TFT model enhances the optimization results by 2.7% for GLEAM and 8.5% for DEAP, respectively. These improvements are both statistically significant and form a basis for better flexibility provisioning from the considered DERs. Furthermore, it is shown that the approach does not affect further objectives.

As previously discussed, several aspects of the presented approaches are worth further investigation in future work. These aspects are considered out of scope for the present thesis but could lead to a deeper understanding of the opportunities for flexibility provision by EHs. First, throughout the thesis it is assumed that the pre-defined target load provided by a system operator as well as the generation by RESs and prices for different energy carriers are known in advance. With the presented concepts and their modular architecture of the system, in future work implementing probabilistic forecasts for the above mentioned data is possible with minor adjustments. Second, after introducing probabilistic forecasts, a rolling horizon optimization method seems to be an appropriate approach to deal with the changing quality of forecasts according to the time horizon. Third, the presented EH system with its EMS and different optimization options offers the

opportunity to be integrated into hardware-in-the-loop tests. Therefore, the modular component models encapsulated as FMU can be exchanged with real-world hardware, e.g., a CHP or battery, with minor effort: To conduct real-world testing, the communication interface of the EMS needs to be adjusted to the needs of the communication of the real-world hardware.

To overcome the "cold-start" problem at the ML forecasting model, future work could investigate whether a feedback loop can be introduced into the process to train the forecasting models online. Furthermore, it would be interesting to extend the approach by including different objective functions within the prediction of the optimization results. Forecasting models specifically designed for the interval length assignment and focusing on the shape instead of absolute performance could be investigated. Particularly, the impact of such forecasting methods on the variance in optimization DOF and the correlation between forecasting quality and optimization results is interesting. Additionally, the transferability of the trained forecasting models to further instances of EHs, in terms of transfer learning, should be investigated whether the models are beneficial in general or specific to a certain EH configuration. Finally, to improve computational efficiency, possibilities to parallelize the approach should be considered.





# List of Figures

2.1	Venn diagram of smart grid aggregation level . . . . .	11
2.2	Hierarchical communication concept for DERs . . . . .	12
2.3	Pareto front . . . . .	14
2.4	Weighted sum for convex and non-convex Pareto front . . . . .	15
2.5	Cascaded weighted sum for convex and non-convex Pareto front . . . . .	16
2.6	General flowchart of an evolutionary algorithm . . . . .	17
2.7	Encoding and decoding within the evolutionary process . . . . .	18
2.8	Example mapping functions . . . . .	19
2.9	MILP flowchart . . . . .	21
3.1	System efficiency of PEM . . . . .	26
3.2	General simulation setup . . . . .	27
3.3	Energy Hub Gas Overview . . . . .	27
3.4	Energy Hub Gas simulation setup . . . . .	29
3.5	Test case data within the Energy Hub Gas concept . . . . .	34
3.6	Load profile of an exemplary day in March 2021 . . . . .	35
3.7	Single-Line Diagram of the 20 kV Grid of Campus North, KIT . . . . .	36
3.8	Curtailment in Germany from 2018 to 2021 . . . . .	37
3.9	Boxplot of optimization results for comparing GLEAM and DEAP . . . . .	42
3.10	Energy flow chart for March 3 <sup>rd</sup> , 2021 . . . . .	44
3.11	Resulting power w/ and w/o EHG interacting at March 3 <sup>rd</sup> , 2021 . . . . .	45
3.12	PSD of the power flow w/ and w/o the EHG on March 3 <sup>rd</sup> , 2021 . . . . .	46
3.13	Resulting power w/ and w/o EHG interacting on February 25 <sup>th</sup> , 2021 . . . . .	47
3.14	Energy flow chart for February 25 <sup>th</sup> , 2021 . . . . .	48
3.15	PSD of the power flow w/ and w/o the EHG on February 25 <sup>th</sup> , 2021 . . . . .	49
3.16	Exemplary mapping function for EAs . . . . .	50
3.17	Process overview of the evaluation within the EMS . . . . .	54
3.18	Mapping function with DOF . . . . .	55
3.19	Boundary value calculation for storage units . . . . .	56
3.20	Sensitivity Analysis of DOF results . . . . .	58
3.21	Boxplot of the simulated year 2019 with evaluation using the DOF . . . . .	59
4.1	Adaptive optimization process overview . . . . .	68
4.2	Combining schedules with different time resolution . . . . .	70
4.3	Optimization result with low time resolution for an example day . . . . .	71
4.4	Combined schedule for an example day . . . . .	72
4.5	Concept overview of hybrid EA for optimized scheduling an EH . . . . .	74

4.6	Hybrid EA process for scheduling with dynamic time interval length . . . . .	76
4.8	Overview of the process of forecasting the optimization error . . . . .	79
4.9	Target schedule . . . . .	82
4.10	Boxplot results of mean $DOF_{RMSE}$ with GLEAM . . . . .	84
4.11	Boxplot results for each day in the week with GLEAM . . . . .	86
4.12	Boxplot of the $DOF_{Cost}$ considering the operational cost objective with GLEAM . . .	87
4.13	Boxplot results of mean $DOF_{RMSE}$ with DEAP . . . . .	88
4.14	Boxplot results for each day in the week with DEAP . . . . .	89
4.15	Boxplot of the $DOF_{Cost}$ considering the operational cost objective with DEAP . . . .	90
5.1	Interval lengths of the different forecasting models RF, TFT and the Ground Truth for Sunday, April 10 <sup>th</sup> , 2022 . . . . .	93

# List of Tables

2.1	Conversion types within an EH . . . . .	6
2.2	Chromosome encoding example . . . . .	17
2.3	Decoded schedule example . . . . .	18
2.4	Offspring generation . . . . .	20
3.1	Technical parameters of the component models within the EHG . . . . .	32
3.2	Technical parameters of the component models within the Scenario Data . . . . .	32
3.3	Comparison of GLEAM and DEAP . . . . .	40
3.4	Summary of the results for TC1 over the complete year 2021 . . . . .	45
3.5	Summary of the results for TC2 over the complete year 2021 . . . . .	48
4.1	EA settings tests with different population sizes and numbers of generations . . . . .	63
4.2	Overview of the input time series used to forecast the EH power time series . . . . .	80
4.3	Overview of the MAE and RMSE for the optimization target error $\hat{\mathcal{E}}_{\text{opt, rel}}$ . . . . .	83



# Previous Publications

## Journal Article

- [1] M. Chlosta, J. Liu, R. Poppenborg, R. Lutz, K. Förderer, T. Schlachter, and V. Hagenmeyer. An adapter-based architecture for evaluating candidate solutions in energy system scheduling. *Energy Informatics*, 5(S4):56, 2022. ISSN 2520-8942. doi: 10.1186/s42162-022-00246-z. 37.12.02; LK 01.
- [2] G. Mehlmann, U. Kühnapfel, F. Wege, A. Winkens, C. Scheibe, S. Vogel, P. Nogliki, M. Gratza, J. Richter, M. Weber, I. Burlakin, A. Kuri, T. Wagner, S. Hubschneider, R. Poppenborg, T. Heins, K. Förderer, A. Ulbig, A. Monti, V. Hagenmeyer, and M. Luther. The kopernikus ensure co-demonstration platform. *IEEE Open Journal of Power Electronics*, pages 1–16, 2023. doi: 10.1109/OJPEL.2023.3332515.
- [3] R. Poppenborg, M. Chlosta, J. Ruf, C. Hotz, C. Döpmeier, T. Kolb, and V. Hagenmeyer. Energy hub gas: A modular setup for the evaluation of local flexibility and renewable energy carriers provision. *Energies*, 16(6), 2023. ISSN 1996-1073. doi: 10.3390/en16062720.

## Conference Proceedings

- [4] S. Grafenhorst, J. Ohm, R. Poppenborg, K. Förderer, and V. Hagenmeyer. Heuristic vs. analytical energy hub optimization: Design, implementation, and trade-offs. In *2024 IEEE 12th International Conference on Smart Energy Grid Engineering (SEGE)*, (accepted for publication).
- [5] R. Poppenborg, J. Ruf, M. Chlosta, J. Liu, C. Hotz, C. Döpmeier, T. Kolb, and V. Hagenmeyer. Energy hub gas: A multi-domain system modelling and co-simulation approach. In *2021 9th Workshop on Modelling and Simulation of Cyber-Physical Energy Systems (MSCPES)*, pages 67–72, 2021. doi: 10.1145/3470481.3472712.
- [6] R. Poppenborg, M. Chlosta, J. Ruf, C. Hotz, C. Döpmeier, T. Kolb, and V. Hagenmeyer. Energy hub gas: A modular setup for the evaluation of local flexibility and renewable energy carriers provision. In *2022 IEEE 10th International Conference on Smart Energy Grid Engineering (SEGE)*, pages 33–41, 2022. doi: 10.1109/SEGE55279.2022.9889751.

- [7] R. Poppenborg, H. Khalloof, M. Chlosta, T. Hofferberth, C. Döpmeier, and V. Hagenmeyer. Dynamic optimization of energy hubs with evolutionary algorithms using adaptive time segments and varying resolution. In Hujun Yin, David Camacho, and Peter Tino, editors, *Intelligent Data Engineering and Automated Learning – IDEAL 2022*, pages 513–524, Cham, 2022. Springer International Publishing. ISBN 978-3-031-21753-1. doi: 10.1007/978-3-031-21753-1\_50.
- [8] R. Poppenborg, K. Beisswanger, C. Hotz, K. Förderer, T. Kolb, and V. Hagenmeyer. Dynamic mapping for evolutionary algorithm based optimization of energy hub gas scheduling. In *2023 IEEE 11th International Conference on Smart Energy Grid Engineering (SEGE)*, pages 206–211, 2023. doi: 10.1109/SEGE59172.2023.10274571.
- [9] R. Poppenborg, K. Phipps, H. Khalloof, K. Förderer, R. Mikut, and V. Hagenmeyer. Dynamic chromosome interpretation in evolutionary algorithms for distributed energy resources scheduling. In *Proceedings of the Companion Conference on Genetic and Evolutionary Computation, GECCO '23 Companion*, page 755–758, New York, NY, USA, 2023. Association for Computing Machinery. ISBN 9798400701207. doi: 10.1145/3583133.3590666.

# References

- [10] *Sequencing and scheduling: algorithms and complexity*, volume 4 of *Handbooks in Operations Research and Management Science*, pages 445–522. Elsevier, 1993. doi: [https://doi.org/10.1016/S0927-0507\(05\)80189-6](https://doi.org/10.1016/S0927-0507(05)80189-6).
- [11] H2 Barometer, 2024. URL [https://e-bridge.com/wp-content/uploads/2024/05/E-Bridge\\_Hydrogen-Barometer\\_1-2024.pdf](https://e-bridge.com/wp-content/uploads/2024/05/E-Bridge_Hydrogen-Barometer_1-2024.pdf). visited 16.08.2024.
- [12] A. Ahmed and M. Khalid. A review on the selected applications of forecasting models in renewable power systems. *Renewable and Sustainable Energy Reviews*, 100:9–21, 2019. doi: 10.1016/j.rser.2018.09.046.
- [13] E. Ahrens, A. Wehling, W. Köppel, M. Sterner, and N. Lucke. Technisch-Ökonomische Modellierung eines sektorengesetzten Gesamtenergiesystems aus Gas und Strom unter Fortschreibung des regulatorischen Rahmens - SMARAGD. DVGW-Förderkennzeichen G201708, 2018.
- [14] K. AlRafea, M. Fowler, A. Elkamel, and A. Hajimiragha. Integration of renewable energy sources into combined cycle power plants through electrolysis generated hydrogen in a new designed energy hub. *International Journal of Hydrogen Energy*, 41(38):16718–16728, 2016. ISSN 0360-3199. doi: <https://doi.org/10.1016/j.ijhydene.2016.06.256>.
- [15] R. R. Appino, J. Á. González-Ordiano, R. Mikut, T. Faulwasser, and V. Hagenmeyer. On the use of probabilistic forecasts in scheduling of renewable energy sources coupled to storages. *Applied Energy*, 210:1207–1218, 2018. doi: 10.1016/j.apenergy.2017.08.133.
- [16] Association of German Engineers. VDI-Standard: VDI 4602 part 2., 2013. URL [https://www.vdi.de/fileadmin/pages/vdi\\_de/redakteure/richtlinien/inhaltsverzeichnis/1929951.pdf](https://www.vdi.de/fileadmin/pages/vdi_de/redakteure/richtlinien/inhaltsverzeichnis/1929951.pdf).
- [17] K. R. Baker and D. Trietsch. *Principles of sequencing and scheduling*. John Wiley, Hoboken, N.J, 2009. ISBN 9780470391655.
- [18] Z. Bao, Q. Zhou, Z. Yang, Q. Yang, L. Xu, and T. Wu. A multi time-scale and multi energy-type coordinated microgrid scheduling solution—part i: Model and methodology. volume 30, pages 2257–2266, 2015. doi: 10.1109/TPWRS.2014.2367127.

- [19] S. D. Beigvand, H. Abdi, and M. La Scala. A general model for energy hub economic dispatch. *Applied Energy*, 190:1090–1111, 2017. doi: 10.1016/j.apenergy.2016.12.126.
- [20] Aharon Ben-Tal and Arkadi Nemirovski. *1. Linear Programming*. Society for Industrial and Applied Mathematics, 2001. doi: 10.1137/1.9780898718829.ch1.
- [21] P. J. Bentley, S. L. Lim, A. Gaier, and L. Tran. Evolving through the looking glass: Learning improved search spaces with variational autoencoders. In *Parallel Problem Solving from Nature–PPSN XVII: 17th International Conference, PPSN 2022, Dortmund, Germany, September 10–14, 2022, Proceedings, Part I*, pages 371–384. Springer, 2022.
- [22] Peter J. Bentley, Soo Ling Lim, Adam Gaier, and Linh Tran. Coil: Constrained optimization in learned latent space: learning representations for valid solutions. In *Proceedings of the Genetic and Evolutionary Computation Conference Companion, GECCO '22*, page 1870–1877, New York, NY, USA, 2022. Association for Computing Machinery. ISBN 9781450392686. doi: 10.1145/3520304.3533993.
- [23] C. M. Bishop and N. M. Nasrabadi. *Pattern recognition and machine learning*, volume 4. Springer, 2006. ISBN 978-0-387-31073-2.
- [24] V. S. Bisht, N. Joshi, G. S. Jethi, and A. S. Bhakuni. *A Review on Genetic Algorithm and Its Application in Power System Engineering*, pages 107–130. Springer Singapore, Singapore, 2021. ISBN 978-981-15-7571-6. doi: 10.1007/978-981-15-7571-6\_5.
- [25] T. Blochwitz, M. Otter, M. Arnold, C. Bausch, C. Clauß, H. Elmqvist, A. Junghanns, J. Mauss, M. Monteiro, T. Neidhold, D. Neumerkel, H. Olsson, J.-V. Peetz, and S. Wolf. The functional mockup interface for tool independent exchange of simulation models. pages 105–114, 03 2011. ISBN 978-91-7393-096-3. doi: 10.3384/ecp11063105.
- [26] C. Blume and W. Jakob. GLEAM - an evolutionary algorithm for planning and control based on evolution strategy. In E. Cantú-Paz, editor, *Late Breaking papers at the Genetic and Evolutionary Computation Conference (GECCO-2002), New York, USA, 9-13 July 2002*, pages 31–38. AAAI, 2002.
- [27] C. Blume and W. Jakob. Gleam - general learning evolutionary algorithm and method : ein evolutionärer algorithmus und seine anwendungen. Technical report, Karlsruher Institut für Technologie (KIT), 2009.
- [28] J. Branke. *Evolutionary optimization in dynamic environments*. PhD thesis, Boston, Mass. [u.a.], 2002.
- [29] Jörg Bremer, Barbara Rapp, and Michael Sonnenschein. Support vector based encoding of distributed energy resources’ feasible load spaces. In *2010 IEEE PES Innovative Smart Grid Technologies Conference Europe (ISGT Europe)*, pages 1–8, 2010. doi: 10.1109/ISGTEUROPE.2010.5638940.



- 
- [30] P. Brucker. *Computational Complexity*, pages 37–60. Springer Berlin Heidelberg, Berlin, Heidelberg, 2007. ISBN 978-3-540-69516-5. doi: 10.1007/978-3-540-69516-5\_3.
- [31] Peter Brucker and Sigrid Knust. *Complex scheduling*. GOR-Publications. Springer, Berlin, 2006. ISBN 3540295453; 9783540295457.
- [32] Bundesnetzagentur. Bericht zum Redispatch nach Artikel 13 Verordnung (EU) 2019/943. Technical report, Bundesnetzagentur für Elektrizität, Gas, Telekommunikation, Post und Eisenbahnen. URL [https://www.bundesnetzagentur.de/SharedDocs/Downloads/DE/Sachgebiete/Energie/Unternehmen\\_Institutionen/Versorgungssicherheit/Engpassmanagement/RedispatchBericht2020.pdf?\\_\\_blob=publicationFile&v=1](https://www.bundesnetzagentur.de/SharedDocs/Downloads/DE/Sachgebiete/Energie/Unternehmen_Institutionen/Versorgungssicherheit/Engpassmanagement/RedispatchBericht2020.pdf?__blob=publicationFile&v=1). visited 16.08.2024.
- [33] Michael L. Bynum, Gabriel A. Hackebeil, William E. Hart, Carl D. Laird, Bethany L. Nicholson, John D. Siirola, Jean-Paul Watson, and David L. Woodruff. *Pyomo-optimization modeling in python*, volume 67. Springer Science & Business Media, third edition, 2021. ISBN 978-3-030-68927-8. doi: 10.1007/978-3-030-68928-5.
- [34] E. Cantú-Paz. *Efficient and Accurate Parallel Genetic Algorithms*. Springer US, Boston, MA, 2001. ISBN 978-1-4615-4369-5. doi: 10.1007/978-1-4615-4369-5.
- [35] C. Challu, K. G. Olivares, B. N. Oreshkin, F. Garza, M. Mergenthaler, and A. Dubrawski. N-hits: Neural hierarchical interpolation for time series forecasting. *Proceedings of the AAAI Conference on Artificial Intelligence*, 37(6):6989–6997, 2023. doi: 10.1609/aaai.v37i6.25854.
- [36] T. Chen and C. Guestrin. XGBoost: A scalable tree boosting system. In *Proceedings of the 22nd ACM SIGKDD International Conference on Knowledge Discovery and Data Mining, KDD '16*, pages 785–794, New York, NY, USA, 2016. ACM. ISBN 978-1-4503-4232-2. doi: 10.1145/2939672.2939785.
- [37] S. Cheng, R. Wang, J. Xu, and Z. Wei. Multi-time scale coordinated optimization of an energy hub in the integrated energy system with multi-type energy storage systems. volume 47, page 101327, 2021. doi: 10.1016/j.seta.2021.101327.
- [38] C. A. Coello Coello, G. B. Lamont, and D. A. Van Veldhuizen. *Evolutionary algorithms for solving multi-objective problems*. Genetic and evolutionary computation series. Springer, New York, NY, 2. ed. edition, 2007. ISBN 9780387332543; 0387332545.
- [39] International Electrotechnical Commission. *Communication networks and systems for power utility automation*. International Electrotechnical Commission, Geneva, Switzerland, IEC 61850:2021 edition, 2021.
- [40] R. W. Conway, W. L. Maxwell, and L. W. Miller. *Theory of scheduling*. Addison-Wesley, Reading, Mass. [u.a.], 1967. ISBN 0201011891.

- [41] R. D'Agostino and E. S. Pearson. Tests for departure from normality. empirical results for the distributions of  $b_2$  and  $\sqrt{b_1}$ . *Biometrika*, 60(3):613–622, 1973. ISSN 00063444. doi: 10.2307/2335012.
- [42] V. Davatgaran, M. Saniei, and S. S. Mortazavi. Optimal bidding strategy for an energy hub in energy market. *Energy*, 148:482–493, 2018. doi: 10.1016/j.energy.2018.01.174.
- [43] François-Michel De Rainville, Félix-Antoine Fortin, Marc-André Gardner, Marc Parizeau, and Christian Gagné. Deap: a python framework for evolutionary algorithms. In *Proceedings of the 14th Annual Conference Companion on Genetic and Evolutionary Computation, GECCO '12*, page 85–92, New York, NY, USA, 2012. Association for Computing Machinery. ISBN 9781450311786. doi: 10.1145/2330784.2330799.
- [44] K. Deb. An efficient constraint handling method for genetic algorithms. *Computer Methods in Applied Mechanics and Engineering*, 186(2-4):311–338, 2000.
- [45] K. Deb, A. Pratap, S. Agarwal, and T. Meyarivan. A fast and elitist multiobjective genetic algorithm: Nsga-ii. *IEEE Transactions on Evolutionary Computation*, 6(2):182–197, 2002. doi: 10.1109/4235.996017.
- [46] K. Deb, A. Pratap, S. Agarwal, and T. Meyarivan. A fast and elitist multiobjective genetic algorithm: NSGA-II. *IEEE Transactions on Evolutionary Computation*, 6(2):182–197, 2002. doi: 10.1109/4235.996017.
- [47] Kalyanmoy Deb and Himanshu Jain. An evolutionary many-objective optimization algorithm using reference-point-based nondominated sorting approach, part i: Solving problems with box constraints. *IEEE Transactions on Evolutionary Computation*, 18(4):577–601, 2014. doi: 10.1109/TEVC.2013.2281535.
- [48] T. Ding, W. Jia, M. Shahidehpour, O. Han, Y. Sun, and Z. Zhang. Review of optimization methods for energy hub planning, operation, trading, and control. *IEEE Transactions on Sustainable Energy*, 13(3):1802–1818, 2022. doi: 10.1109/TSTE.2022.3172004.
- [49] B. Efron and T. Hastie. *Computer Age Statistical Inference: Algorithms, Evidence, and Data Science*. Institute of Mathematical Statistics Monographs. Cambridge University Press, 2016. doi: 10.1017/CBO9781316576533.
- [50] Agoston E. Eiben and James E. Smith. *Introduction to Evolutionary Computing*. Natural Computing Series. Springer, Berlin, Heidelberg, 2nd ed. 2015 edition, 2015. doi: 10.1007/978-3-662-44874-8.
- [51] A. N. Elmachtoub, J. C. N. Liang, and R. McNellis. Decision trees for decision-making under the predict-then-optimize framework. In *International Conference on Machine Learning*, pages 2858–2867. PMLR, 2020.

- 
- [52] Sandbag (Ember). Entwicklung des Emissionsfaktors der Stromerzeugung in Deutschland und Frankreich im Zeitraum 2000 bis 2023 (in g CO<sub>2</sub>-Äquivalent pro Kilowattstunde Strom). URL <https://de.statista.com/statistik/daten/studie/1421117/umfrage/emissionen-strom-deutschland-und-frankreich/>. visited 16.08.2024.
- [53] L. Fiorini and M. Aiello. Energy management for user's thermal and power needs: A survey. volume 5, pages 1048–1076, 2019. doi: 10.1016/j.egy.2019.08.003.
- [54] D. B. Fogel. *Introduction to Evolutionary Computation*, chapter 1, pages 1–23. John Wiley & Sons, Ltd, 2008. ISBN 9780470225868. doi: <https://doi.org/10.1002/9780470225868.ch1>.
- [55] Kevin Michael Förderer. *Modeling and Communicating Flexibility in Smart Grids Using Artificial Neural Networks as Surrogate Models*. PhD thesis, Karlsruher Institut für Technologie (KIT), 2021.
- [56] M. R. Garey and D. S. Johnson. *Computers and intractability : a guide to the theory of NP-completeness*. A series of books in the mathematical sciences. Freeman, New York, NY [u.a.], 1979. ISBN 9780716710455.
- [57] M. Geidl. *Integrated Modeling and Optimization of Multi-Carrier Energy Systems*. PhD thesis, ETH Zürich, 2007.
- [58] M. Geidl and G. Andersson. A modeling and optimization approach for multiple energy carrier power flow. In *2005 IEEE Russia Power Tech*, pages 1–7, 2005. doi: 10.1109/PTC.2005.4524640.
- [59] M. Geidl and G. Andersson. Optimal power flow of multiple energy carriers. *IEEE Transactions on Power Systems*, 22(1):145–155, 2007. doi: 10.1109/TPWRS.2006.888988.
- [60] M. Geidl, G. Koepfel, P. Favre-Perrod, B. Klockl, G. Andersson, and K. Frohlich. Energy hubs for the future. *IEEE Power and Energy Magazine*, 5(1):24–30, 2007. doi: 10.1109/MPAE.2007.264850.
- [61] D. Gong, B. Xu, Y. Zhang, Y. Guo, and S. Yang. A similarity-based cooperative co-evolutionary algorithm for dynamic interval multiobjective optimization problems. *IEEE Transactions on Evolutionary Computation*, 24(1):142–156, 2020. doi: 10.1109/TEVC.2019.2912204.
- [62] J. Á. González-Ordiano, T. Mühlfordt, E. Braun, J. Liu, H. Çakmak, U. Kühnapfel, C. Döpmeier, S. Waczowicz, T. Faulwasser, R. Mikut, V. Hagenmeyer, and R. R. Appino. Probabilistic forecasts of the distribution grid state using data-driven forecasts and probabilistic power flow. *Applied Energy*, 302:117498, 2021. ISSN 0306-2619. doi: 10.1016/j.apenergy.2021.117498.

- [63] M. Gorges-Schleuter. Explicit parallelism of genetic algorithms through population structures. In H.-P. Schwefel and R. Männer, editors, *Parallel Problem Solving from Nature*, pages 150–159, Berlin, Heidelberg, 1991. Springer Berlin Heidelberg. ISBN 978-3-540-70652-6.
- [64] M. Gorges-Schleuter. A comparative study of global and local selection in evolution strategies. In A. E. Eiben, T. Bäck, M. Schoenauer, and H.-P. Schwefel, editors, *Parallel Problem Solving from Nature - PPSN V*, pages 367–377, Berlin, Heidelberg, 1998. Springer Berlin Heidelberg. ISBN 978-3-540-49672-4.
- [65] M. Götz, J. Lefebvre, F. Mörs, A. McDaniel Koch, F. Graf, S. Bajohr, R. Reimert, and T. Kolb. Renewable power-to-gas: A technological and economic review. *Renewable Energy*, 85:1371–1390, 2016. ISSN 0960-1481. doi: 10.1016/j.renene.2015.07.066.
- [66] John J. Grefenstette. Optimization of control parameters for genetic algorithms. *IEEE Transactions on Systems, Man, and Cybernetics*, 16(1):122–128, 1986. doi: 10.1109/TSMC.1986.289288.
- [67] Gurobi Optimization, LLC. Gurobi Optimizer Reference Manual, 2023. URL <https://www.gurobi.com>.
- [68] A. Hajimiragha, C. Canizares, M. Fowler, M. Geidl, and G. Andersson. Optimal energy flow of integrated energy systems with hydrogen economy considerations. In *2007 iREP Symposium - Bulk Power System Dynamics and Control - VII. Revitalizing Operational Reliability*, pages 1–11, 2007. doi: 10.1109/IREP.2007.4410517.
- [69] William E Hart, Jean-Paul Watson, and David L Woodruff. Pyomo: modeling and solving mathematical programs in python. *Mathematical Programming Computation*, 3(3):219–260, 2011. doi: 10.1007/s12532-011-0026-8.
- [70] L. He, H. Ishibuchi, A. Trivedi, H. Wang, Y. Nan, and D. Srinivasan. A survey of normalization methods in multiobjective evolutionary algorithms. *IEEE Transactions on Evolutionary Computation*, 25(6):1028–1048, 2021. ISSN 1089-778X. doi: 10.1109/TEVC.2021.3076514.
- [71] B. Heidrich, A. Bartschat, M. Turowski, O. Neumann, K. Phipps, S. Meisenbacher, K. Schmieder, N. Ludwig, R. Mikut, and V. Hagenmeyer. pywatts: Python workflow automation tool for time series. *ArXiv*, abs/2106.10157, 2021.
- [72] B. F. Hobbs, editor. *The next generation of electric power unit commitment models*. International series in operations research & management science. Kluwer Academic Publishers, Boston, 2001. ISBN 0792373340.

- 
- [73] IEC 61850-7-520. Communication networks and systems for power utility automation: Part 7-520: Basic communication structure - distributed energy resources modelling concepts and guidelines, 2015-03-21.
- [74] International Electrotechnical Commission. Communication networks and systems for power utility automation: Part 7-520: Basic communication structure – distributed energy resources modelling concepts and guidelines.
- [75] W. Jakob. Evo file documentation - gleam. Technical report, KIT, Insititute for Automation and Applied Informatics, 2020. URL <https://github.com/KIT-IAI/Gleam/blob/main/Docu/EVO-File-Docu.pdf>.
- [76] W. Jakob. Applying evolutionary algorithms successfully - a guide gained from real-world applications. *KIT Scientific Working Papers*, 2021. ISSN 2194-1629.
- [77] W. Jakob and C. Blume. Pareto optimization or cascaded weighted sum: A comparison of concepts. *Algorithms*, 7(1):166–185, 2014. ISSN 1999-4893. doi: 10.3390/a7010166.
- [78] W. Jakob, A. Quinte, K.-U. Stucky, and W. Süß. Fast multi-objective scheduling of jobs to constrained resources using a hybrid evolutionary algorithm. In *Proceedings of the 10th International Conference on Parallel Problem Solving from Nature — PPSN X - Volume 5199*, page 1031–1040, Berlin, Heidelberg, 2008. Springer-Verlag. ISBN 9783540876991.
- [79] W. Jakob, S. Strack, A. Quinte, G. Bengel, K.-U. Stucky, and W. Süß. Fast rescheduling of multiple workflows to constrained heterogeneous resources using multi-criteria memetic computing. *Algorithms*, 6(2):245–277, 2013. ISSN 1999-4893. doi: 10.3390/a6020245. URL <https://www.mdpi.com/1999-4893/6/2/245>.
- [80] W. Jakob, J. Á. González Ordiano, N. Ludwig, R. Mikut, and V. Hagenmeyer. Towards coding strategies for forecasting-based scheduling in smart grids and the energy lab 2.0. In *Proceedings of the Genetic and Evolutionary Computation Conference Companion, GECCO '17*, page 1271–1278, New York, NY, USA, 2017. Association for Computing Machinery. ISBN 9781450349390. doi: 10.1145/3067695.3082481.
- [81] S. Jiang, J. Zou, S. Yang, and X. Yao. Evolutionary dynamic multi-objective optimisation: A survey. *ACM Computing Surveys*, 2022. ISSN 0360-0300. doi: 10.1145/3524495.
- [82] H. Khalloof, W. Jakob, J. Liu, E. Braun, S. Shahoud, C. Düepmeier, and V. Hagenmeyer. A generic distributed microservices and container based framework for metaheuristic optimization. In *Proceedings of the Genetic and Evolutionary Conference Companion, Kyoto, J, July 15-19, 2018*, pages 1363–1370. Association for Computing Machinery (ACM), 2018. doi: 10.1145/3205651.3208253.

- [83] H. Khalloof, W. Jakob, S. Shahoud, C. Düepmeier, and V. Hagenmeyer. A generic scalable method for scheduling distributed energy resources using parallelized population-based metaheuristics. In *Proceedings of the Future Technologies Conference (FTC) 2020, Volume 2. Ed.: K. Arai*, volume 1289 of *Advances in Intelligent Systems and Computing (AISC)*, pages 1–21. Springer Nature, 2021. ISBN 978-3-030-63088-1. doi: 10.1007/978-3-030-63089-8\_1.
- [84] Hatem Khalloof. *A Generic Flexible and Scalable Method for Using Evolutionary Algorithms in Cluster Computing Environments*. PhD thesis, Karlsruher Institut für Technologie (KIT), 2023. 37.12.03; LK 01.
- [85] A. Konak, D. W. Coit, and A. E. Smith. Multi-objective optimization using genetic algorithms: A tutorial. *Reliability Engineering & System Safety*, 91(9):992–1007, 2006. ISSN 09518320. doi: 10.1016/j.res.2005.11.018.
- [86] G. Kumari, A. Sharma, H. P. Singh, R. K. Viral, S. K. Sinha, and N. Anwer. *Energy Management System for Hybrid Energy System: Renewable Integration, Modeling and Optimization, Control Aspects and Conceptual Framework*, pages 195–206. Springer Singapore, Singapore, 2021. ISBN 978-981-15-7571-6. doi: 10.1007/978-981-15-7571-6\_9.
- [87] M. Kumawat, N. Gupta, N. Jain, V. Shrivastava, and G. Sharma. *Applications of Metaheuristics in Renewable Energy Systems*, pages 253–282. Springer Singapore, Singapore, 2021. ISBN 978-981-15-7571-6. doi: 10.1007/978-981-15-7571-6\_12.
- [88] A. Kurita, H. Okubo, K. Oki, S. Agematsu, D.B. Klapper, N.W. Miller, W.W. Price, J.J. Sanchez-Gasca, K.A. Wirgau, and T.D. Younkins. Multiple time-scale power system dynamic simulation. volume 8, pages 216–223, 1993. doi: 10.1109/59.221237.
- [89] K. D. Le and J. T. Day. Rolling horizon method: A new optimization technique for generation expansion studies. volume PAS-101, pages 3112–3116, 1982. doi: 10.1109/TPAS.1982.317523.
- [90] C. Li, X. Liu, Y. Cao, P. Zhang, H. Shi, L. Ren, and Y. Kuang. A time-scale adaptive dispatch method for renewable energy power supply systems on islands. volume 7, pages 1069–1078, 2016. doi: 10.1109/TSG.2015.2485664.
- [91] H. Li and D. Landa-Silva. An adaptive evolutionary multi-objective approach based on simulated annealing. *Evolutionary computation*, 19(4):561–595, 2011. doi: 10.1162/EVCO\_a\_00038.
- [92] Zhengping Liang, Shunxiang Zheng, Zexuan Zhu, and Shengxiang Yang. Hybrid of memory and prediction strategies for dynamic multiobjective optimization. *Information Sciences*, 485:200–218, 2019. ISSN 0020-0255. doi: 10.1016/j.ins.2019.01.066.

- [93] B. Lim, S. Ö. Arık, N. Loeff, and T. Pfister. Temporal fusion transformers for interpretable multi-horizon time series forecasting. *International Journal of Forecasting*, 37(4):1748–1764, 2021. ISSN 0169-2070. doi: 10.1016/j.ijforecast.2021.03.012.
- [94] H. Liu, W. Du, and Z. Guo. A multi-population evolutionary algorithm with single-objective guide for many-objective optimization. *Information Sciences*, 503:39–60, 2019. ISSN 00200255. doi: 10.1016/j.ins.2019.06.051.
- [95] J. Liu, E. Braun, C. Düpmeier, P. Kuckertz, D. S. Ryberg, M. Robinius, D. Stolten, and V. Hagemeyer. Architectural concept and evaluation of a framework for the efficient automation of computational scientific workflows: An energy systems analysis example. *Applied Sciences*, 9(4), 2019. ISSN 2076-3417. doi: 10.3390/app9040728.
- [96] J. Liu, C. Düpmeier, and V. Hagemeyer. A new concept of a generic co-simulation platform for energy systems modeling. In *FTC 2017 - Future Technologies Conference 2017*, pages 97–103, 29-30 November 2017. URL [https://saiconference.com/Downloads/FTC2017/Proceedings/11\\_Paper\\_211-A\\_New\\_Concept\\_of\\_a\\_Generic\\_Co-Simulation.pdf](https://saiconference.com/Downloads/FTC2017/Proceedings/11_Paper_211-A_New_Concept_of_a_Generic_Co-Simulation.pdf).
- [97] M. Lösch. *Utilization of Electric Prosumer Flexibility Incentivized by Spot and Balancing Markets*. PhD thesis, Karlsruhe Institute of Technology (KIT), 2022.
- [98] A. Maroufmashat, S. T. Taqvi, A. Miragha, M. Fowler, and A. Elkamel. Modeling and optimization of energy hubs: A comprehensive review. volume 4, 2019. doi: 10.3390/inventions4030050.
- [99] Ingo Mauser, Jan Müller, Kevin Förderer, and Hartmut Schmeck. Definition, modeling, and communication of flexibility in smart buildings and smart grid. In *ETG Congress 2017 – Die Energiewende, Bonn, November 28 – 29, 2017*, ETG-Fachberichte, pages 605–610. VDE Verlag, 2017. ISBN 978-3-8007-4505-0. 37.06.01; LK 01.
- [100] R.-A. Mehdi. Scheduling deferrable appliances and energy resources of a smart home applying multi-time scale stochastic model predictive control. volume 32, pages 338–347, 2017. doi: 10.1016/j.scs.2017.04.006.
- [101] Z. Michalewicz. *Genetic algorithms + data structures = evolution programs ; with 36 tables*. Springer, Berlin, 3., rev. and extended edition, 1996. ISBN 0387606769. doi: 10.1007/978-3-662-03315-9.
- [102] S. Mischinger, H. Seidl, E.-L. Limbacher, S. Fasbender, and F. Stalleicken. dena innovation report ancillary services actual achievements and actions needed at present for stable operation of the electric power system up to 2030. 2018. URL <https://www.dena.de/newsroom/>.

- [103] M. Mohammadi, Y. Noorollahi, B. Mohammadi-ivatloo, and H. Yousefi. Energy hub: From a model to a concept – a review. *Renewable and Sustainable Energy Reviews*, 80:1512–1527, 2017. ISSN 1364-0321. doi: <https://doi.org/10.1016/j.rser.2017.07.030>.
- [104] M. Mohammadi, Y. Noorollahi, B. Mohammadi-ivatloo, M. Hosseinzadeh, H. Yousefi, and S. Torabzadeh Khorasani. Optimal management of energy hubs and smart energy hubs - a review. *Renewable and Sustainable Energy Reveiws*, 89:33–50, 2018. doi: 10.1016/j.rser.2018.02.035.
- [105] M. Mostafavi Sani, H. Mostafavi Sani, M. Fowler, A. Elkamel, A. Noorpoor, and A. Ghasemi. Optimal energy hub development to supply heating, cooling, electricity and freshwater for a coastal urban area taking into account economic and environmental factors. *Energy*, 238:121743, 2022. ISSN 0360-5442. doi: 10.1016/j.energy.2021.121743.
- [106] MTU Solutions. Power generation: Series 4000 gas generator set. URL [https://www.mtu-solutions.com/content/dam/mtu/download/applications/power-generation/16120795\\_PG\\_NaturalGas\\_S4000\\_brochure.pdf/\\_jcr\\_content/renditions/original./16120795\\_PG\\_NaturalGas\\_S4000\\_brochure.pdf](https://www.mtu-solutions.com/content/dam/mtu/download/applications/power-generation/16120795_PG_NaturalGas_S4000_brochure.pdf/_jcr_content/renditions/original./16120795_PG_NaturalGas_S4000_brochure.pdf). visited 16.08.2024.
- [107] M. Nemati, M. Braun, and S. Tenbohlen. Optimization of unit commitment and economic dispatch in microgrids based on genetic algorithm and mixed integer linear programming. *Applied Energy*, 210:944–963, 2018. ISSN 0306-2619. doi: <https://doi.org/10.1016/j.apenergy.2017.07.007>.
- [108] T. T. Nguyen, S. Yang, J. Branke, and X. Yao. Evolutionary dynamic optimization: Methodologies. In S. Yang and X. Yao, editors, *Evolutionary Computation for Dynamic Optimization Problems*, pages 39–64, Berlin, Heidelberg, 2013. Springer Berlin Heidelberg. ISBN 978-3-642-38416-5.
- [109] Jorge Nocedal and Stephen J. Wright. *Numerical optimization*. Springer series in operations research. Springer, New York, 2nd ed. edition, 2006. ISBN 978-0-387-30303-1.
- [110] P. Palensky, A. A. Van Der Meer, C. D. Lopez, A. Joseph, and K. Pan. Cosimulation of intelligent power systems: Fundamentals, software architecture, numerics, and coupling. *IEEE Industrial Electronics Magazine*, 11(1):34–50, 2017. doi: 10.1109/MIE.2016.2639825.
- [111] M Parizeau, Ol. Gagnon, M.-A. Gardner, and Y. Hold-Geoffroy. Scoop 0.7 2.0 documentation. Technical report, 2016. URL <https://scoop.readthedocs.io/en/latest/index.html>.
- [112] F. Pedregosa, G. Varoquaux, A. Gramfort, V. Michel, B. Thirion, O. Grisel, M. Blondel, P. Prettenhofer, R. Weiss, V. Dubourg, J. Vanderplas, A. Passos, D. Cournapeau, M. Brucher, M. Perrot, and E. Duchesnay. Scikit-learn: Machine learning in Python. *Journal of Machine Learning Research*, 12:2825–2830, 2011.



- [113] D.D. Peng, M. Fowler, A. Elkamel, A. Almansoori, and S. B. Walker. Enabling utility-scale electrical energy storage by a power-to-gas energy hub and underground storage of hydrogen and natural gas. *Journal of Natural Gas Science and Engineering*, 35:1180–1199, 2016. ISSN 1875-5100. doi: <https://doi.org/10.1016/j.jngse.2016.09.045>.
- [114] F. Petropoulos, D. Apiletti, V. Assimakopoulos, M. Z. Babai, D. K. Barrow, S. B. Taieb, C. Bergmeir, R. J. Bessa, J. Bijak, J. E. Boylan, et al. Forecasting: theory and practice. *International Journal of Forecasting*, 38(3):705–871, 2022. ISSN 0169-2070. doi: [10.1016/j.ijforecast.2021.11.001](https://doi.org/10.1016/j.ijforecast.2021.11.001).
- [115] H. Qiu, W. Gu, Y. Xu, and B. Zhao. Multi-time-scale rolling optimal dispatch for ac/dc hybrid microgrids with day-ahead distributionally robust scheduling. volume 10, pages 1653–1663, 2019. doi: [10.1109/TSTE.2018.2868548](https://doi.org/10.1109/TSTE.2018.2868548).
- [116] H. Richter. Coupled map lattices as spatio-temporal fitness functions: Landscape measures and evolutionary optimization. *Physica D: Nonlinear Phenomena*, 237(2):167–186, 2007. ISSN 01672789. doi: [10.1016/j.physd.2007.08.016](https://doi.org/10.1016/j.physd.2007.08.016).
- [117] J. Ruf, M. Zimmerlin, P. S. Sauter, W. Köppel, M. R. Suriyah, M. Kluwe, S. Hohmann, T. Leibfried, and T. Kolb. Simulation framework for multi-carrier energy systems with power-to-gas and combined heat and power. In *2018 53rd International Universities Power Engineering Conference (UPEC)*, pages 1–6, 2018. doi: [10.1109/UPEC.2018.8542066](https://doi.org/10.1109/UPEC.2018.8542066).
- [118] Susanne Sass, Timm Faulwasser, Dinah Elena Hollermann, Chrysoula Dimitra Kappatou, Dominique Sauer, Thomas Schütz, David Yang Shu, André Bardow, Lutz Gröll, Veit Hagenmeyer, Dirk Müller, and Alexander Mitsos. Model compendium, data, and optimization benchmarks for sector-coupled energy systems. *Computers & Chemical Engineering*, 135:106760, April 2020. ISSN 00981354. doi: [10.1016/j.compchemeng.2020.106760](https://doi.org/10.1016/j.compchemeng.2020.106760).
- [119] F. Sayedin, A. Maroufmashat, S. Al-Adwani, S. S. Khavas, A. Elkamel, and M. Fowler. Evolutionary optimization approaches for direct coupling photovoltaic-electrolyzer systems. In *2015 International Conference on Industrial Engineering and Operations Management (IEOM)*, pages 1–8, 2015. doi: [10.1109/IEOM.2015.7093884](https://doi.org/10.1109/IEOM.2015.7093884).
- [120] P. Schäfer and A. Mitsos. Tailored time grids for nonlinear scheduling subject to time-variable electricity prices by wavelet-based analysis. In S. Pierucci, F. Manenti, G. L. Bozzano, and D. Manca, editors, *30th European Symposium on Computer Aided Process Engineering*, volume 48 of *Computer Aided Chemical Engineering*, pages 1123–1128. Elsevier, 2020. doi: [10.1016/B978-0-12-823377-1.50188-9](https://doi.org/10.1016/B978-0-12-823377-1.50188-9).
- [121] P. Schäfer, A. M. Schweidtmann, P. H. A. Lenz, H. M. C. Markgraf, and A. Mitsos. Wavelet-based grid-adaptation for nonlinear scheduling subject to time-variable electricity prices. *Computers & Chemical Engineering*, 132:106598 –, 2020. ISSN 0098-1354. doi: [10.1016/j.compchemeng.2019.106598](https://doi.org/10.1016/j.compchemeng.2019.106598).

- [122] S. Schütte, S. Scherfke, and M. Tröschel. Mosaik: A framework for modular simulation of active components in smart grids. In *2011 IEEE First International Workshop on Smart Grid Modeling and Simulation (SGMS)*, pages 55–60, 2011. doi: 10.1109/SGMS.2011.6089027.
- [123] H.-P. Schwefel. *Evolution and optimum seeking*. Sixth-generation computer technology series A Wiley-Interscience publication. Wiley, New York [u.a.], 1. print. edition, 1995. ISBN 0471571482.
- [124] V. Senthil Kumar and M.R. Mohan. Solution to security constrained unit commitment problem using genetic algorithm. *International Journal of Electrical Power & Energy Systems*, 32(2):117–125, 2010. ISSN 0142-0615. doi: 10.1016/j.ijepes.2009.06.019.
- [125] A. Sharif, A. Almansoori, M. Fowler, A. Elkamel, and K. Alrafea. Design of an energy hub based on natural gas and renewable energy sources. *International Journal of Energy Research*, 38(3):363–373, 2014. ISSN 0363907X. doi: 10.1002/er.3050.
- [126] A. Sheikhi, A.M. Ranjbar, and H. Oraee. Financial analysis and optimal size and operation for a multicarrier energy system. *Energy and Buildings*, 48:71–78, 2012. ISSN 0378-7788. doi: 10.1016/j.enbuild.2012.01.011.
- [127] T. Smolinka, N. Wiebe, P. Sterchele, A. Palzer, F. Lehner, M. Jansen, S. Kiemel, R. Mieke, S. Wahren, and F. Zimmermann. Studie indwede: Industrialisierung der wasserelektrolyse in deutschland: chancen und herausforderungen für nachhaltigen wasserstoff für verkehr, strom und wärme.
- [128] Y.-G. Son, B.-C. Oh, M. A. Acquah, R. Fan, D.-M. Kim, and S.-Y. Kim. Multi energy system with an associated energy hub: A review. *IEEE Access*, 9:127753–127766, 2021. doi: 10.1109/ACCESS.2021.3108142.
- [129] C. Steinbrink, M. Blank-Babazadeh, A. El-Ama, S. Holly, B. Lüers, M. Nebel-Wenner, R. P. Ramírez Acosta, T. Raub, J. S. Schwarz, S. Stark, A. Nieße, and S. Lehnhoff. Cpes testing with mosaik: Co-simulation planning, execution and analysis. *Applied Sciences*, 9(5), 2019. ISSN 2076-3417. doi: 10.3390/app9050923.
- [130] M. Sterner and I. Stadler. *Energiespeicher – Bedarf, Technologien, Integration // Energiespeicher - Bedarf, Technologien, Integration*. Springer Vieweg, Berlin, 2. korrigierte und ergänzte auflage edition, 2017. ISBN 978-3-662-48893-5. doi: 10.1007/978-3-662-48893-5.
- [131] V. Svetnik, A. Liaw, C. Tong, J. C. Culberson, R. P. Sheridan, and B. P. Feuston. Random forest: a classification and regression tool for compound classification and qsar modeling. *Journal of Chemical Information and Computer Sciences*, 43(6):1947–1958, 2003. doi: 10.1021/ci034160g.

- 
- [132] Z. Tang and P. A. Fishwick. Feedforward neural nets as models for time series forecasting. *ORSA Journal on Computing*, 5(4):374–385, 1993. doi: 10.1287/ijoc.5.4.374.
- [133] C.-L. Tseng. *On power system generation unit commitment problems*. University of California, Berkeley, 1996.
- [134] T. Wagner and H. Trautmann. Integration of preferences in hypervolume-based multiobjective evolutionary algorithms by means of desirability functions. *IEEE Transactions on Evolutionary Computation*, 14(5):688–701, 2010. ISSN 1089-778X. doi: 10.1109/TEVC.2010.2058119.
- [135] S. Walker, T. Labeodan, W. Maassen, and W. Zeiler. A review study of the current research on energy hub for energy positive neighborhoods. *Energy Procedia*, 122:727 – 732, 2017. ISSN 1876-6102. doi: 10.1016/j.egypro.2017.07.387. CISBAT 2017 International Conference Future Buildings & Districts – Energy Efficiency from Nano to Urban Scale.
- [136] R. Wang, J. Xiong, H. Ishibuchi, G. Wu, and T. Zhang. On the effect of reference point in moea/d for multi-objective optimization. *Applied Soft Computing*, 58:25–34, 2017. ISSN 15684946. doi: 10.1016/j.asoc.2017.04.002.
- [137] E. Widl, T. Jacobs, D. Schwabeneder, S. Nicolas, D. Basciotti, S. Henein, T. Noh, O. Terros, and A. Schuelke. Studying the potential of multi-carrier energy distribution grids: A holistic approach. *Energy*, 153:519–529, 2018. doi: 10.1016/j.energy.2018.04.047.
- [138] D.H. Wolpert and W.G. Macready. No free lunch theorems for optimization. *IEEE Transactions on Evolutionary Computation*, 1(1):67–82, 1997. doi: 10.1109/4235.585893.
- [139] S. Xia, Z. Ding, T. Du, D. Zhang, M. Shahidehpour, and T. Ding. Multitime scale coordinated scheduling for the combined system of wind power, photovoltaic, thermal generator, hydro pumped storage, and batteries. *IEEE Transactions on Industry Applications*, 56(3): 2227–2237, 2020. doi: 10.1109/TIA.2020.2974426.
- [140] H. Yang, M. Li, Z. Jiang, and P. Zhang. Multi-time scale optimal scheduling of regional integrated energy systems considering integrated demand response. volume 8, pages 5080–5090, 2020. doi: 10.1109/ACCESS.2019.2963463.
- [141] Z. Yi, Y. Xu, W. Gu, and W. Wu. A multi-time-scale economic scheduling strategy for virtual power plant based on deferrable loads aggregation and disaggregation. volume 11, pages 1332–1346, 2020. doi: 10.1109/TSTE.2019.2924936.
- [142] Meiling Yue, Hugo Lambert, Elodie Pahon, Robin Roche, Samir Jemei, and Daniel Hissel. Hydrogen energy systems: A critical review of technologies, applications, trends and challenges. *Renewable and Sustainable Energy Reviews*, 146:111180, 2021. ISSN 1364-0321. doi: 10.1016/j.rser.2021.111180.

- [143] R. Zafar, J. Ravishankar, J. E. Fletcher, and H. R. Pota. Multi-timescale model predictive control of battery energy storage system using conic relaxation in smart distribution grids. volume 33, pages 7152–7161, 2018. doi: 10.1109/TPWRS.2018.2847400.
- [144] Y. Zhou and X. Jiao. Knowledge-driven multi-objective evolutionary scheduling algorithm for cloud workflows. *IEEE Access*, 10:2952–2962, 2022. doi: 10.1109/ACCESS.2021.3139137.